

Hydrogen Peroxide Sensing with Prussian Blue-Based Fiber-Optic Sensors

by

Hamed Akbari Khorami
B.Sc., Sharif University of Technology, Iran, 2008
M.Sc., Materials and Energy Research Center, Iran, 2010

A Dissertation Submitted in Partial Fulfillment
of the Requirements for the Degree of
DOCTOR OF PHILOSOPHY
in the Department of Mechanical Engineering

© Hamed Akbari Khorami, 2016
University of Victoria

All rights reserved. This dissertation may not be reproduced in whole or in part, by photocopy or other means, without the permission of the author.

Hydrogen Peroxide Sensing with Prussian Blue-Based Fiber-Optic Sensors

by

Hamed Akbari Khorami

B.Sc., Sharif University of Technology, Iran, 2008

M.Sc., Materials and Energy Research Center, Iran, 2010

Supervisory Committee

Dr. Nedjib Djilali, Department of Mechanical Engineering
Co-supervisor

Dr. Peter Wild, Department of Mechanical Engineering
Co-supervisor

Dr. Alexandre G. Brolo, Department of Chemistry
Outside Member

Supervisory Committee

Dr. Nedjib Djilali, Department of Mechanical Engineering
Co-supervisor

Dr. Peter Wild, Department of Mechanical Engineering
Co-supervisor

Dr. Alexandre G. Brolo, Department of Chemistry
Outside Member

Abstract

Hydrogen peroxide (H_2O_2) is extensively used in a broad range of industrial and medical applications, such as aseptic processing of food and pharmaceuticals, disinfection, water treatment plants, and decontamination of industrial effluents. H_2O_2 is believed to be responsible for chemical degradation of polymer membranes in Polymer-Electrolyte-Membrane (PEM) fuel cells. Therefore, a versatile H_2O_2 sensor that functions in different environments with different conditions is of practical importance in various fields. This dissertation presents the fabrication of a fiber-optic H_2O_2 sensing probe (optrode) and its H_2O_2 sensing behavior in different conditions.

An H_2O_2 optrode is fabricated using chemical deposition of Prussian blue (PB) onto the tip of a multimode optical fiber. Sensing tests are performed in aqueous solutions at a constant pH and different concentrations of H_2O_2 . Sensing features of the optrode (i.e. repeatability, durability, and reproducibility) are assessed by performing multiple sensing tests with several optrodes. The results show the prepared optrode is able to detect concentrations of H_2O_2 in aqueous solutions at a constant pH of 4 and the optrode features a repeatable and durable response at this condition.

The functionality of optrodes at different pH values is further investigated by performing additional sensing experiments. These experiments are carried out in aqueous solutions with different concentrations of H_2O_2 at different pH values (i.e. pH 2-7). The sensor detects the presence of H_2O_2 at a range of pH values. Sensing behavior of optrodes toward detection and measurement of H_2O_2 concentrations is studied at the pH value corresponding to an operating PEM fuel cell (i.e. pH 2). The optrode is able to detect concentrations of H_2O_2 at this condition with a repeatable and durable response.

The stability of PB films, prepared through different conditions, is investigated to address the stability of optrodes at elevated temperatures. PB films are first deposited onto the glass slides through three different chemical processes, and then at different synthesis temperatures. The PB films are left in Phosphate-Buffer-Solutions (PBS) with pH 2 and at elevated temperatures for a day. Finally, PB films are characterized using Fourier transform infrared spectroscopy (FTIR) to analyze their stability following PBS processing at operating temperatures and pH value corresponding to an operating PEM fuel cell (i.e. 80 °C and pH 2). The results of these experiments illustrate the PB films prepared through the single-source precursor (SSP) technique and at synthesis temperatures above 60 °C remain stable after the PBS processing.

The proposed optrode shows reliable sensing behavior toward detection and measurement of H_2O_2 concentrations in aqueous solutions at different conditions. The prepared optrode has the potential for being developed and used in different industrial and medical fields, as well as an operating PEM fuel cell, to detect and measure H_2O_2 concentrations.

Table of Contents

| | |
|---|------|
| Supervisory Committee | ii |
| Abstract | iii |
| Table of Contents | v |
| List of Tables | viii |
| List of Figures | ix |
| List of Symbols and Abbreviations..... | xi |
| Acknowledgements..... | xii |
| Dedication | xiv |
| 1. Introduction | 1 |
| 1.1. Research Motivation..... | 1 |
| 1.2. Literature Review | 2 |
| 1.2.1. Membrane Degradation by H ₂ O ₂ in PEM Fuel Cell | 2 |
| 1.3. Detection of H ₂ O ₂ | 5 |
| 1.3.1. Electrochemical Techniques | 6 |
| 1.3.2. Spectroscopic Techniques Using Optical Fibers..... | 7 |
| 1.4. Prussian Blue | 11 |
| 1.4.1. H ₂ O ₂ Detection mechanism by Prussian Blue | 11 |
| 1.4.2. Preparation of Prussian Blue Films..... | 13 |
| 1.5. Objectives | 14 |
| 1.6. Structure of Dissertation..... | 15 |
| 2. Summary of Key Results..... | 17 |

| | |
|--|----|
| 2.1. Spectroscopic Detection of Hydrogen Peroxide with an Optical Fiber Probe using Chemically Deposited Prussian Blue | 17 |
| 2.2. pH-dependent Response of a Hydrogen Peroxide Sensing Probe | 19 |
| 2.3. Effect of Deposition Conditions on Stability of PB Films at PEMFC's Operating Temperatures and pH..... | 20 |
| 3. Spectroscopic Detection of Hydrogen Peroxide with an Optical Fiber Probe using Chemically Deposited Prussian Blue | 22 |
| Preamble | 22 |
| Abstract | 22 |
| 3.1. Introduction | 23 |
| 3.2. Experimental..... | 25 |
| 3.2.1. Materials..... | 25 |
| 3.2.2. Chemical Deposition of Prussian Blue..... | 26 |
| 3.2.3. Characterization of the Prussian Blue | 27 |
| 3.2.4. Sensing Test Procedures and Instrumentation | 27 |
| 3.3. Results and Discussion | 29 |
| 3.3.1. Chemical Deposition of Prussian Blue..... | 29 |
| 3.3.2. Sensing Behavior..... | 33 |
| 3.3.3. Repeatability..... | 37 |
| 3.3.4. Reproducibility | 37 |
| 3.3.5. Durability | 40 |
| 3.4. Conclusions | 41 |
| 4. pH-dependent Response of a Hydrogen Peroxide Sensing Probe | 43 |
| Preamble | 43 |
| Abstract | 43 |
| 4.1. Introduction | 44 |
| 4.2. Experimental..... | 47 |
| 4.2.1. Materials..... | 47 |
| 4.2.2. Sensor Fabrication..... | 48 |
| 4.2.3. Sensing Test Procedure and Instrumentation | 48 |
| 4.3. Results and Discussion | 49 |
| 4.3.1. pH-dependent Response | 49 |

| | | |
|----------|---|----|
| 4.3.2. | Sensing Behavior at PEM Fuel Cell's Operating pH..... | 52 |
| 4.3.2.1. | Repeatability..... | 54 |
| 4.3.2.2. | Reproducibility..... | 56 |
| 4.3.2.3. | Durability..... | 57 |
| 4.3.3. | pH-dependent Sensitivity..... | 58 |
| 4.4. | Conclusions..... | 59 |
| 5. | Effect of Deposition Conditions on Stability of PB Films at PEMFC's Operating Temperatures and pH..... | 60 |
| | Preamble..... | 60 |
| | Abstract..... | 60 |
| 5.1. | Introduction..... | 61 |
| 5.2. | Experimental..... | 63 |
| 5.2.1. | Deposition of Prussian Blue Films..... | 63 |
| 5.2.2. | PBS Processing of Samples..... | 65 |
| 5.3. | Results and Discussion..... | 65 |
| 5.3.1. | Effect of Synthesis Process and Precursors..... | 65 |
| 5.3.2. | Effect of Synthesis Temperature..... | 67 |
| 5.4. | Summary..... | 68 |
| 6. | Conclusions and Future Work..... | 69 |
| 6.1. | Conclusions and Contributions..... | 69 |
| 6.1.1. | Spectroscopic Detection of Hydrogen Peroxide with an Optical Fiber Probe using Chemically Deposited Prussian Blue..... | 70 |
| 6.1.2. | pH-dependent Response of a Hydrogen Peroxide Sensing Probe..... | 71 |
| 6.1.3. | Effect of Deposition Conditions on Stability of PB Films at PEMFC's Operating Temperatures and pH..... | 72 |
| 6.1.4. | Conclusions..... | 72 |
| 6.2. | Future work..... | 73 |
| | Bibliography..... | 74 |
| | Appendix A: Polymer Electrolyte Membrane Fuel Cell..... | 81 |
| | Appendix B: Prussian Blue..... | 85 |

List of Tables

| | |
|---|----|
| Table 4-1: Slopes of intensity variation at different concentrations of H ₂ O ₂ | 55 |
| Table 5-1: Source of Chemicals..... | 64 |

List of Figures

| | |
|--|----|
| Figure 1-1: Schematic of fuel cell's components and reactions. | 3 |
| Figure 1-2: Nafion structure (http://en.wikipedia.org/wiki/File:Nafion2.svg). | 3 |
| Figure 1-3: (a) Surface and (b) cross-section SEM micrographs of the Nafion membranes treating in H ₂ O ₂ /metal ions containing solution for 48 h (taken from [6], Reproduced with permission from Elsevier). | 5 |
| Figure 1-4: Configuration of a fiber-optic sensor. | 9 |
| Figure 1-5: An illustration of excitation and fluorescence. | 10 |
| Figure 1-6: (a) Electrochemical and (b) spectroscopic characteristics of PB (taken from [38], Reproduced with permission from Taylor & Francis). | 12 |
| Figure 1-7: Detection mechanism of H ₂ O ₂ using an optrode based on PB/PW system. .. | 12 |
| Figure 3-1: Detection mechanism of H ₂ O ₂ using fiber-optic sensing probe based on PB/PW system. | 24 |
| Figure 3-2: Experimental setup. | 28 |
| Figure 3-3: Raman spectra in the range of 2025-3010 cm ⁻¹ of red line) uncoated glass substrate, blue line) sample synthesized in darkness, and green line) sample synthesized under the fluorescent lamp light exposure. The inset is the Raman spectra of same samples in the range of 100-3200 cm ⁻¹ | 31 |
| Figure 3-4: The light reflection from the distal end of an optical fiber during synthesis a) in darkness and in 720 ± 15 nm, b) under the light exposure in 720 ± 15 nm, c) in darkness and in 420 ± 15 nm, and d) under the light exposure in 420 ± 15 nm. | 32 |
| Figure 3-5: Response of the sensing probe to immersion in solutions with random H ₂ O ₂ concentration. | 34 |
| Figure 3-6: Response of the sensing probe and its inverse exponential fit to immersion in 100 μM H ₂ O ₂ solution. | 35 |
| Figure 3-7: Time response of sensing probe versus H ₂ O ₂ concentration. | 36 |
| Figure 3-8: Average time response of sensing probe versus H ₂ O ₂ concentration. | 37 |
| Figure 3-9: Response of three different sensing probes to immersion in solutions containing H ₂ O ₂ | 38 |

| | |
|---|----|
| Figure 3-10: Time response of three different sensing probes versus H ₂ O ₂ concentration. | 39 |
| Figure 3-11: Response of a sensing probe to immersion in solutions containing H ₂ O ₂ four and seven months after its fabrication. | 40 |
| Figure 3-12: Time response of a sensing probe versus H ₂ O ₂ concentration four and seven months after its fabrication. | 41 |
| Figure 4-1: Detection mechanism of H ₂ O ₂ using an optrode based on PB/PW system (taken from [56]). | 46 |
| Figure 4-2: Sensing test experimental Setup including white light source, optical fiber, optrode, and spectrometer. | 49 |
| Figure 4-3: Intensity response of the optrode to immersion in solutions with different pH values and 100 μmol L ⁻¹ of H ₂ O ₂ | 50 |
| Figure 4-4: Time constant of the optrode versus pH of the test solutions with 100 μmol L ⁻¹ of H ₂ O ₂ | 52 |
| Figure 4-5: Intensity response of the optrode to immersion into solutions with different H ₂ O ₂ concentrations at pH 2. | 53 |
| Figure 4-6: Time constant of the optrode versus H ₂ O ₂ concentration at pH 2. | 53 |
| Figure 4-7: Successive intensity responses of the optrode to red) 50 μmol L ⁻¹ of H ₂ O ₂ , green) 100 μmol L ⁻¹ of H ₂ O ₂ , blue) 200 μmol L ⁻¹ of H ₂ O ₂ , and orange) 400 μmol L ⁻¹ of H ₂ O ₂ (For interpretation of the references to colour in this figure legend, the reader is referred to the web version of this article). | 54 |
| Figure 4-8: Time constant of the optrode versus H ₂ O ₂ concentration. | 55 |
| Figure 4-9: Time constant of two different optrodes versus H ₂ O ₂ concentration at pH 2.56 | |
| Figure 4-10: Time constant of an optrode versus H ₂ O ₂ concentration (A) five, (B) six, and (C) nine months after its fabrication. | 57 |
| Figure 4-11: Time constant of an optrode versus H ₂ O ₂ concentration in solutions with (A) pH 6, (B) pH 5, and (C) pH 2. | 58 |
| Figure 5-1: Experimental procedure | 65 |
| Figure 5-2: FTIR spectra of PB films synthesized through (a) sol-gel process, (b) chemical process using potassium ferrocyanide and iron (III) chloride, and (c) SSP process using potassium ferricyanide, before (solid line) and after (dashed line) PBS processing. | 66 |
| Figure 5-3: FTIR spectra of PB films synthesized at (a) 40 °C, (b) 60 °C, and (c) 80 °C, before (solid line) and after (dashed line) PBS processing. | 67 |
| Figure A-1: Schematic of fuel cell's components and reactions. | 82 |
| Figure A-2: Nafion structure (http://en.wikipedia.org/wiki/File:Nafion2.svg). | 84 |
| Figure A-3: CL at cathode electrode (taken from [2], Reproduced with permission from Elsevier). | 84 |
| Figure B-1: Face-centered-cubic crystal structure of PB (taken from [38], Reproduced with permission from Taylor & Francis). | 85 |

List of Symbols and Abbreviations

| Symbol or Abbreviation | Meaning |
|------------------------|---|
| PB | Prussian blue, ferric ferrocyanide |
| PW | Prussian white, potassium ferrous ferrocyanide |
| BG | Berlin green, ferric ferrocyanide |
| ABS | Acetate buffer solution |
| PBS | Phosphate buffer solution |
| TEOS | Tetraethyl orthosilicate |
| PTFE | Polytetrafluoroethylene |
| PEM | Polymer electrolyte membrane |
| MEA | Membrane electrode assembly |
| CL | Catalyst layer |
| GDL | Gas diffusion layer |
| SSP | Single source precursor, synthesis approach |
| ESA | Electrostatic self-assembly, deposition technique |
| LbL | Layer-by-layer, deposition technique |
| FTIR | Fourier transform infrared spectroscopy |
| STDEV | Estimated standard deviation |
| R^2 | R-squared is a statistical measure of how close the data are to the fitted regression line |
| τ | Characteristic response time is the time elapsed for the signal to reach $(1 - 1/e)$ equal to 63% of the intensity at plateau state |
| T | Transmittance |
| c_i | Amount concentration of material |
| ϵ_i | Molar attenuation coefficient |
| l | Path length of the beam through a thin layer of material |

Acknowledgements

First and foremost I would like to express my special appreciation and thanks to my supervisors, Dr. Ned Djilali and Dr. Peter Wild. It has been an honor for me to be your Ph.D. student. I would like to thank you for encouraging my research and for allowing me to grow as a research scientist. You have taught me how to work in a professional manner and how important is to have good research questions. Thank you for all the support you have provided and all the lessons you have taught me during the years of my Ph.D. studies

I would also like to thank Dr. Alexandre Brolo from the Department of Chemistry for providing access to his laboratory facilities and for being my committee member. I cannot forget to thank Dr. Harry Kowk from the Department of Electrical and Computer Engineering who had been my supervisor before I started my Ph.D. in the Department of Mechanical Engineering.

A special thanks goes to my family. Words cannot express how grateful I am to my parents and parents-in-law for all their lifetime support. I would like to extend my appreciation to Dr. Nazi Ghabaee who has always been beside my family and I, ready to provide us with her support and love.

Starting my Ph.D. studies coincided with leaving my home country for the first time and immigrating to a new country with a different language, culture, geography, and weather than my home country. This could have been very challenging and difficult without the support of my dear friend Dr. Alireza Tari, the family of Shayeste Kia, and Dr. Mahyar Mazloumi. Thanks for welcoming me with your open arms and thanks for all your support and love. I want to extend my gratitude to my dear friends Dr. Amirali Baniasadi, Dr. Porya Shirazian, and Reza Bayesteh who were always ready to provide help and emotionally support me. Thank you all for giving me your friendship and becoming a part of my life.

I would like to thank Susan Walton, Pauline Shepherd, and Peggy White in IESVic and Dorothy Burrows, and Susan Wignall in the Department of Mechanical Engineering.

Thanks to all my friends, classmates and colleagues at UVic, Dr. Juan F. Botero-Cadavid, Dr. Nigel David, Majid Soleimani nia, Alireza Akhgar, and Koh Yiin Hong.

I would also like to acknowledge financial support from the Natural Sciences and Engineering Research Council of Canada (NSERC), as well as The German Academic Exchange Service (DAAD) for supporting me as an exchange Ph.D. student at the University of Oldenburg, Germany.

Dedication

To my wife Nina Taherimakhsousi

It would not have been possible without your love, endless support, encouragement, and infinite patience

Chapter 1

Introduction

This dissertation describes the development of a fiber-optic sensing probe (optrode) that detects and measures concentrations of hydrogen peroxide (H_2O_2) in an environment similar to that in an operating Polymer-Electrolyte-Membrane (PEM) fuel cell. The process of optrode preparation is studied to find suitable processes and conditions yielding optrodes that remain stable under operating condition corresponding to a PEM fuel cell (i.e. pH 2 and temperature range of 60 to 80 °C). Sensing behavior of the optrode is then systematically investigated under a range of conditions. Section 1.1 of this chapter discusses the research motivation. A literature review on membrane degradation, by H_2O_2 , in PEM fuel cells is provided in Section 1.2. H_2O_2 sensing techniques and H_2O_2 detector agent are described in Sections 1.3 and 1.4. The objectives and the structure of the dissertation are described in Sections 1.5 and 1.6.

1.1. Research Motivation

PEM fuel cells convert chemical energy directly into electricity. When using hydrogen and oxygen as reactants, the only by-products of fuel cells are water and heat. PEM fuel cells are prospective power sources for multiple applications (e.g. transportation systems and portable electronics). For using PEM fuel cells in transportation systems, high power density, fast start-up, high efficiency, and durability need to be optimized or improved in order to make PEM fuel cells competitive with internal combustion engines [1].

A key component of a PEM fuel cell is the polymer electrolyte membrane. The chemical and mechanical stability of the membrane are crucial to fuel cell performance, efficiency and life time. However, under certain operating conditions, H_2O_2 is produced and causes chemical degradation of the membrane resulting in a decrease in fuel cell efficiency and life time. Monitoring H_2O_2 and understanding underlying conditions that promote its formation is a challenging problem. This requires the development of a suitable H_2O_2 sensor to measure concentrations of H_2O_2 *in operando* within a fuel cell, to investigate production rates and controlling factors.

1.2. Literature Review

This section briefly describes PEM fuel cells and reviews progress reported in the literature on understanding of membrane degradation by H_2O_2 in PEM fuel cells. Further information on PEM fuel cell operation is provided in Appendix A.

1.2.1. Membrane Degradation by H_2O_2 in PEM Fuel Cell

A PEM fuel cell consists of an anode, a cathode, and a proton exchange membrane (PEM) that all together form the so-called Membrane Electrode Assembly (MEA). The anode and cathode electrodes are connected to an external circuit. At the anode electrode, hydrogen fuel is oxidized and forms hydrogen cations and electrons. Hydrogen cations migrate to the cathode side through the electrolyte membrane. Conversely, electrons are blocked by the electrolyte membrane, and flow through the external circuit, drive the load, and return to the cathode side. At the cathode, oxygen reacts with hydrogen cations and consumes electrons. As long as the anode and cathode are fed with hydrogen and oxygen, the electrons continue to flow through the external circuit [1, 2]. Figure 1-1 is a schematic of the fuel cell components and shows the key reactions of fuel cell operation.

The electrolyte membrane in the PEM fuel cell is formed from a hydrophobic and inert polymer backbone which is sulfonated with hydrophilic and ionically conductive acid clusters. Nafion is the most used and studied polymer electrolyte for fuel cells and is synthesized by sulphonation (SO_3^-) of the basic polytetrafluoroethylene (PTFE) structure, Nafion structure is shown in Figure 1-2. The PTFE is not ionically conductive but provides chemical stability and durability for the membrane. Clustering of the sulfonic

acid side groups and hydration level are determining factors for the ionic conductivity of the electrolyte.

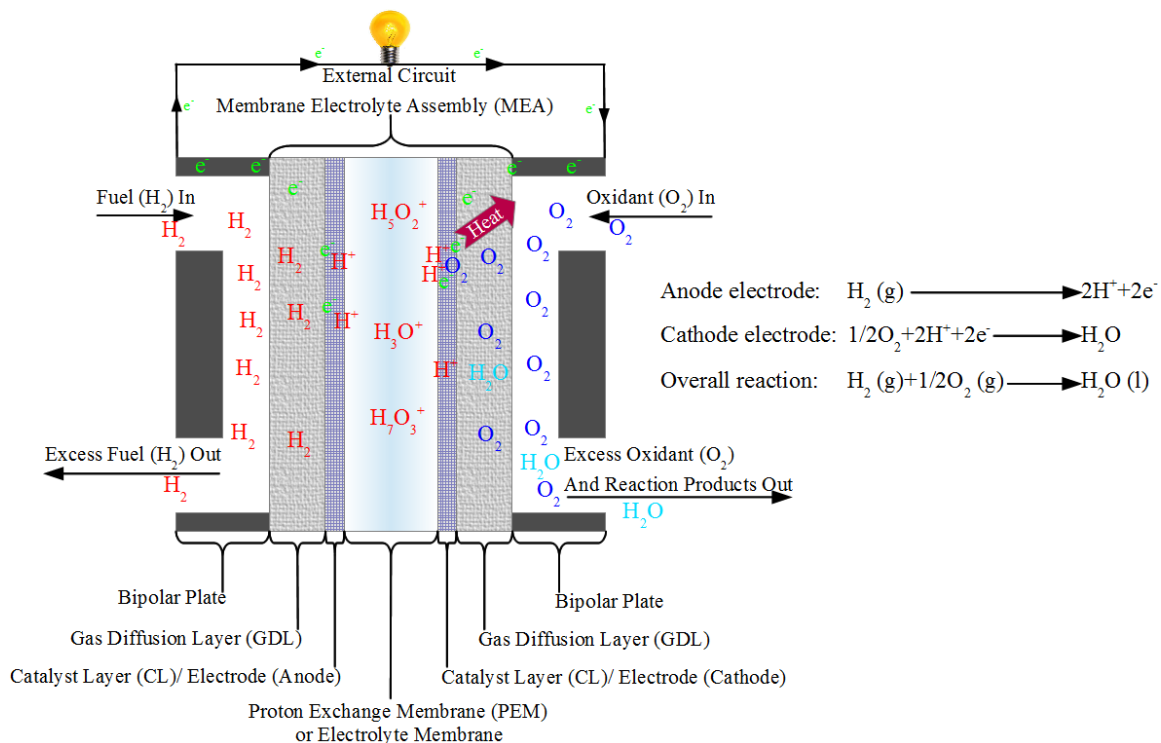


Figure 1-1: Schematic of fuel cell's components and reactions.

The performance of the PEM fuel cell degrades gradually due to deterioration of cell components [1]. In particular, degradation of the electrolyte membrane which may leads to many aspects of the damage such as gas crossover, local membrane breakdown or thinning, lowering of catalyst utilization in MEA. Consequently, the chemical and mechanical stability and durability of the electrolyte membrane are crucial to fuel cell performance, efficiency and life time [1].

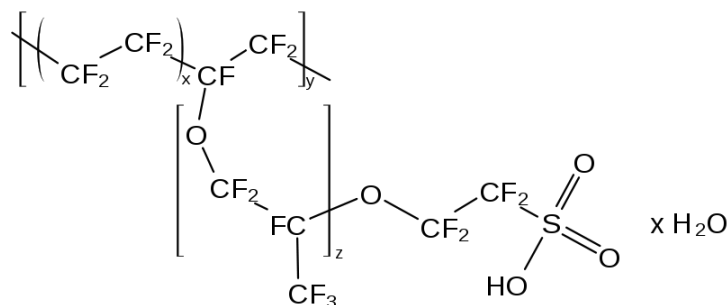


Figure 1-2: Nafion structure (<http://en.wikipedia.org/wiki/File:Nafion2.svg>).

H_2O_2 is one of the chemicals that is believed to play a leading role in chemical degradation of the polymer membrane in PEM fuel cells [3, 4, 5, 6]. Both the thermodynamic and the kinetic factors necessary for formation of H_2O_2 exist in the PEM fuel cell environment [7]. H_2O_2 presence in PEM fuel cells has been detected by analysis of the effluent water condensate from the anode and cathode during fuel cell operation [8]. In that work, the H_2O_2 flux was less than $0.02 \mu\text{mol h}^{-1} \text{cm}^{-2}$. However, this flow may not represent the total amount of H_2O_2 formed in the cell [8].

Two pathways have been proposed for the formation of H_2O_2 in PEM fuel cells. First, H_2O_2 is formed at the cathode side through the oxygen reduction, reaction (1-1). Next, H_2O_2 is formed at the anode side through reactions (1-2) and (1-3) [9]. The necessary oxygen molecules for reaction (1-3) to take place are provided at the anode side through oxygen crossover from the cathode to the anode or air bleed on the anode side.



The effect of H_2O_2 on membrane degradation has been investigated by introducing Nafion membranes into H_2O_2 solutions at 80°C [4, 9]. After H_2O_2 processing of Nafion, fluoride and sulfate ions (F^- and SO_4^{2-}) are detected in the solution which are derived from the C-F bonds and the sulfonic acid groups, respectively. Kinumoto et al. [4] observed that the loss of sulfonic acid groups leads to decrease in the proton conductivity, and the decomposition of the C-F bonds causes formation of holes in Nafion membrane and membrane thinning. The proton conductivity, water uptake and water self-diffusion coefficient in membrane gradually decrease with H_2O_2 processing [9]. Moreover, Nafion is used in the catalyst layer to enhance ionic conductivity. Therefore, decomposition of Nafion inside the catalyst layer also reduces the effective reaction area and raises the overpotential of the cell [4].

Another cause of membrane degradation is the formation of hydroxyl ($\text{OH}\cdot$) and hydroperoxyl ($\text{OOH}\cdot$) radicals from H_2O_2 decomposition in the presence of transition metal ions (M^{n+}) [6, 10]. These reactions are represented by

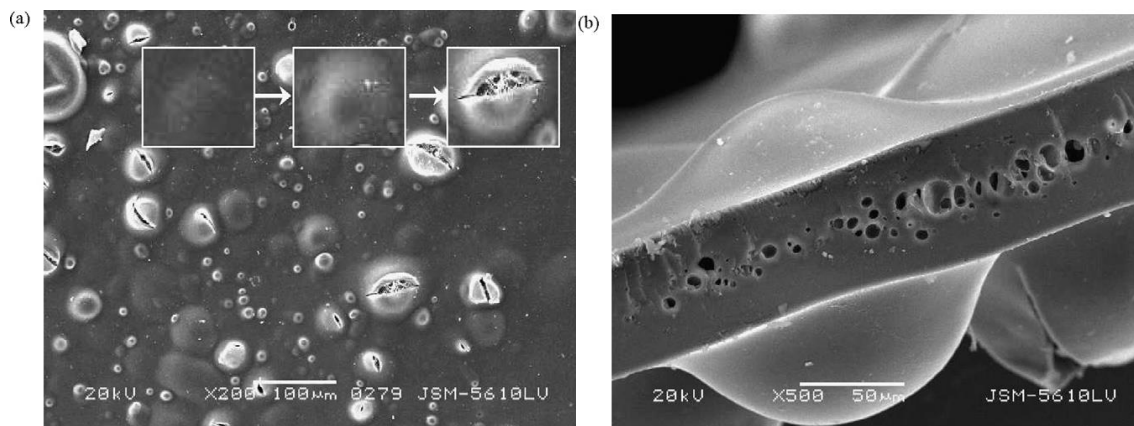


Figure 1-3: (a) Surface and (b) cross-section SEM micrographs of the Nafion membranes treating in H_2O_2 /metal ions containing solution for 48 h (taken from [6], Reproduced with permission from Elsevier).

Nafion decomposition was investigated in solutions containing $\text{H}_2\text{O}_2/\text{M}^{n+}$ (M: Fe, Cr and Ni) by Tang et al. [6]. FTIR and NMR analyses indicate that decomposition of Nafion starts from the ends of the main chain, resulting in the loss of the repeat units. This causes formation of holes in the membrane and leads to the membrane hazard of gas crossover, Figure 1-3.

In the following section, detection techniques for H_2O_2 are reviewed in the context of *in situ* sensing in PEM fuel cells.

1.3. Detection of H_2O_2

Conventional techniques to detect H_2O_2 comprise titrimetric, colorimetric, and gasometric methods. The titrimetric method is based on a redox reaction in which a solution of a substance with unknown concentration is treated with a titrant reagent of known concentration. The latter solution is added to the former until an expected change

happens (e.g. color of the auxiliary detector agent, potential of the reaction, etc). At this point, the volume of the titrant is used to determine the concentration of the substance with unknown concentration using the stoichiometry of the reaction. For example, the potentiometric titration of H_2O_2 is performed by known concentration of a KMnO_4 solution. In colorimetric technique, the concentration of a substance in a solution is determined by evaluating the change of color intensity of the solution as a result of treating with a colorimetric reagent. This color change is due to production of a colored compound through the reaction [11]. For instance, treating an H_2O_2 solution with titanium sulfate reagent leads to perititanic acid production with yellow color [12]. Gasometric technique is performed by measurement of a derivative gas from a reaction between H_2O_2 and a reagent such as NaBrO [13].

These techniques require complex equipment and time consuming sample preparation; they are sensitive to interference from other chemical species; and their limits of detection limit the use of these techniques [14]. Therefore, they are not suitable for *in situ* detection of H_2O_2 in PEM fuel cells.

Electrochemical and spectroscopic techniques on the other hand are able to determine small concentrations of H_2O_2 [14, 15, 16, 17, 18, 19] which might be suitable for *in situ* detection of H_2O_2 in PEM fuel cells. These two techniques are briefly discussed in Sections 1.3.1 and 1.3.2.

1.3.1. Electrochemical Techniques

Electrochemical techniques engage an electrochemical cell consisting of at least two electrodes and measuring the current and the potential. Depending on whether the current is passed through the cell and how the current or the potential is controlled. Electrochemical techniques are divided into potentiometry, coulometry, and voltammetry.

Potentiometry measures the potential of a solution between an indicator electrode and a reference electrode while there is no current passing through the cell. The measured potential is then related to the concentration of analytes.

Coulometry measures the charge versus time while a current or a potential is applied to the cell. This method is based on the complete conversion of an analyte from one oxidation state to another. The number of charges transferred in the course of a redox reaction in the cell is determined in accordance with Faraday's laws. Thus, the concentration of analytes can be determined by knowing the number of electrons involved in the electrochemical reaction.

Voltammetry measures the current of the cell as a function of potential while a fixed or variable potential is applied to the electrode surface. Hydrodynamic and cyclic voltammetries, amperometry, and polarography are examples of voltammetry methods with different functions of the applied potential to the cell.

In spite of this wide variety of electrochemical techniques, these methods are not promising for *in situ* measurement of H_2O_2 inside PEM fuel cells since they require complex instrumentation. Further, the current inside PEM fuel cells may interfere with the current from the electrochemical cell that needs to be measured in case of coulometry and voltammetry methods. Potentiometry, in particular, needs to be done in a current free environment which is not the case in an operating PEM fuel cell.

However, the only report so far on *in situ* detection of H_2O_2 is based on the electrochemical method [7]. An electrochemical technique using Pt wires as working electrodes was used to detect H_2O_2 in a PEM fuel cell. This sensor detected H_2O_2 inside the PEM fuel cell but was not able to quantify the amount of H_2O_2 produced in the cell. Also, the existence of an electrical field in a PEM fuel cell can interfere with the function of amperometric sensors, which detect current signal in nanoampere to picoampere range [20]. As mentioned earlier, this limits the application of electrochemical sensors for monitoring trace of H_2O_2 in PEM fuel cells.

1.3.2. Spectroscopic Techniques Using Optical Fibers

Recently, fiber-optic sensors have been used for *in situ* sensing of temperature and relative humidity in PEM fuel cells [21, 22]. Optical fibers are attractive for this application for several reasons. The small size of optical fibers allows for high spatial resolution and easy integration of the sensing probe into the fuel cells. The optical signal

does not interfere with electrochemical processes in the fuel cell and is not affected by the electromagnetic noise. The fiber material is compatible with the harsh environment inside the fuel cell while conductor wires of electrical sensors may suffer corrosion due to the temperature, humidity, and electrochemically active atmosphere in PEM fuel cells [23].

Fiber-optic sensors and sensing mechanism for detecting H_2O_2 including absorption [16, 17, 24, 25, 26, 27, 28, 29], fluorescence [30, 31], and chemiluminescence [32, 33] techniques are briefly explained in below.

Fiber-optic sensors: Fiber-optic sensors engage spectroscopic techniques for converting the analyte concentration to optical signal. These devices are generally composed of a light source, a light detector, and an optrode, Figure 1-4 [34]. An optrode consists of a source fiber and a receiver fiber which is connected to a sensing fiber and, in some cases, sensing material which is coated onto the tip of the sensing fiber. Moreover, computer software might be required for interpreting the optical signals collected by the light detector.

Figure 1-4 illustrates one of the configurations of an extrinsic fiber-optic sensor using a bifurcated optical fiber, which is ultimately used in this research. The light generated by a light source is carried along the source fiber and through the sensing fiber, reaching the sensing material on the distal end of the optrode. The light is influenced indirectly by the analyte and part of the scattered light from the sensing material is collected by the optical fiber and guided back through the receiver fiber into a light detector. In an extrinsic fiber-optic sensor, an interaction happens between the analyte and the sensing material, influencing the characteristics of the sensing material such as its refractive index, reflection, absorption, or scattering properties. Therefore, the sensing material is used for sensing purpose and the optical fiber is used for transmitting the light to and from the sensing region.

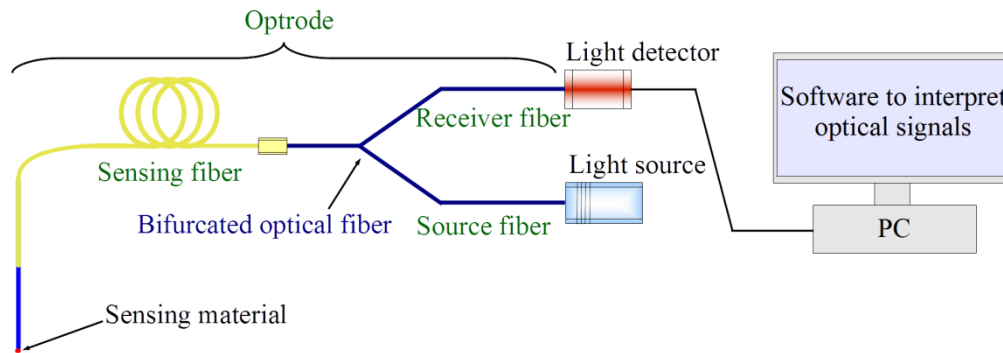


Figure 1-4: Configuration of a fiber-optic sensor.

There are also intrinsic fiber-optic sensors in which the optical fiber is used not only for guiding the light, but also for sensing purpose. The sensing of measureand by optical fibers occurs when the optical fiber structure is influenced by the measureand. This causes some changes in parameters like intensity, wavelength, phase, or polarization of the output light. The fiber-Bragg-grating sensor used for temperature measurements in PEM fuel cells is an example of a wavelength-modulated intrinsic fiber-optic sensor [21].

Absorption: Absorption-based fiber-optic sensors involve the absorption of light by the analyte, or by a sensing material whose absorption is influenced by the analyte. Therefore, the changes in the concentration of the analyte correlate to absorption-based optical signals. In these sensors, white light passes through an optical fiber to the sensing material and the amount of the light absorbed by the sensing material is determined by measuring the light reflected back. The sensing scheme explained in previous section and illustrated in Figure 1-4 is an example of an absorption-based fiber-optic sensor.

Fluorescence: In general, luminescence is emission of light by a substance as a result of stimuli except heat. Fluorescence is a form of luminescence that is initiated by photoexcitation. When a fluorescent molecule (fluorophore) absorbs light at certain wavelength (excitation), the emission of light happens after a period of time (lifetime) and at longer wavelength (fluorescence), Figure 1-5. The lifetime is defined as the average amount of time that fluorophore stays in the excited state between the photon absorption and the fluorescence emission. The wavelengths at which the excitation and emission occur are unique fingerprints of each fluorophore. Therefore, measuring the

fluorescent intensity or fluorescent lifetime allows us not only to determine the presence of the analyte, but also to correlate the fluorescent intensity to the concentration of the analyte.

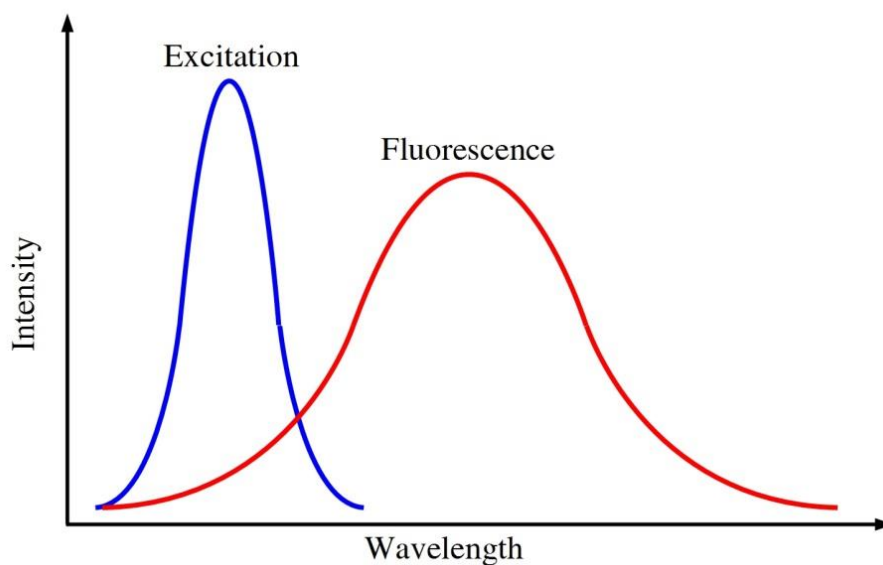
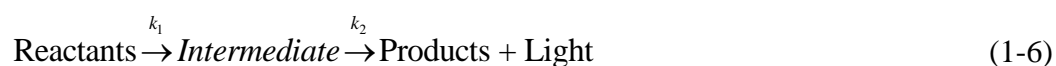


Figure 1-5: An illustration of excitation and fluorescence.

Chemiluminescence: Chemiluminescence is another form of luminescence that is initiated by a chemical reaction. Since no light is required for excitation of molecules, no light source is needed for the sensor application. There is usually an intermediate state involved in a chemiluminescence, reaction (1-6), in which the step from the reactants to the intermediate state is called exciting step and the step from the intermediate state to the final products is called emission step.



A chemiluminescence-based H_2O_2 sensor involves oxidation of a chemical compound and requires the presence of a catalyst. For example, oxidation of luminol ($\text{C}_8\text{H}_7\text{N}_3\text{O}_2$) by H_2O_2 in the presence of hemin ($\text{C}_{34}\text{H}_{32}\text{ClFeN}_4\text{O}_4$) results in chemiluminescence. The reaction of luminol and H_2O_2 initially forms an excited state of 3-aminophthalate (intermediate). This excited state then decays to a lower energy level producing 3-aminophthalate and light [35].

Among the three aforementioned techniques, absorption-based techniques are one of the simplest detection systems for sensing H_2O_2 and these methods do not require expensive and complex instrumentation. Conversely, fluorescence-based techniques require complex instrumentation including specialized light sources and detectors. The performance of the chemiluminescence-based sensor, on the other hand, is highly dependent on pH of the sensing environment with the maximum intensity of emitted light in the pH value ranging from 8.5 to 9, and a very low response in acidic environments. Therefore, the chemiluminescence-based technique is mostly suitable for developing biosensors; and it does not seem suitable for application in PEM fuel cells with an operating pH of 2.

Therefore, the absorption-based technique is chosen in this research for developing H_2O_2 sensor suitable to be used in PEM fuel cells. This leads to the next step which is choosing a sensing material for developing the H_2O_2 optrode.

1.4. Prussian Blue

Prussian blue (PB) is one of the sensing materials which has been successfully demonstrated as an indicator of H_2O_2 in both electrochemical and spectroscopic manners [36, 37]. PB is briefly described in Appendix B. The sensing mechanism of H_2O_2 by PB through the absorption-based technique and the PB films preparation technique which is used in this research are briefly described in Sections 1.4.1 and 1.4.2.

1.4.1. H_2O_2 Detection mechanism by Prussian Blue

The detection mechanism of the proposed optrode relies on the redox reactions of PB/PW compound, and the evaluation of corresponding changes of the optical properties of the compound, Figure 1-6. PB is reduced to PW in the presence of a reducing agent, such as ascorbic acid. The reverse reaction happens when PW is exposed to an oxidizing agent, such as H_2O_2 , resulting in PB. PB has a strong intervalence charge transfer absorption band near 700 nm because transition from $\text{Fe}^{\text{III}}\text{Fe}^{\text{II}}$ to $\text{Fe}^{\text{II}}\text{Fe}^{\text{III}}$ states absorbs red photons, and reflects blue light. On the other hand, transparent PW does not have any distinct bands in the visible range of its absorption spectrum [38]. As a result, the increasing absorbance in the visible range while PW is oxidizing to PB by H_2O_2 is used

to detect the presence of this oxidant. Moreover, the initial PW state is recovered by exposing PB to ascorbic acid. Figure 1-7 illustrates the detection mechanism of H_2O_2 using optrodes based on chemically deposited PB/PW system onto the tip of an optical fiber.

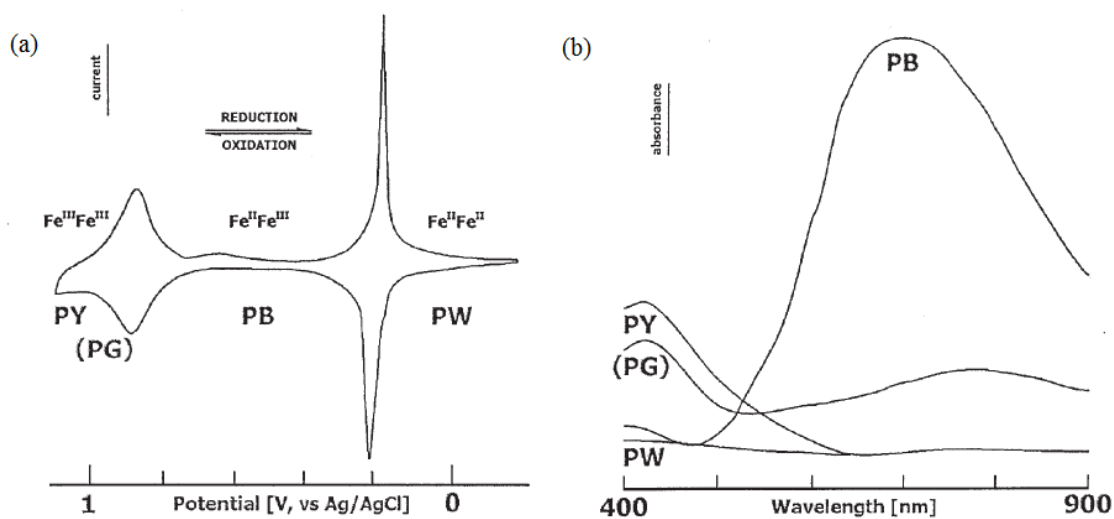


Figure 1-6: (a) Electrochemical and (b) spectroscopic characteristics of PB (taken from [38], Reproduced with permission from Taylor & Francis).

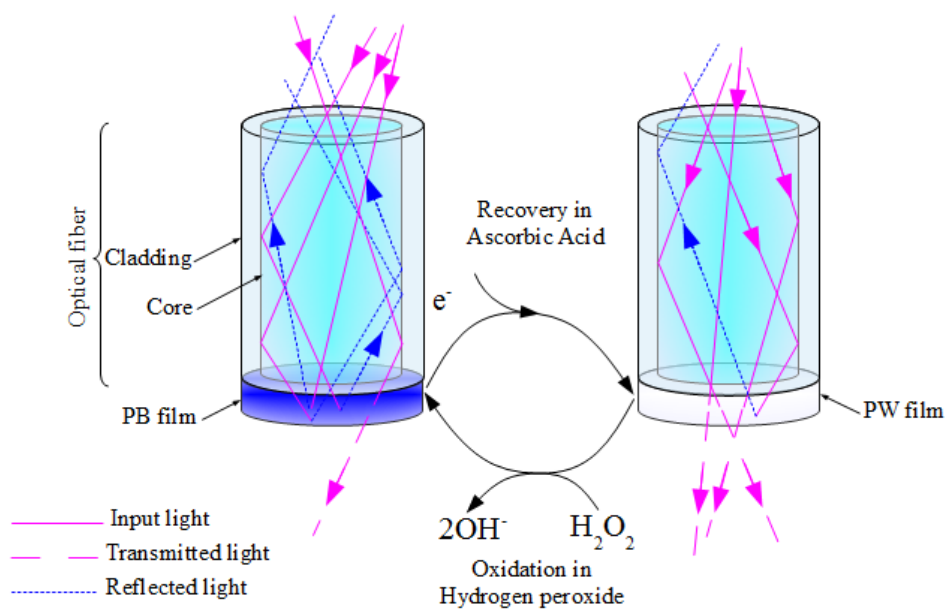


Figure 1-7: Detection mechanism of H_2O_2 using an optrode based on PB/PW system.

1.4.2. Preparation of Prussian Blue Films

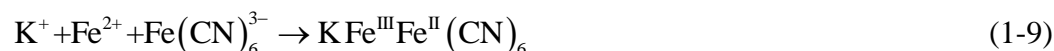
Generally, PB can be synthesized by electrochemical [39, 40, 41, 42, 43] or chemical [44, 45, 46, 47, 48, 49] paths. In the former case, the substrate should be electrically conductive. Considering that optical fibers are made of non-conductive materials, the chemical synthesis of PB is a more suitable approach. Several chemical methods such as sol-gel [50, 51], sonochemical [46], photochemical [52], hydrothermal [47], and layer-by-layer (LbL) electrostatic self-assembly (ESA) [48] are used to synthesize or immobilize PB nanoparticles and thin films onto non-conductive substrates.

In the chemical paths PB films are normally synthesized using a solution containing two components: iron (II) salt and hexacyanoferrate (III), or iron (III) salt and hexacyanoferrate (II) [53]. Using these precursors, PB forms directly in the presence of both iron valences.

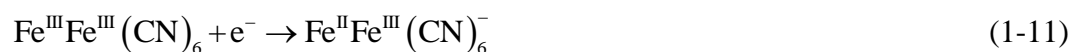
Among the aforementioned techniques, Single-source precursor (SSP) is the most straightforward chemical technique that is used in this research to prepare PB films. SSP is a synthesis approach in which all the elements that are required in the final product are incorporated into one compound. In SSP technique, the precursor may participate in several consecutive reactions to afford the final product. Potassium hexacyanoferrate (III) (or potassium ferricyanide) was used as a single-source precursor containing just one of the iron valences, (i.e. iron (III)) whereas both iron valences are required for formation of PB. Therefore, redox reactions are required to occur in the course of PB formation to provide both iron valences.

There are two possible mechanisms for chemical formation of PB from a single source hexacyanoferrate (III). First, partial decomposition of hexacyanoferrate (III) occurs in a high acidity environment of reacting mixture (1-7) [36]. Free iron (III) cations from the associated complex are reduced to iron (II) cations (1-8). The iron (II) cations then react with undissociated hexacyanoferrate (III) anions to form soluble PB (1-9) [54]. Since the reduction of iron (III) to iron (II) is unfavorable thermodynamically, the driving force would be provided by the reaction of iron (II) cations and hexacyanoferrate (III)

anions [54]. The standard free energy change for the combined reactions is -177 kJ mol^{-1} [54].



In the second case, the iron (III) cations produced in (1-7) and hexacyanoferrate (III) anions present in the solution can form a highly reactive complex of ferric ferricyanide or Berlin green (BG) (1-10) [36]. This mixture has an oxidation potential higher than that of each component, and it even causes oxidation of water [55]. For BG to become PB, the presence of a reducing agent is necessary. It is reported that BG can oxidize water (solvent), solution impurities, and liberate cyanides through reaction (1-11) [39, 40, 54, 36]. However, liberated cyanides can play the role of main reducing agent – more than water and the impurities– for the process of PB formation [36]. The reduced BG reacts with free iron (III) cations in the solution and forms insoluble PB (1-12) [36].



Itaya et al. reported the chemical synthesis of PB using hexacyanoferrate (III) and iron (III) chloride [39]. They studied the ratio of the total charges consumed in the reduction of prepared PB and its oxidized form. Based on this ratio, they demonstrated that the PB is insoluble [39], in agreement with the second interpretation.

1.5. Objectives

The overall objective of this research is to develop an H_2O_2 optrode that is able to detect and measure H_2O_2 concentrations at operating temperature and pH corresponding

to an operating PEM fuel cell (i.e. 80 °C and pH 2). This overall objective is broken to several steps as follows:

- (1) To develop optrodes by depositing PB¹ films onto the tip of the optical fibers, Chapter 3.
- (2) To demonstrate the capability of the sensor to detect and measure H₂O₂ concentrations at room temperature and pH 4², Chapter 3.
- (3) To assess the functionality of the sensor to detect and measure H₂O₂ concentrations at different pH values including pH 2 (i.e. pH of PEM fuel cells), Chapter 4.
- (4) To find the deposition conditions that result in a stable PB film at the high temperature and the low pH of the PEM fuel cell's environment (i.e. temperature range of 60 to 80 °C and pH 2), Chapter 5.

1.6. Structure of Dissertation

This dissertation comprises the current introductory chapter that serves to provide context and framework that links the following chapters in terms of the research motivation, background information, and objectives. A summary of key contributions of this research is presented in Chapter 2. Chapters 3, 4 and 5 present these contributions in the manuscript format. Each of these manuscripts is a proof-of-concept study on the development of an optrode which responds to H₂O₂ concentrations in solutions at similar temperature and pH to an operating PEM fuel cell. The relevant background, experimental, and detailed aspects of the research are presented in Chapters 3 to 5, and each chapter terminates with a conclusion. Finally the sixth chapter list all the conclusions and possible future considerations for this work.

Chapter 3 presents the peer-reviewed published article [56] and describes the sensor fabrication process and demonstrates the sensor response to H₂O₂ concentrations at room temperature and pH 4. PB film is deposited onto the tip of an optical fiber through the SSP method. SSP is a synthesis approach in which all the elements that are required in

¹ The PB serves as an indicator of H₂O₂ in a spectroscopic manner.

² pH 4 is chosen because the most reliable response of PB to H₂O₂ concentrations is reported at this pH [59].

the final product are incorporated into one compound. The effect of light exposure, during the deposition of PB films, on the purity of PB compound is investigated. The sensor response to H_2O_2 concentrations is evaluated and the reliability of the sensor response is examined by performing multiple sensing tests with several different sensors. This proof-of-concept leads to the next step which is investigating the functionality of the sensor at different pH values with a focus on operating pH of PEM fuel cells.

Chapter 4 presents the peer-reviewed published article [57] and demonstrates the sensor response to H_2O_2 concentrations at room temperature and different pH values (i.e. pH 2 to 7). In spite of the effect of pH of the sensing test solution on sensor response, the sensor is found to be functional for detecting and measuring H_2O_2 concentrations at different pH values. More sensing tests are performed at pH 2 to evaluate the behavior of the sensor in terms of the repeatability, reproducibility and durability of the sensor response at this specific pH. The final stage of the research is to make sure that the sensor remains functional at temperatures between 60 °C to 80 °C (PEM fuel cell's operating temperature).

Chapter 5 presents the peer-reviewed published article [58] and explains a methodology for assessing stability of PB films in solutions with pH 2 and at elevated temperatures. PB films are deposited on glass slides through different chemical techniques. Then PB films are soaked in Phosphate-Buffer-Solutions (PBS) with pH 2 and at elevated temperatures for a day. These PB films are characterized using Fourier transform infrared spectroscopy (FTIR) to analyze their stability following PBS processing. Extra samples are prepared at different temperatures through the deposition technique that leads to the most stable PB films. The same PBS processing is performed on these samples following with FTIR analysis to find the temperature in which the most stable PB films are prepared.

Conclusions from all contributions are summarized in Chapter 6 and suggestions for possible future works are made in Chapter 6 as well.

Chapter 2

Summary of Key Results

This chapter provides a summary of key results from the three studies presented in this dissertation. These studies, which are presented in Chapters 3 to 5, have been published in peer-reviewed journals. The first study describes the process of sensor development and analyzes the sensor response to H₂O₂ concentrations in aqueous solutions at room temperature and pH 4. This work is extended in the second study which evaluates the sensor behavior in environments with pH values ranging from 2 to 7. The third study presents a systematic assessment of the stability of PB films, prepared under different conditions, at elevated temperatures and in acidic environments (i.e. 80-90 °C and pH 2).

2.1. Spectroscopic Detection of Hydrogen Peroxide with an Optical Fiber Probe using Chemically Deposited Prussian Blue

The objectives of this study are: (1) to develop an H₂O₂ sensor that is immune to electromagnetic interference and; (2) to study the response of the prepared sensor to H₂O₂ concentrations in aqueous solutions at room temperature and pH 4. A spectroscopic technique using optical fibers is chosen for H₂O₂ detection in this study because the special features of an optrode make it a suitable candidate for integration into an operating PEM fuel cell. The special features of optrodes include; immunity to electromagnetic interference, small size, flexibility, and compatibility of the fiber material (i.e. silica glass) with electrochemically active environment of a PEM fuel cell.

The process of the sensor development includes deposition of PB films onto the distal end of the fiber. Since the fiber material is not conductive, only chemical techniques can be considered for PB deposition on the tip of the fiber, unless the fiber surface is modified with a conductive material. Therefore, PB films are deposited chemically in aqueous solutions using potassium ferricyanide as a single-source precursor. Although PB films are deposited successfully onto the distal end of optical fibers, analysis of PB films prepared through the same deposition technique but different conditions of lighting reveals the effect of light on purity of PB compound. The light exposure leads to formation of pure PB film, whereas deposition in darkness leads to co-precipitation of PB and BG.

The prepared PB-based optrodes are used to detect H_2O_2 concentrations in buffered solutions at room temperature of pH 4. This pH value was chosen because the previous PB-based optrodes have demonstrated reliable response to H_2O_2 concentrations at this pH value [59, 17]. The sensing test is performed by exposing the optrode to solutions with different concentrations of H_2O_2 and collecting the reflected light, from the distal end of the optical fiber, using a spectrometer. Different response times are obtained at different concentrations of H_2O_2 . These response times are found to vary linearly with H_2O_2 concentrations, on a log-log scale. This allows us not only to detect the presence of H_2O_2 , but also to measure its concentration.

Additional sensing tests are performed with multiple optrodes to investigate sensor characteristics in terms of the repeatability, reproducibility and durability. Performing multiple sensing tests with the optrode shows that sensor response is repeatable with an adjusted-r-squared value of 0.91.

The optrode preparation through the SSP technique is tested for reproducibility by preparing multiple optrodes at different times and then performing the same sensing test with each optrode. This experiment demonstrates that the response times of optrodes vary linearly with the change of H_2O_2 concentrations with a similar slope on a log-log scale.

In the final stage of this study, the durability of sensor response is investigated by performing several sensing tests with an optrode four and seven months after optrode

preparation. Comparing those results reveals that the sensor behavior remains linear although the slope of linear response is slightly changed. This change in the slope necessitates periodic recalibration of the sensor.

The key findings of this study are as follows. (1) The SSP is a reproducible technique for preparing PB-based optrodes. (2) The lighting conditions during PB synthesis affect the purity of PB films. (3) The sensor detects concentrations of H_2O_2 , (i.e. 2 μM – 400 μM of H_2O_2) in aqueous solutions at room temperature and pH 4. (4) The sensor responds to H_2O_2 concentrations seven months after its fabrication; however, periodic recalibration is necessary because of the change in the slope of the sensor response.

This study is published in *Electrochimica Acta* [56] and is presented in Chapter 3.

2.2. pH-dependent Response of a Hydrogen Peroxide Sensing Probe

The objectives of this study are: (1) to investigate the functionality of the sensor at different pH values ranging from 2 to 7; (2) to evaluate the sensor response and performance at pH 2 (i.e. PEM fuel cells operating pH). Investigating the sensor behavior at different pH values is a crucial step to assess the functionality of the sensor in environments with a pH fluctuation. This step also determines the possibility of using this sensor in other environments with different pH values than that of an operating PEM fuel cell. Evaluating the sensor performance at PEM fuel cell operating pH is also another critical step to assess the suitability of this sensor for being used as an *in situ* sensor inside a PEM fuel cell.

In this study, an optrode is first exposed to buffered solutions with different pH values, ranging from 2 to 7, and a constant concentration of H_2O_2 . Both the intensity and time response of the sensor change in solutions with a constant concentration of H_2O_2 and different pH values. Therefore, the pH of the sensing environment affects the sensor behavior. This indicates the optrode requires recalibration prior to be used in each pH value.

In the next step of this study, the sensor response to H_2O_2 concentrations and the sensor characteristics are investigated at pH 2 (i.e. PEM fuel cell operating pH). An optrode is exposed to solutions with different concentrations of H_2O_2 . The response times of the sensor is plotted versus H_2O_2 concentration on a log-log scale which shows the sensor behavior at pH 2 is also linear with a different slope than that of at pH 4. Repeating the same sensing experiment with the same optrode showed the sensor response to H_2O_2 concentrations is reproducible at pH 2. Therefore, the sensor can be used for *in situ* sensing of H_2O_2 inside a PEM fuel cell.

In the final step of this study, the optrode is exposed to solutions at different pH values with different concentrations of H_2O_2 in each pH value. The sensor behavior is consistent at different pH values, which allows us to detect and measure H_2O_2 concentrations at different pH values. However, the slope of the response time versus H_2O_2 concentration plots varies with pH. This indicates that the sensitivity of the sensor is different at different pH values with the higher sensitivity at lower pH values.

The key findings of this study are as follows. (1) The proposed optrode is functional in solutions with pH values ranging from 2 to 7. (2) The pH of the sensing environment affects the sensor behavior; making the sensor recalibration necessary before using the optrode in each pH value. (3) The sensor detects H_2O_2 concentrations at pH 2; validating the application of the sensor inside an operating PEM fuel cell, provided that the sensor withstands the high temperatures inside PEM fuel cells. (4) The sensitivity of the sensor is higher at lower pH values.

This study is published in *Sensors and Actuators B: Chemical* [57] and is presented in Chapter 4.

2.3. Effect of Deposition Conditions on Stability of PB Films at PEMFC's Operating Temperatures and pH

The objective of this study is to find the deposition conditions which result in a PB film that is stable at the PEM fuel cell operating temperature and pH. This study is motivated by previous studies that have shown that PB films tested in solutions at elevated temperatures are prone to leaching [60].

Three different deposition methods are used to prepare PB films: sol-gel dip coating, direct chemical process (i.e. using both iron valences as precursors), and SSP. All samples are prepared in reaction mixtures at temperature of 60 °C. The prepared PB films are left in PBS with pH 2 and at elevated temperatures for a day³. FTIR analyses are performed with all PB films before and after PBS processing. The results show the film prepared through the SSP method has the highest stability after PBS processing.

Additional samples are prepared through the SSP method and at different deposition temperatures (i.e. 40 °C, 60 °C, and 80 °C) to find the temperature that leads to the most stable PB film. PBS processing of the samples is performed and followed by the FTIR analysis. The FTIR analysis reveals that the film prepared at 40 °C is completely leached into the PBS, while the films prepared at 60 °C and 80 °C are sufficiently robust to sustain the PBS processing. Therefore, the deposition temperature of over 60 °C is chosen for optrode preparation for *in situ* sensing tests.

The key findings of this study are as follows. (1) The PB film prepared through the SSP technique is more stable than the PB films prepared through the sol-gel dip coating and direct chemical process. (2) The optrode that is prepared by deposition of PB film through the SSP method and at deposition temperatures over 60 °C remains stable at PEM fuel cell operating temperatures and pH.

This study is published in Journal of The Electrochemical Society [58] and is presented in Chapter 5.

³ The temperature and time period for PBS processing are overestimated based on the condition through which *in situ* sensing tests may be performed inside PEM fuel cells.

Chapter 3

Spectroscopic Detection of Hydrogen Peroxide with an Optical Fiber Probe using Chemically Deposited Prussian Blue

(*Electrochimica Acta*, volume **115**, 2014, 416–424)

Reproduced with permission from Elsevier

Preamble

The primary objectives of this research are to develop a fiber-optic sensor, and to demonstrate the sensor capability to detect and measure H₂O₂ concentrations in solutions at room temperature and with a constant pH value. These are two major contributions that validate the proof-of-concept in this research. In the first part, the process of sensor development is described with a focus on the deposition process of PB films onto the tip of optical fibers. The second part presents an investigation of the sensor behavior and the sensor characteristics in terms of the stability and reliability of sensor response.

The Body of this chapter was published in *Electrochimica Acta*.

Abstract

A novel fiber-optic hydrogen peroxide sensing probe was fabricated using chemically deposited ferric ferrocyanide, often referred to as Prussian blue (PB). The probe features a fast linear response and durability, due to the robustness and purity of the PB film. Potassium ferricyanide was used as a single source precursor in a straightforward chemical deposition of nanostructured PB onto the tip of a multimode optical fiber. Spectroscopic detection of hydrogen peroxide (H₂O₂) was performed based

on the reduction of PB to Prussian white (PW) by agents like ascorbic acid, and oxidation of PW to PB by H_2O_2 . Measurement of H_2O_2 concentration is based on the changes of the absorption spectrum, under visible light, of PB and PW. The fiber-optic probes exhibit a linear response to concentration on a log-log scale and are found suitable for determining small concentrations of H_2O_2 . Multiple tests were performed to investigate the repeatability and durability of a sensor response and though requiring recalibration, the probes were found to remain functional for an extended period of time.

Keywords: Chemical deposition, Hydrogen peroxide, Optical fiber sensor, Prussian blue, Single source precursor, Spectroscopic detection.

3.1. Introduction

H_2O_2 is commonly used in many industrial and medical processes such as water treatment plants and disinfection [61, 62]. It is also a by-product of oxidative metabolisms [63]. Detection and determination of small concentrations of hydrogen peroxide remains a major challenge in many fields where it plays a main role in a variety of damage mechanisms. For example, H_2O_2 induces cellular damage in human cells [64, 65] and its presence can be used to diagnose illnesses such as asthma [66]. It is also believed to be responsible for chemical degradation of polymer membranes in PEM-Fuel cells [3, 4, 5, 6]. Conventional techniques to detect H_2O_2 comprise titrimetric, colorimetric, and gasometric methods which, in general, require complex equipment and time consuming sample preparation, or have poor selectivity and limits of detection [14]. Electrochemical and spectroscopic techniques on the other hand are able to determine small concentrations of H_2O_2 and have good selectivity [14, 15, 16, 17, 18, 19], with spectroscopic techniques being preferred for many biochemical and industrial applications because of their immunity to electromagnetic interference. Spectroscopic detection includes chemiluminescent [32, 33], fluorescent [30, 31], and absorptive [16, 17, 24, 25, 26, 27, 28, 29] techniques.

The absorptive technique chosen in the present work relies on a detector agent film deposited onto the tip of optical fiber. It affords a small size, flexible fiber-optic sensing probe that is immune to electromagnetic interference. The prepared sensing probe has

potential for developing *in-situ* sensors for PEM-Fuel cells, as well as portable biosensors.

PB was chosen as an H_2O_2 indicator for the proposed fiber-optic probe because of its sensitivity and selectivity toward H_2O_2 [16, 55]. PB is a ferric ferrocyanide with the basic face-centered-cubic crystalline structure consisting of iron ions linked by the cyanide groups with two chemical forms $\text{Fe}_4^{\text{III}}[\text{Fe}^{\text{II}}(\text{CN})_6]_3$ and $\text{KFe}^{\text{III}}\text{Fe}^{\text{II}}(\text{CN})_6$ [39, 40]. These two chemical forms are commonly known as “insoluble” and “soluble”, respectively [40]. Both insoluble and soluble forms of PB are highly insoluble ($K_{\text{sp}} = 10^{-40}$), the difference refers to the simplicity of potassium peptization [54]. Large metal cations and water molecules, as well as other small molecules like H_2O_2 , can be accommodated in the open structure of PB [54]. Chemical reduction and oxidation of PB leads to PW (potassium ferrous ferrocyanide) and Berlin green (BG) (ferric ferricyanide), with chemical formula $\text{K}_2\text{Fe}^{\text{II}}\text{Fe}^{\text{II}}(\text{CN})_6$, and $\text{Fe}^{\text{III}}\text{Fe}^{\text{III}}(\text{CN})_6$, respectively [39, 54].

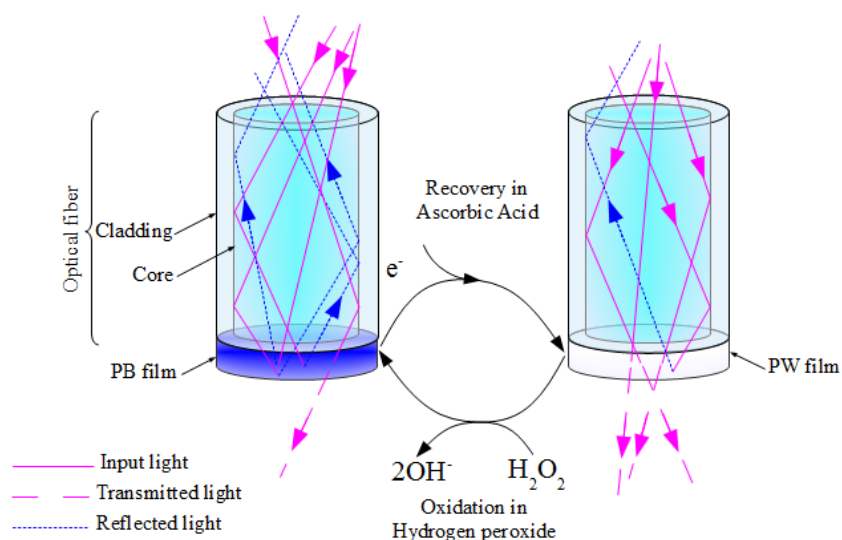


Figure 3-1: Detection mechanism of H_2O_2 using fiber-optic sensing probe based on PB/PW system.

The H_2O_2 detection mechanism in the absorptive technique based on PB relies on the redox reactions of PB/PW system, and the evaluation of corresponding changes of the optical properties of the compound. PB will be reduced to PW in the presence of a reducing agent, such as ascorbic acid. The reverse reaction happens when PW is exposed to an oxidizing agent, such as H_2O_2 , resulting in PB. PB has a strong intervalence charge

transfer absorption band near 700 nm because transition from $\text{Fe}^{\text{III}}\text{Fe}^{\text{II}}$ to $\text{Fe}^{\text{II}}\text{Fe}^{\text{III}}$ states absorbs red photons, and reflects blue light. On the other hand, transparent PW does not have any distinct bands in the visible range of its absorption spectrum [38]. As a result, the increasing absorbance in the visible range while PW is oxidizing to PB by H_2O_2 can be used to detect the presence of this oxidant. Moreover, the initial PW state can be recovered by exposing PB to ascorbic acid. Figure 3-1 illustrates the detection mechanism of H_2O_2 using fiber-optic sensing probe based on chemically deposited PB/PW system onto the tip of an optical fiber.

Generally, PB can be synthesized by electrochemical [39, 40, 41, 42, 43] or chemical [44, 45, 46, 47, 48, 49] paths. In the former case, the substrate should be electrically conductive. Considering that optical fibers are made of non-conductive materials, the chemical synthesis of PB would be a more suitable approach. Several chemical methods such as sol-gel [50, 51], sonochemical [46], photochemical [52], hydrothermal [47], and electrostatic self-assembly [48] have been used to synthesize or immobilize PB nanoparticles and thin films onto non-conductive substrates.

In the present work, a PB thin film was chemically deposited onto the tip of an optical fiber through the single-source precursor approach which, to the best of our knowledge, is the simplest method for synthesizing PB nanoparticles. This method allows the particle size, shape, and porosity to be adjusted by tuning the synthesis parameters such as solution pH, concentration of precursor, temperature and time of synthesis, and reaction environment light [46, 52]. After the synthesis of PB, the optical fiber probe was annealed and sensing measurements were performed at room temperature in H_2O_2 buffered solutions with pH 4. Repeatability, durability, and reproducibility of sensor responses were analyzed using multiple sensing probes.

3.2. Experimental

3.2.1. Materials

Potassium hexacyanoferrate (III) (product No. 13746-66-2) from Sigma-Aldrich was used as single-source precursor in an aqueous solution of Hydrochloric acid (HCl) (37%) for synthesizing PB onto the tip of an optical fiber. L-ascorbic acid from Aldrich,

(catalog No. 25,556-4), was used as the reducing agent for the PB to PW reaction. Glacial acetic acid, (product No. 00598-468) from Anachemia and Sodium acetate trihydrate, (product No. S-1850) from ACP Chemicals were used to prepare an acetate buffer solution (ABS) at pH 4.0 in which the H₂O₂ solutions and ascorbic acid were prepared. The reducing solution was prepared in ABS with 0.04 mol L⁻¹ of L-ascorbic acid. H₂O₂ (30 wt%) from ACP Chemicals was used to prepare the oxidizing solutions at different concentrations in ABS. Sodium hydroxide (NaOH) and Hydrochloric acid (HCl) at concentrations of 0.1 mol L⁻¹ were used to adjust the pH of the solutions to the desired values. All chemicals were used as received with no further purification. The water used in the experiments was purified with a four-cartridge purification system (Super- Q Plus, Millipore, Billerica, MA) and had a resistivity of 18.2 MΩ cm. The optical fiber was a multi-mode AFS50/125Y from Thorlabs (Newton, NJ), with core and cladding diameters of 50 μm and 125 μm, respectively.

3.2.2. Chemical Deposition of Prussian Blue

The PB film was deposited chemically using the distal end of an optical fiber as a substrate. The optical fiber was cleaved and cleansed with isopropanol. In a synthesis process, 0.25 mmol of K₃Fe(CN)₆ were added to 25mL of an aqueous solution of 0.1 mol L⁻¹ hydrochloric acid. The optical fiber was immersed in this prepared mix, and was kept at 40°C under continuous stirring at 300 rpm for 10 hours. The synthesis process was done under the fluorescent lamp light exposure. Finally, the optical fiber was left inside the solution to cool to room temperature. The prepared fiber-optic probe was removed from the solution and left at room temperature and relative humidity for one day, and then it was annealed at 100°C for 15 min.

In the present work, the sensing region with PB was located at the distal end of the optical fiber rather than along the fiber in order to facilitate the eventual integration of the probe into the membrane of a PEM fuel cell. With the distal end PB deposition, the probe operates based on the reflected light from the sensing region and only requires an inlet port into the membrane. In the other case, the operation of the probe would relies on the attenuation of the transmitted light through the optical fiber, similarly to the fiber sensor presented by Hu and Tao [20]; This requires both inlet and outlet ports, which would

impose additional design constraints to ensure proper alignment and sealing of the sensing probe within a fuel cell.

3.2.3. Characterization of the Prussian Blue

The effect of light exposure in synthesis process was characterized by Raman spectroscopy. Two samples were prepared on plain microscope slides in two conditions: (a) under fluorescent lamp light exposure, and (b) in darkness. The Raman spectra were recorded using Renishaw inVia microRaman system equipped with a He-Ne laser source with excitation at 785 nm and a laser power of 1mW. The light reflection from the distal end of optical fibers during synthesis in both conditions were recorded and analyzed.

3.2.4. Sensing Test Procedures and Instrumentation

The sensing behavior of the probe to solutions with concentrations of H_2O_2 ranging from $2 \mu\text{mol L}^{-1}$ to $400 \mu\text{mol L}^{-1}$ was evaluated in liquid phase. H_2O_2 solutions were prepared in ABS with a pH of 4.0 ± 0.1 . L-ascorbic acid in solution was used as a reducing agent in all tests. This solution was prepared at a concentration of 0.04 mol L^{-1} using ABS as solvent and adjusting its pH to 4.0 ± 0.1 . The pH measurements of all the prepared solutions were performed using a digital pH-meter (AR25 accumet[®], Fisher Scientific, Hampton, NH) using an (Ag|AgCl) electrode.

The sensing measurement method, as described in detail in [59], includes the following steps. The sensing probe is immersed in the ascorbic acid and H_2O_2 solutions alternately for the recovery and oxidation steps of the PB/PW system. Three sequences of concentrations of H_2O_2 solutions were used during the tests. In the first, H_2O_2 concentrations were chosen randomly in the range of $2 \mu\text{mol L}^{-1}$ to $400 \mu\text{mol L}^{-1}$. In the second, the concentration of H_2O_2 increased from $2 \mu\text{mol L}^{-1}$ to $200 \mu\text{mol L}^{-1}$ and then decreased back to $2 \mu\text{mol L}^{-1}$. In the final sequence, H_2O_2 concentrations decreased from $400 \mu\text{mol L}^{-1}$ to $5 \mu\text{mol L}^{-1}$ and increased back to $400 \mu\text{mol L}^{-1}$.

In each of the sequences, the sensing probe was initially immersed in an ascorbic acid solution to promote the reduction of PB to PW. When the intensity of reflected light from the sensing probe plateaued to a minimum level, it was considered to have reached the PW state. The optical fiber was then removed from the ascorbic acid and placed in the

H₂O₂ solution and kept there until the intensity plateaued to a maximum, indicating the oxidation from PW to PB.

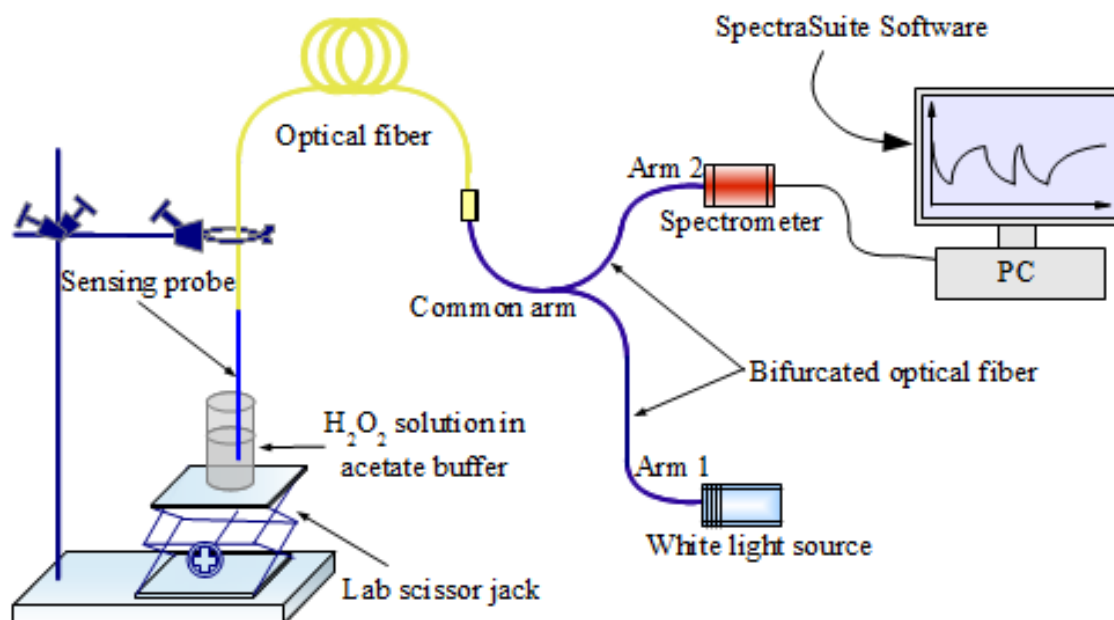


Figure 3-2: Experimental setup.

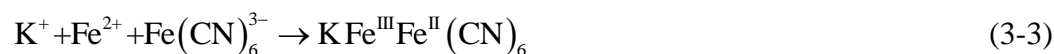
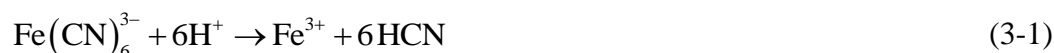
Figure 3-2 illustrates the experimental setup that was used for the measurements of the reflected light coming from the PB/PW system deposited on the distal end of the optical fiber. The light generated by a white light source (LS-1, OceanOptics, Dunedin, FL), is carried along the arm 1 of a bifurcated optical fiber (BIF200- UV-Vis, OceanOptics) and through the common arm of the bifurcated optical fiber, reaching the sensing film on the distal end of the fiber-optic probe connected to the common arm. Part of the scattered light from this sensing film of PB/PW is collected by the optical fiber and guided back through the common arm and arm 2 of the bifurcated optical fiber into an optical fiber spectrometer (USB2000, OceanOptics), which measured the intensity of the light in a wavelength range of 370 to 1048 nm. The reflected spectrum was sampled at a frequency rate of 1Hz using the software SpectraSuite (OceanOptics, Dunedin, FL). The integrated values of intensity over the full range of the spectrometer (i.e. 370 to 1048 nm) were evaluated to study the response of the PB/PW system during both the oxidizing and the reducing steps.

3.3. Results and Discussion

3.3.1. Chemical Deposition of Prussian Blue

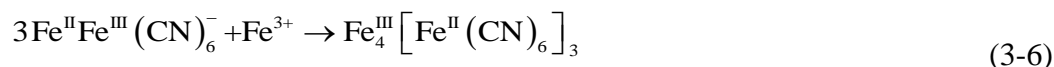
PB films are normally synthesized using a solution containing two components: iron (II) salt and hexacyanoferrate (III), or iron (III) salt and hexacyanoferrate (II) [53]. Using these precursors, PB forms directly in the presence of both iron valences. In the current work, potassium hexacyanoferrate (III) was used as a single-source precursor. In this case, a redox reaction needs to occur during synthesis to provide both iron valences.

There are two possible mechanisms for chemical formation of PB from a single source hexacyanoferrate (III). In the first, partial decomposition of hexacyanoferrate (III) occurs in a high acidity environment of reacting mixture (3-1) [36]. Free iron (III) cations from the associated complex are reduced to iron (II) cations (3-2). The iron (II) cations then react with undissociated hexacyanoferrate (III) anions to form soluble PB (3-3) [54]. Since the reduction of iron (III) to iron (II) is unfavorable thermodynamically, the driving force would be provided by the reaction of iron (II) cations and hexacyanoferrate (III) anions [54]. The standard free energy change for the combined reactions is -177 kJ mol^{-1} [54].



In the second case, the iron (III) cations produced in (3-1) and hexacyanoferrate (III) anions present in the solution can form a highly reactive complex of ferric ferricyanide or BG (3-4) [36]. This mixture has an oxidation potential higher than that of each component, and it even causes oxidation of water [55]. For BG to become PB, the presence of a reducing agent is necessary. It has been reported that BG can oxidize water (solvent), solution impurities, and liberate cyanides through reaction (3-5) [39, 40, 54, 36]. However, liberated cyanides can play the role of main reducing agent –more than

water and the impurities— for the process of PB formation [36]. The reduced BG reacts with free iron (III) cations in the solution and forms insoluble PB (3-6) [36].



Itaya et al. reported the electrochemical synthesis of PB using hexacyanoferrate (III) and iron (III) chloride [39]. They studied the ratio of the total charges consumed in the reduction of prepared PB and its oxidized form. Based on this ratio, they demonstrated that the PB is insoluble [39], in agreement with the second interpretation.

To study the effect of light on PB formation, PB films were synthesized in two conditions: (a) under the light, and (b) in darkness. The reflected light coming from the distal end of optical fiber during the synthesis process in both conditions were measured and recorded using the experimental setup shown in Figure 3-2. Simultaneously, a microscopic glass slide was dipped into the reaction mixture to prepare a sample for investigation of the Raman spectra of produced compounds in each condition.

Figure 3-3 shows the Raman spectra of samples synthesized under the light, in darkness, and uncoated glass substrate in the range of 2025 to 3010 cm^{-1} ; the inset shows the spectra of the same samples in the range 100 to 3200 cm^{-1} . In the inset of Figure 3-3, the broad peaks in the range of 1000 to 2300 cm^{-1} correspond to the fluorescence spectra of glass substrate. The peaks at 273 and 539 cm^{-1} correspond to iron-cyanide bending vibration modes, and the peaks at 2088, 2149, and 2154 cm^{-1} correspond to cyanide vibration modes [67]. In Figure 3-3, the spectra of sample synthesized under the light have a weak peak at 2088 cm^{-1} and a very strong peak at 2154 cm^{-1} . On the other hand, the spectra of sample synthesized in darkness have a very weak peak at 2088 cm^{-1} and a strong peak consisting of two maxima at 2149 and 2154 cm^{-1} .

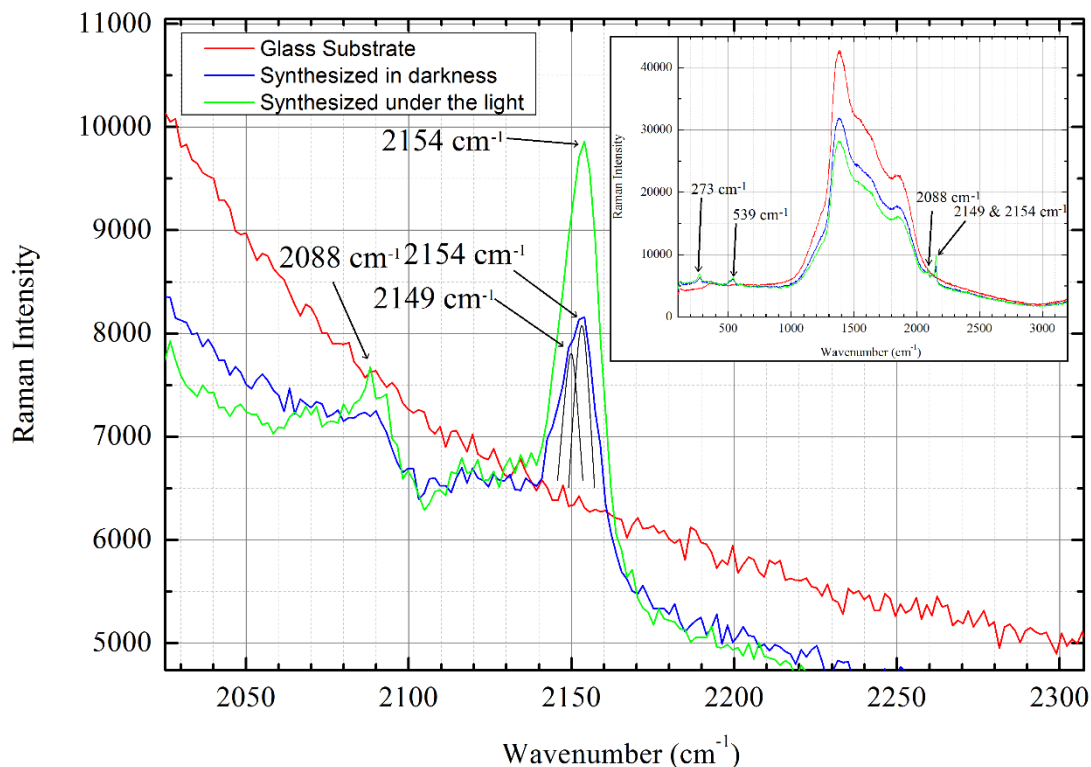


Figure 3-3: Raman spectra in the range of 2025-3010 cm^{-1} of red line) uncoated glass substrate, blue line) sample synthesized in darkness, and green line) sample synthesized under the fluorescent lamp light exposure. The inset is the Raman spectra of same samples in the range of 100-3200 cm^{-1} .

The weak peak around 2088 and very strong peak at 2154 cm^{-1} are the characteristic peaks for PB [67]. As shown in Figure 3-3 the sample synthesized under the light has the same characteristic peaks, and since it does not exhibit any extra peaks, it is therefore pure PB. The strong peak at 2149 cm^{-1} is the characteristic peak for BG [67]. The sample synthesized in darkness has a strong peak at 2149 cm^{-1} which indicates the presence of BG in the sample. It also has a very weak peak around 2088 cm^{-1} and a distinct peak at 2154 cm^{-1} , which are the characteristic peaks of PB. Therefore, the sample synthesized in darkness has both PB and BG in the form of $\{\text{Fe}_4^{\text{III}}[\text{Fe}^{\text{II}}(\text{CN})_6]_3\}_x\{\text{Fe}^{\text{III}}\text{Fe}^{\text{III}}(\text{CN})_6\}_{1-x}$.

These results show that iron (III) is reduced to iron (II) even in the absence of light. Although, the iron (II) production rate is not sufficient to form just PB, and another reaction also occurs between iron (III) and hexacyanoferrate (III) to form BG. On the other hand, it is found that exposure to light during the synthesis process promotes the

reduction of iron (III) to iron (II). The iron (II) production rate, in this case, is sufficiently high to form just PB.

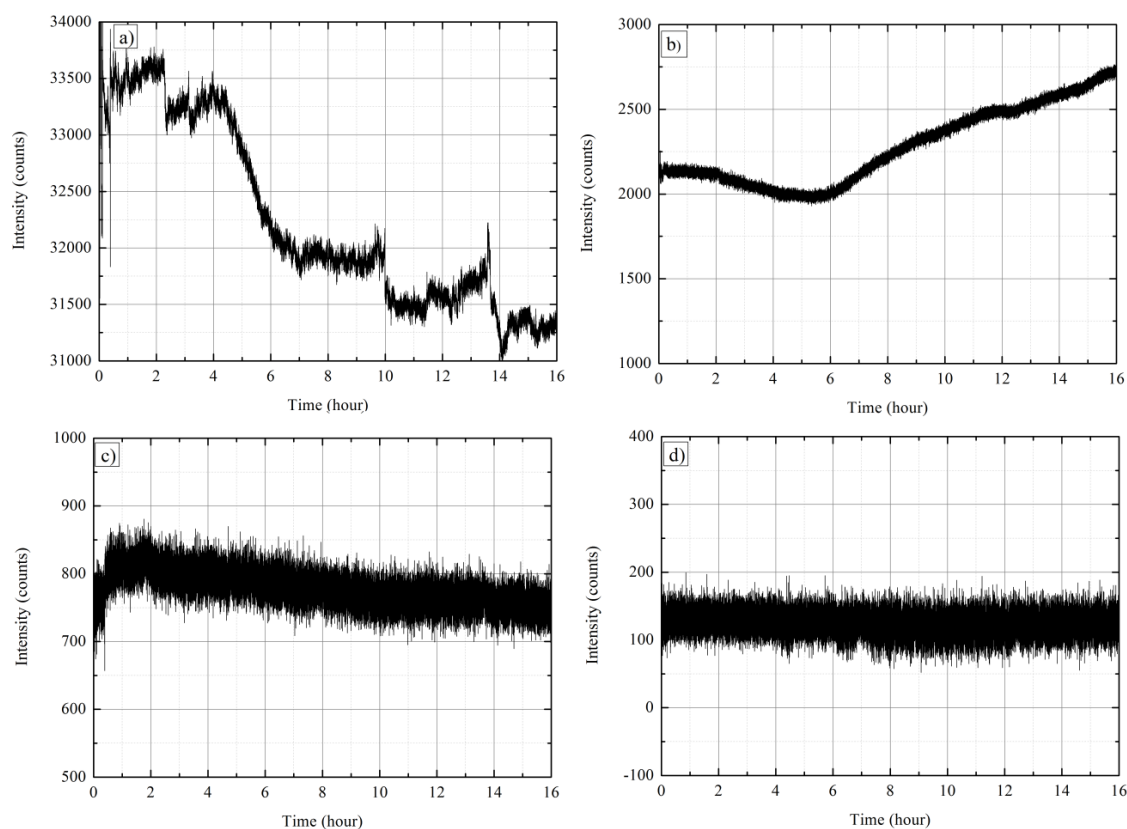


Figure 3-4: The light reflection from the distal end of an optical fiber during synthesis a) in darkness and in 720 ± 15 nm, b) under the light exposure in 720 ± 15 nm, c) in darkness and in 420 ± 15 nm, and d) under the light exposure in 420 ± 15 nm.

Figure 3-4 depicts the intensity of reflected light coming from the distal end of an optical fiber during the synthesis processes. The intensities integrated over the range of 720 ± 15 nm and 420 ± 15 nm are shown respectively in Figure 3-4 (a) and (b), and Figure 3-4 (c) and (d). Figure 3-4 (a) and (c), and Figure 3-4 (b) and (d) belong to samples synthesized in darkness and under the light, respectively.

In general, two phenomena affect the amount of light reflection from the distal end of an optical fiber: changes in the reaction mixture that generally result in changes in the imaginary part of the reaction mixture's refractive index; and variation in the precipitation of the compounds, with each having its own characteristics absorbance spectrum, onto the distal end of optical fiber.

As seen in Figure 3-4 (a), the intensity of light around 720 nm decreases during the synthesis in darkness. This may happen when no PB is being produced, or when PB is produced but its formation rate is very low. Traces of PB are seen in the Raman result for the sample synthesized in darkness. Therefore, PB is produced in darkness but the effect of changes of reaction mixture's refractive index is dominant and causes a decrease in light reflection from the distal end of the optical fiber. Figure 3-4 (c) depicts the intensity of light around 420 nm for sample synthesized in darkness, which initially increases, and starts to decrease after an hour. Increasing the intensity at this wavelength is evidence for formation of BG and it shows, as soon as introducing the optical fiber to the reaction mixture in darkness the BG starts to form. The decrease of intensity after the initial period is due to the change in the reaction mixture's refractive index, with reflection becoming dominant. The increase of light reflection around 720 nm for the sample synthesized under illumination illustrates the high rate of PB formation in this condition, Figure 3-4 (b). The purity of synthesized PB under illumination is supported by the absence of change in the light reflection around 420 nm, Figure 3-4 (d).

The results of monitoring the light reflection from the distal end of optical fiber during the synthesis in darkness and under the light are in good agreement with Raman spectra of the synthesized samples. Both imply the formation of pure PB while the synthesis is being done under illumination and formation of PB and BG simultaneously while the synthesis is being done in darkness.

3.3.2. Sensing Behavior

The time response of the intensity of the reflected light from the distal end of the sensing probe during its immersion in solutions at random concentrations of H_2O_2 is shown in Figure 3-5. The circles and squares indicate the instant at which the sensing probe was immersed into the H_2O_2 test solution and ascorbic acid, respectively. Since PW has a low absorbance under visible light, when the film is in PW state the majority of the light transmits through the film, and consequently, a lower intensity of reflected light is attained. The intensity of the recorded light starts rising after the immersion of the sensing probe in the H_2O_2 solutions due to oxidation of PW to PB. This behavior continues until plateauing at a maximum reflectance in PB state. Following the

immersion of the probe in ascorbic acid, the intensity decreases as the reagent returns the PB deposited film to its PW state.

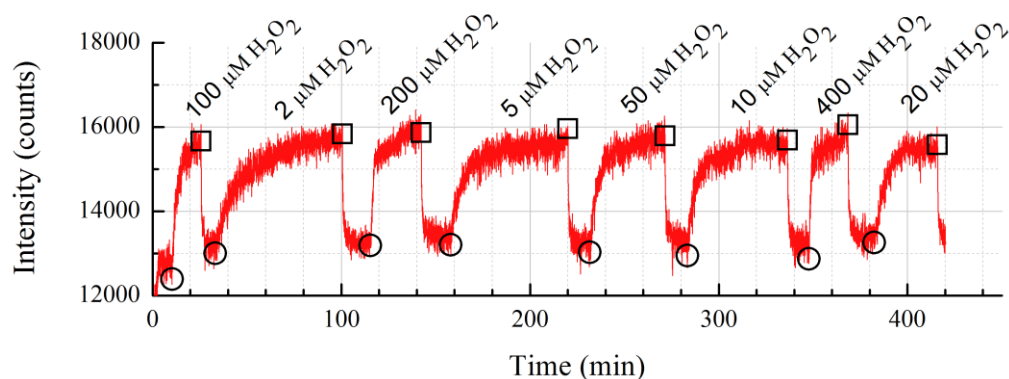


Figure 3-5: Response of the sensing probe to immersion in solutions with random H_2O_2 concentration.

The intensities after each immersion shown in Figure 3-5 reach essentially the same value. Koncki et al. proved earlier that the changes in the intensity of the reflected light from the PB/PW system are related to the total amount of H_2O_2 that enters in contact with the sensing film and the extent of the reaction [36]. In addition to this, the porosity and particle size of the PB/PW structure determine the surface area of the film accessible to H_2O_2 . These parameters control the extension of the reaction between the H_2O_2 and sensing film. As a result, the intensity of the optical signal is related to the extent of reaction and not to the concentration of the H_2O_2 [16, 38, 36]. In the case of the probe used in this work, only the portion of the sensing film that covers the flat portion of the distal end is responsible for the light scattered back into the optical fiber and that is measured by the spectrometer. Due to the small amount of PB/PW compound involved in the reaction and the constant intensity after each test performed, it is believed that the test solutions are able to oxidize almost all the PW to PB even at very low concentrations of H_2O_2 , which directly affects the detection limit of the probe.

Despite this drawback, there is a beneficial distinction between the signals corresponding to the tests at different concentrations of H_2O_2 . The time it takes the signal to reach the saturation level decreases with increasing concentrations of H_2O_2 . This behavior is governed by the increased diffusion rates associated with the higher concentration potentials. This behavior was previously observed in the development of

fiber-optics sensing devices based on immobilizing the PB with electrostatic self-assembly of polyelectrolytes [16, 59].

In the present work, the intensity response of each individual test was brought to the origin of the time axis at the moment of immersion in each H_2O_2 solution, and an inverse exponential curve was fitted to it [59]. All responses fitted well to the following equation:

$$I(t) = I_0 + A \left[1 - \exp\left(-\frac{t}{\tau}\right) \right] \quad (3-7)$$

where: $I(t)$ is the intensity at the time t ; I_0 is the intensity level while the sensing probe was immersed into the H_2O_2 solutions; τ is the time elapsed for the signal to reach $(1 - 1/e)$ equal to 63% of the intensity at saturation and was the parameter used to evaluate the time response of the sensing probe; and A is a constant that related to the geometry of the film, the diffusion conditions through the PB structure, and the oxidation of PW to PB. This inverse exponential behavior is consistent with the diffusion mechanism underlying the operating principle of the sensing probe [59]. Figure 3-6 shows the response of the sensing probe when it was immersed in $100 \mu\text{M}$ of H_2O_2 solution.

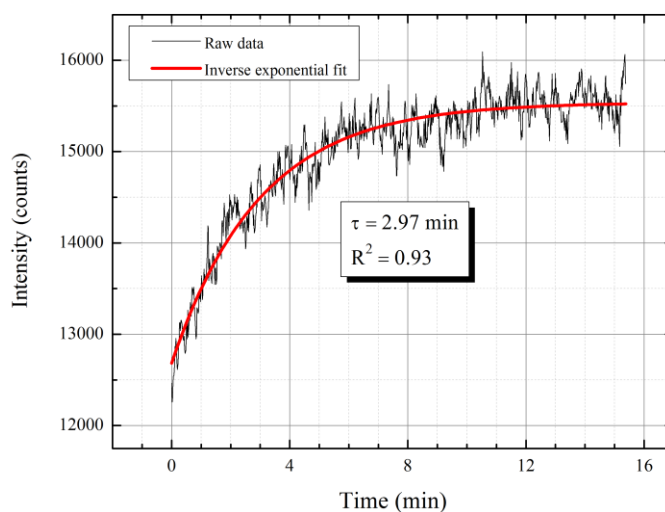


Figure 3-6: Response of the sensing probe and its inverse exponential fit to immersion in $100 \mu\text{M}$ H_2O_2 solution.

The characteristic response time, τ , versus the H_2O_2 concentration plotted in Figure 3-7, shows that the probe exhibits a linear response to H_2O_2 concentration on a log-log scale. Calibration of the probe can thus be performed by fitting the log-log relation to two data points using two solutions with known amounts of H_2O_2 .

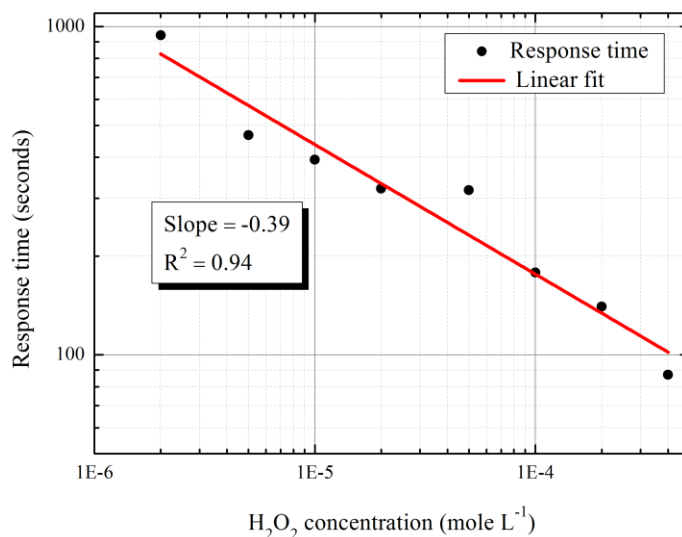


Figure 3-7: Time response of sensing probe versus H_2O_2 concentration.

One of the features of this sensing probe that distinguishes it from previously reported sensors is the nearly-constant signal baselines in the response at either the PB or the PW state, shown in Figure 3-5. Other fiber-optic sensing probes based on the PB/PW system have been fabricated immobilizing PB by the technique of electrostatic self-assembly of polyelectrolytes [16, 17, 59]. Some of the reported baselines in those studies were not stable, suggesting that not all the immobilized PB/PW takes part in the redox reactions. This causes some uncertainty in the interpretation of the behavior of the sensing probe. An additional advantage of the pure chemical deposition used here is the faster response and recovery times, which can be attributed to the easier diffusion in a pure PB/PW, as opposed to the slower diffusion through a multilayered structure of polyelectrolytes.

The uncertainties in determining concentration and response time of the probe were estimated for $100 \mu\text{M}$ H_2O_2 since it is a representative value of the evaluated range. The uncertainties for this case are $\pm 5 \%$ for concentration and $\pm 14 \%$ for the response time.

3.3.3. Repeatability

Various experiments comprising multiple sensing tests were performed with the same sensing probe to demonstrate the repeatability of the results. As noted in the experimental section, in every experiment the sequence of concentrations of the H_2O_2 solutions was different. Figure 3-8 presents the time response vs. concentration for four experiments using the same sensing probe with different sequences of sensing tests. These sequences include two sets with random concentrations, one decreasing and then increasing the concentration, and one increasing and then decreasing the concentration. The error bars are the Estimated Standard Deviation (STDEV) for each concentration. The probe exhibits a linear behavior with slopes similar to those in the single test presented in Figure 3-7.

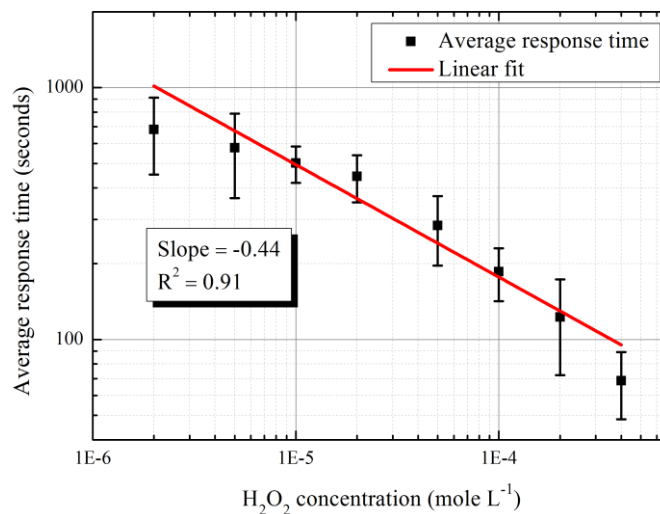


Figure 3-8: Average time response of sensing probe versus H_2O_2 concentration.

3.3.4. Reproducibility

Three sensing probes were prepared in the same manner at different times and multiple sensing experiments were done with each. The intensity response of these probes is plotted vs. time in Figure 3-9. The saturation intensities at PB and PW states are different for different sensing probes, but all these probes exhibited the same behavior and the characteristic decrease in response time with higher H_2O_2 concentration.

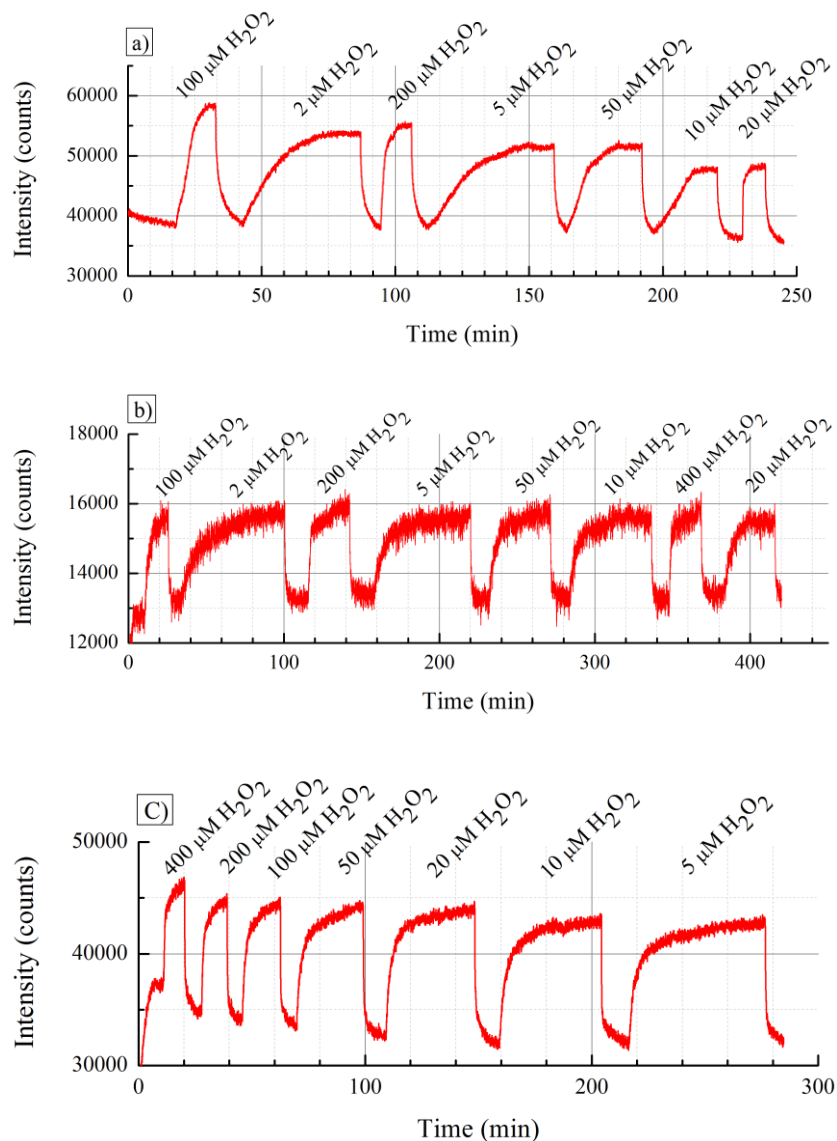


Figure 3-9: Response of three different sensing probes to immersion in solutions containing H_2O_2 .

As discussed earlier, the intensity of the optical signals is related to the extent of reaction. In term of constant H_2O_2 concentration, the extent of reaction is related to the thickness and porosity of the PB/PW film. Also, each prepared optical fiber has its own initial intensity of reflectance, since the flat surface of the distal end of optical fibers does not always have the same angle with the axis of the optical fiber. The offset of the signals from each probe is therefore likely caused by a combination of variation of the PB/PW film thicknesses, porosities, and the angle of flat surface of distal end of optical fiber with the axis of optical fiber. The formation of the PB film is photoinduced with a light source

placed outside the glass container where the reaction takes place. Although solution pH, concentration of reagent, and time and temperature of reaction are well controlled, this fabrication process cannot ensure the same light intensity for all prepared probes. This may have caused different thicknesses and microstructures for the deposited sensing films, and hence different reflected intensities from the distal end of each of the optical fibers.

Figure 3-10 depicts the time response vs. H_2O_2 concentration of sensing probes a-c, extracted from Figure 3-9. The sensing behavior is similar for all three of them. The slopes for the best linear fit on the time response of each sensing probe are roughly the same. However, the intersect with the vertical axis changes. This particularity denotes that each sensor will require an initial calibration with known concentrations of H_2O_2 in order to determine its behavior, prior to be exposed to an unknown amount of H_2O_2 . The different vertical intersects of the sensing probes can be again attributed to the sensing film thickness or the film microstructure which affects the diffusion condition and leads to different diffusion time. However, the similarity observed in the slopes for the different sensing probes suggests that this parameter depends mainly on the nature of the deposited PB/PW film and that is independent of the film thickness and structure.

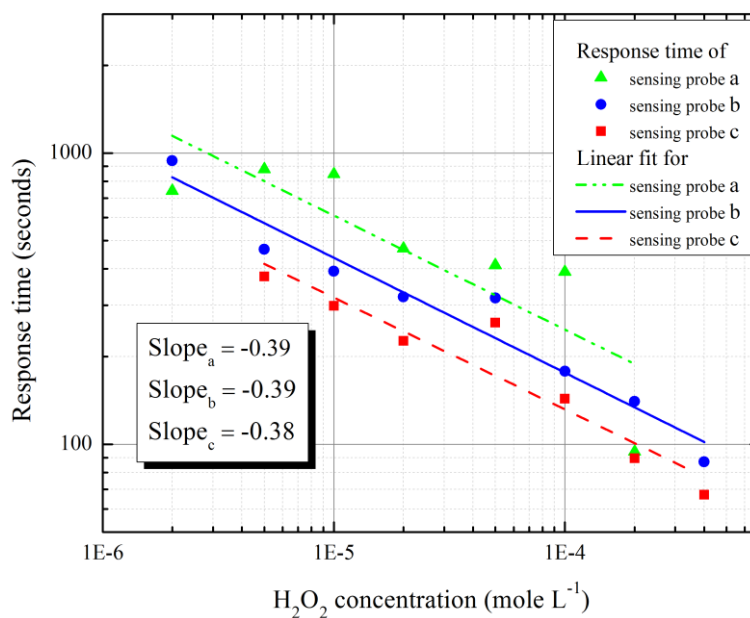


Figure 3-10: Time response of three different sensing probes versus H_2O_2 concentration.

3.3.5. Durability

The durability of a number of the sensing probes and the reliability in the measurements were evaluated by performing similar sensing experiments four and seven months after fabrication. The intensity responses of the sensing probe are presented in Figure 3-11. The maximum intensity that the signal reached is slightly lower for the probe tested in the seventh month. Since the probe was subjected to multiple experiments within the fourth and seventh month, the decrease is likely due to a leaching of the immobilized compound. Hence, to ensure accurate measurements in H_2O_2 concentration, periodic recalibrations may be required in practice.

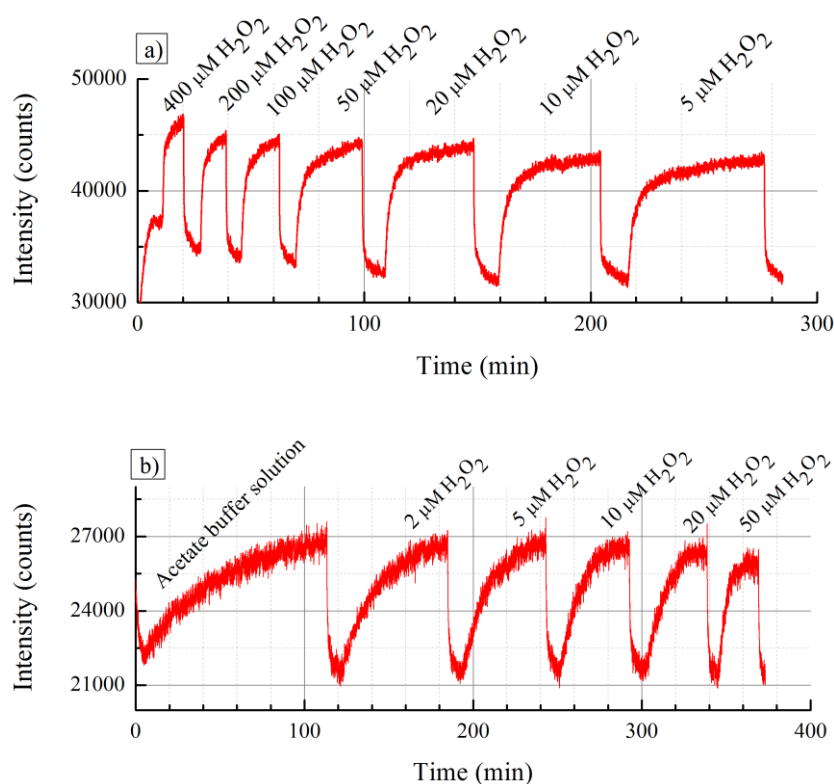


Figure 3-11: Response of a sensing probe to immersion in solutions containing H_2O_2 four and seven months after its fabrication.

Figure 3-12 depicts the time response of the experiments remains linear with the sensing probe for the fourth and seventh months. The response and the slopes are essentially the same for both data sets. However, the vertical intercept is shifted toward slower response times in the more aged probe. Slower diffusion times could again be due to leaching of the structure or possible alterations in the microstructure of the deposited

film that difficult the access of the oxidant to the reaction sites. The sensing probe was found to remain nonetheless functional for an extended period of time and multiple experiments. The results presented here show the prepared sensing probe can be used to detect the H_2O_2 as well as it allows us to quantify the concentration of H_2O_2 , and the fabrication method by the chemical synthesis ease the mass production of the sensing probes.

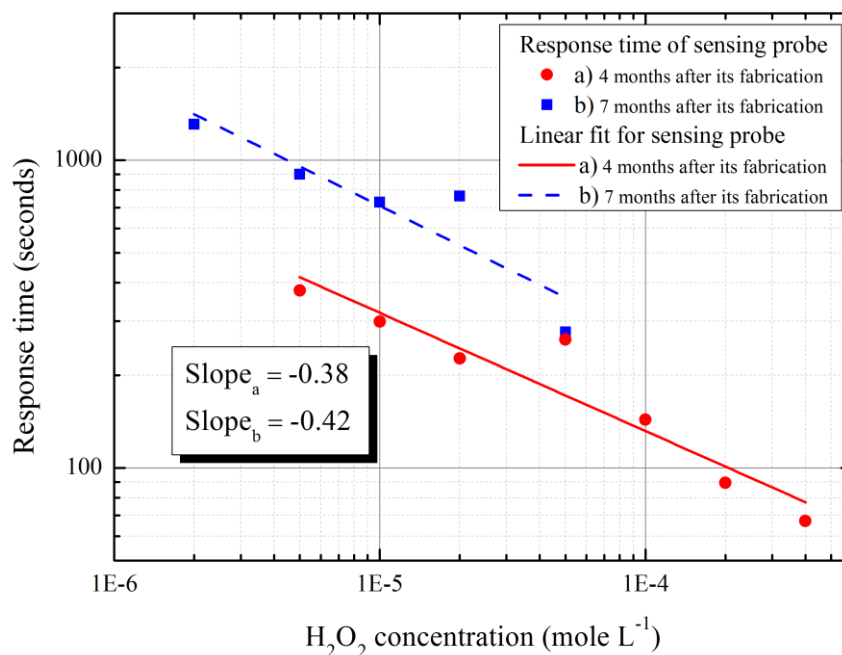


Figure 3-12: Time response of a sensing probe versus H_2O_2 concentration four and seven months after its fabrication.

3.4. Conclusions

A novel fiber-optic probe was developed for the detection and measurement of small concentrations of H_2O_2 in liquid phase. A Prussian blue (PB) film served as an indicator of H_2O_2 in a spectroscopic manner. Pure and robust PB films have been deposited onto the distal end of optical fiber through a simple chemical method using the single-source potassium ferricyanide. The effect of light exposure during synthesis process was analyzed and shows that the light exposure during synthesis will lead to formation of pure PB film, while synthesis in darkness will lead to co-precipitation of PB and BG.

The intensity response of the fiber-optic sensing probes follows an inverse exponential behavior which is in accordance with the physics of diffusion. The characteristic time taken from the inverse exponential equation, which is the $\approx 63\%$ of the time for intensity to reach the saturation level, shows a linear relationship with the H_2O_2 concentration in a log–log scale.

Several sensing experiments with different sequences of H_2O_2 concentrations and testing of several probes fabricated under the same conditions demonstrate the repeatability, reliability, and reproducibility of the probes. Durability of the sensing probe was tested by comparing the sensing behaviors four and seven months after its fabrication. Although the sensing behavior remained unchanged, a small increase in response time observed over the 3-month period, indicating that periodic recalibration of sensing probes is required in practice.

The probes demonstrated in this study capitalize on some of the unique advantages of the fiber-optic devices such as small size, flexibility, and immunity to electromagnetic interference combined with the sensing properties of the synthesized PB, and in particular high sensitivity and selectivity toward H_2O_2 , the proposed optical sensors can pave the way for a high performance and portable H_2O_2 sensing probe applicable for *in situ* measurements in polymer electrolyte membrane fuel cells, as well as in minimally invasive biosensor.

Chapter 4

pH-dependent Response of a Hydrogen Peroxide Sensing Probe

(Sensors and Actuators B: Chemical, volume **237**, 2016, 113–119)

Reproduced with permission from Elsevier

Preamble

The previous chapter demonstrates the process of sensor development and H₂O₂ sensing at room temperature and a pH of 4. This proof-of-concept leads to the next step which is investigating the functionality of the sensor at different pH values especially at pH 2 which is typical of an operating PEM fuel cell. The sensor behavior at different pH values (i.e. pH 2 to 7) and sensor characteristics at pH 2 are evaluated and presented in this chapter.

The Body of this chapter was published in the *Sensors and Actuators B: Chemical*.

Abstract

The response of a fiber-optic hydrogen peroxide (H₂O₂) sensing probe is investigated under a range of pH conditions. The H₂O₂ optrode is prepared by depositing a thin layer of Prussian blue (PB) onto the tip of a multimode optical fiber, and its detection mechanism is based on the PB/Prussian white (PW) redox reaction. PW is oxidized to PB by H₂O₂ leading to changes in the absorption of visible light. The sensor can be restored after usage by reducing the PB to PW with ascorbic acid. This optrode was previously shown to have good repeatability and sensitivity to H₂O₂ concentrations at room temperature and a pH of 4. For practical applications, the sensor must be capable

of detecting H_2O_2 in environments spanning a range of pH conditions, including biological and industrial environments which together span pH values from 7 to less than 3. We present experiments using multiple PB optrodes, at pH values ranging from 7 to 2, and for different concentrations of H_2O_2 . The work demonstrates that the optrode remains functional and provides stable and reproducible measurements of H_2O_2 under a range of pH conditions that correspond, in particular, to those in an operating PEM fuel cell.

Keywords: Hydrogen peroxide, Optrode, PEM Fuel cell, pH-dependent Response, Prussian blue, Spectroscopic detection.

4.1. Introduction

Hydrogen peroxide (H_2O_2) is a by-product of oxidative metabolisms [68, 63]. It is involved in many biological processes and plays a leading role in a variety of damage mechanisms. For example, H_2O_2 induces cellular damage in human cells [64, 65] and its presence in exhaled breath and breast cancer cells can be used to diagnose illnesses such as asthma and human breast cancer, respectively [66, 3]. On the other hand, H_2O_2 is used in a broad range of industrial and medical applications, such as aseptic processing of food and pharmaceuticals, disinfection, water treatment plants, and decontamination of industrial effluents [61, 62, 69]. H_2O_2 is also believed to play a central role in chemical degradation of polymer membranes in PEM fuel cells [4]. A versatile H_2O_2 sensor that functions in environments spanning a range of pH values is therefore of practical importance in various fields. In this study we investigate the functionality of an H_2O_2 optrode at different pH values, and in particular, at pH value corresponding to those in an operating fuel cell, to assess its suitability for eventual *in situ* monitoring of H_2O_2 in PEM fuel cells.

H_2O_2 sensors are usually based on the electrochemical and spectroscopic techniques [15, 14, 16, 17, 18, 19, 70], with spectroscopic techniques being preferred for many biochemical and industrial applications because of their immunity to electromagnetic interference. On the other hand, Prussian blue (PB), ferric ferrocyanide, is widely used for making sensors and biosensors for detection and measurements of H_2O_2 [15, 71]. In particular, optrodes based on PB have shown reliable response to H_2O_2

concentration [59, 56]. These sensors were prepared by depositing PB onto the tip of multimode optical fibers, with PB serving as a spectroscopic indicator of H_2O_2 . Because optical fibers are made of non-conductive materials, the chemical deposition of PB has been preferred for constructing PB-based fiber-optic sensors. Among chemical deposition methods, single-source precursor and layer-by-layer (LbL) techniques have been used successfully to prepare PB-based H_2O_2 optrodes [17, 56]. However, the performance of PB-based H_2O_2 sensors prepared with LbL is limited in environments spanning a range of pH values and although the performance of this type of sensors is slightly improved by adding capping bilayers on the LbL-based PB film, long-term stability is poor.

The single-source precursor technique is a synthesis approach in which all the elements required in the final product are incorporated into one compound. In this technique, the precursor may participate in several consecutive reactions to arrive at the final product. The single-source precursor technique was selected in this work to deposit PB onto the optical fiber because this approach leads to sensors with better long-term stability in aqueous solutions at pH 4 [56]. The single-source precursor technique is a more straightforward process than the LbL technique and results in more stable PB film on the tip of the optical fiber. This is likely due to the different structure of PB that is afforded through the single-source precursor technique compared to the structure that is obtained through the LbL technique. It has been observed that the pH stability of the PB film also depends on the deposition process [71].

A potential application of such a sensor is integration into a PEM fuel cell for *in situ* detection and measurement of H_2O_2 concentrations. The sensor is well suited for this application because of its small size, immunity to electromagnetic interference, and compatibility of the fiber material (*i.e.* silica glass) with the electrochemically active environment inside a fuel cell. Since H_2O_2 is a product of glucose oxidation in the presence of glucose oxidase and oxygen, the proposed optrode has also potential for indirect measurement of glucose content [72].

The H_2O_2 spectroscopic detection mechanism relies on the redox reactions of the PB/PW system, and the evaluation of corresponding changes of the optical properties of the compound. The optrode is first reset by reducing PB to PW in the presence of a

reducing agent, such as ascorbic acid, as shown in Equation 4-1. When the PW-modified fiber is exposed to an oxidizing agent, such as H_2O_2 , the reverse reaction (*i.e.* PB formation) occurs, as shown in Equation 4-2. PB has a strong intervalence charge transfer absorption band near 700 nm due to a transition from $\text{Fe}^{\text{III}}\text{Fe}^{\text{II}}$ to $\text{Fe}^{\text{II}}\text{Fe}^{\text{III}}$ states. On the other hand, PW does not have any distinct absorption bands in the visible range [73]. As a result, the increasing absorbance in the visible range as PW oxidizes to PB, in the presence of H_2O_2 , can be used to detect the presence of this oxidant. Moreover, the initial PW state can be recovered by exposing PB to ascorbic acid. Fig. 4-1 illustrates the detection mechanism of H_2O_2 using the optrode based on chemically deposited PB/PW system onto the tip of an optical fiber.

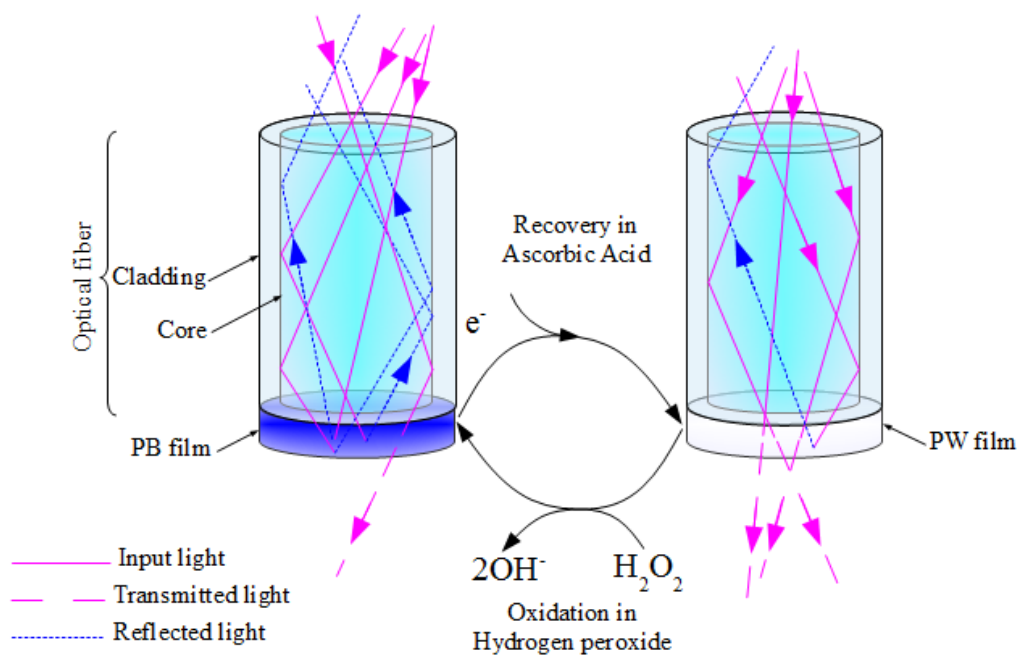
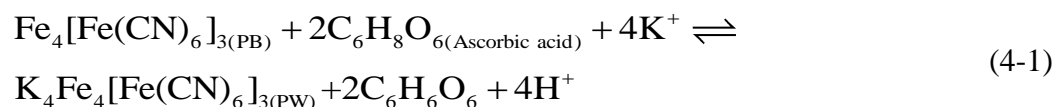


Figure 4-1: Detection mechanism of H_2O_2 using an optrode based on PB/PW system (taken from [56]).



In this study we investigate the functionality of an H₂O₂ optrode at different pH values, and in particular, at pH value corresponding to those in an operating fuel cell, to assess its suitability for eventual *in situ* monitoring of H₂O₂ in PEM fuel cells. An H₂O₂ optrode was prepared using the single-source precursor technique for deposition of PB onto the tip of multimode optical fibers. Sensing measurements in H₂O₂ buffered solutions with pH values, ranging from 7 to 2, were performed to investigate the functionality of the optrode. The sensing behavior of the probe, including stability and reproducibility, was investigated at the operating pH of PEM fuel cells (*i.e.* 2). Furthermore, sensing experiments were performed at three additional pH values, (*i.e.* 2, 5, and 6) and in each pH with different concentrations of H₂O₂ to study the pH dependency of the sensor response.

4.2. Experimental

4.2.1. Materials

Potassium hexacyanoferrate (III) (product No. 13746-66-2) from Sigma-Aldrich was used as a single-source precursor in an aqueous solution of hydrochloric acid (HCl) (37%) for synthesizing PB onto the tip of an optical fiber. L-ascorbic acid from Aldrich, (catalog No. 25,556-4), was used as the reducing agent for the PB to PW reaction. H₂O₂ (30 wt%) from ACP Chemicals was used to prepare the oxidizing solutions at different concentrations.

Potassium phosphate monobasic (product No. 7778-77-0) from Caledon, sodium phosphate dibasic (product No. 7558-79-4) from EM science, sodium phosphate monobasic (product No. 13472-35-0) from EM science, and Phosphoric acid (product No. 7664-38-2) from Caledon were used to prepare phosphate buffer solutions (PBS) at a range of pH values (*i.e.* 2, 3, 5, 6, and 7). The reducing solution is prepared in PBS with 0.04 mol L⁻¹ of L-ascorbic acid. Sodium hydroxide and phosphoric acid were used to adjust the pH of the solutions to the desired values.

All chemicals were used *as received* with no further purification. The water used in the experiments was purified with a four-cartridge purification system (Super-Q Plus, Millipore, Billerica, MA) and has a resistivity of 18.2 MΩ cm. The optical fiber is a

multi-mode AFS50/125Y from Thorlabs (Newton, NJ), with core and cladding diameters of 50 μm and 125 μm , respectively.

4.2.2. Sensor Fabrication

The PB-based optrode was prepared using chemical deposition of PB film onto the tip of a multimode optical fiber. As reported in our previous work [56], 10 mmol L^{-1} of potassium ferricyanide, as a single-source precursor, is added to 25 mL of an aqueous solution of 0.1 mol L^{-1} HCl. The optical fiber is then immersed in this prepared mixture, and held at 40 $^{\circ}\text{C}$ under continuous stirring at 300 rpm for 10 hours. The synthesis process is performed with exposure to fluorescent lamp light (Philips Alto, F28T5 25W). Finally, the optical fiber is left in the solution to cool to room temperature. The prepared optrode is then removed from the solution and left at room temperature for one day. We have explored a range of annealing temperatures and times and found that annealing at 100 $^{\circ}\text{C}$ for 15 min leads to the best performance of the optrode. Therefore, the sensor was annealed under these conditions.

4.2.3. Sensing Test Procedure and Instrumentation

The sensing test procedure comprises three steps: First, the sensor response to aqueous solutions with different pH values (*i.e.* 2, 3, 5, 6, and 7) and containing 100 $\mu\text{mol L}^{-1}$ of H_2O_2 is evaluated. Then, the sensor behavior in concentrations of H_2O_2 ranging from 5 $\mu\text{mol L}^{-1}$ to 400 $\mu\text{mol L}^{-1}$ is examined in solutions with a pH of 2.0 ± 0.1 , which is the typical operating pH of a PEM fuel cell. Additional sensing measurements are performed at pH of 2.0 ± 0.1 with multiple sensors to study the performance of the sensors in terms of repeatability, durability, and reproducibility. Finally, several sensing tests are carried out in solutions containing various concentrations of H_2O_2 at a range of pH values (*i.e.* 2, 5, and 6). Ascorbic acid and H_2O_2 solutions are prepared in PBS at each pH. The pH of all of the prepared solutions are determined using a digital pH-meter (AR25 accuMET[®], Fisher Scientific, Hampton, NH).

Each sensing test is performed by alternately immersing the optrode to an ascorbic acid and H_2O_2 solutions, for the recovery and oxidation steps of the PB/PW system. When the intensity of reflected light from the optrode plateaus to a minimum level, it is

considered to have reached the PW state. The optrode is then removed from the ascorbic acid and placed in the H_2O_2 solution and kept there until the intensity plateaus to a maximum, indicating the oxidation from PW to PB.

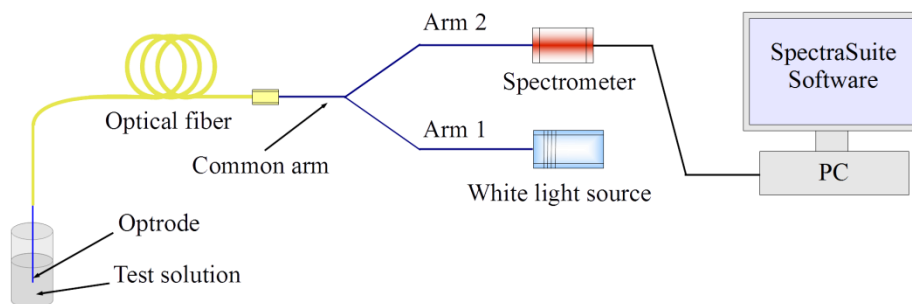


Figure 4-2: Sensing test experimental Setup including white light source, optical fiber, optrode, and spectrometer.

Fig. 4-2 illustrates the experimental setup used for collecting and measuring the reflected light from the optrode. The light from the white light source (LS-1, OceanOptics, Dunedin, FL), is carried to the optrode through arm 1 of a bifurcated optical fiber (BIF200- UV-Vis, OceanOptics) and the common arm. Part of the scattered light from the PB/PW film on the tip of the optrode is collected by the optical fiber and guided back through the common arm and arm 2 of the bifurcated optical fiber into an optical fiber spectrometer (USB2000, Ocean Optics), which measures the intensity of the light in a wavelength range from 370 nm to 1048 nm. The reflected spectrum is sampled at a frequency of 1 Hz using the software, SpectraSuite (Ocean Optics, Dunedin, FL). The intensity data is integrated over the full range of the spectrometer (*i.e.* 370 to 1048 nm) and is used to study the response of the PB/PW system during both the oxidizing and the reducing steps.

4.3. Results and Discussion

4.3.1. pH-dependent Response

The pH-dependent response of the optrode is investigated in $100 \mu\text{mol L}^{-1} \text{H}_2\text{O}_2$ solutions at different pH values. Ascorbic acid and H_2O_2 test solutions are prepared in PBS with pH of 2, 3, 5, 6, and 7. Fig. 4-3 illustrates the intensity of the light reflected from the optrode at different pH values. The circles and squares in Fig. 4-3 indicate the

times at which the optrode is immersed in either the ascorbic acid or H_2O_2 test solutions, respectively. The PB at the fiber tip is reduced to PW when immersed in ascorbic acid, and the PW is oxidized to PB when immersed in the H_2O_2 test solutions. The reactions are time dependant because of the diffusion of the reducing/ oxidizing agent into the PB/PW structure. PW has a low absorbance under visible light and, therefore, the majority of the light transmits through the sensing film while it is in the PW state. Consequently, the intensity of the reflected light decreases as the amount of PW increases in the presence of ascorbic acid. On the other hand, PB has a strong absorption band near 700 nm which causes an increase in the intensity of the reflected light in the presence of H_2O_2 . The intensity of the reflected light changes in either case (*i.e.* reduction or oxidation of the film) until an equilibrium state is reached.

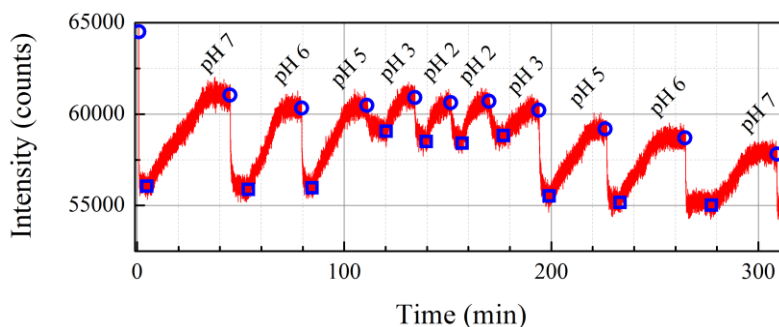


Figure 4-3: Intensity response of the optrode to immersion in solutions with different pH values and $100 \mu\text{mol L}^{-1}$ of H_2O_2 .

As shown in Fig. 4-3, the optrode is first immersed in an ascorbic acid solution with pH 7 to recover the sensor to the PW state and the subsequent detection step was done using an H_2O_2 test solution with pH 7. Afterwards, the recovery step in ascorbic acid and the subsequent detection step in H_2O_2 test solutions are performed at lower pH values down to pH 2, and thereafter at higher pH values up to 7. It is observed in Fig. 4-3 that the optrode detects H_2O_2 at a wide range of pH (from pH 2 to 7). The ability of this optrode to detect H_2O_2 across this pH range suggests that it can be applied in a variety of physiological and industrial environments. As shown in Fig. 4-3, pH influences the intensity of the reflected light at minimum plateaued state, achieved during the recovery step in ascorbic acid. A similar behaviour was observed before by [16].

The precise reason for the increased intensity when the film is in PW state at lower pH values shown in Fig. 4-3 is unknown as several factors are involved, such as the various equilibria involved (*e.g.* ionization equilibrium of acid ascorbic) and even the microstructured environment of the film. The reduction potential of ascorbic acid also decreases with increasing pH, according to the Nernst equation, which should also contribute to this effect. A similar trend has been observed in another study [74] on reduction of PB nanoparticles in different reaction media with different pH values. In that study, the intensity of the absorbance of PB nanoparticles after reduction in different pH values showed no significant change between pH 2 and 3 while the intensity changed significantly between pH 3 and 5.

The intensity response of the optrode when it is at equilibrium in the presence of H₂O₂ is similar for all tests, regardless of the pH of the test solution, as shown in Fig. 4-3. This suggests that the extent of PW oxidation to PB in the presence of H₂O₂ is also similar at all pH values. However the intensity response of the optrode at equilibrium in the presence of either H₂O₂ or ascorbic acid decreases slightly after several tests, which can be attributed to leaching or possible alterations in the microstructure of the deposited PB/PW film. Possible leaching of the PB film would reduce the durability of the optrode. Therefore, the durability of the optrode has been investigated and discussed in section 3.2.3.

To investigate the optrode response to test solutions, the time constant of the optrode was extracted from the intensity response of each test. For this calculation, the moment of immersion in each H₂O₂ solution is defined as $t=0$, and the data is fit to an inverse exponential function (Equation 4-3):

$$I(t) = I_0 + A \left[1 - \exp\left(-\frac{t}{\tau}\right) \right] \quad (4-3)$$

where $I(t)$ and I_0 are the intensities at time t and the instant the optrode was initially immersed into the H₂O₂ solutions, respectively. τ is a constant equal to the time elapsed when the intensity reaches 63% of the intensity at equilibrium and is the parameter used to evaluate the response of the optrode. A is a constant related to the geometry of the film,

the diffusion conditions through the PB structure, and the oxidation of PW to PB. This inverse exponential behavior is consistent with the diffusion mechanism underlying the operating principle of the optrode [59].

Fig. 4-4 depicts the average time constant of the optrode versus pH of the test solutions containing $100 \mu\text{mol L}^{-1} \text{H}_2\text{O}_2$, on a log-log scale. It is apparent that pH affects the time constant of the optrode. The time constant is smaller for the test H_2O_2 solutions at lower pH values.

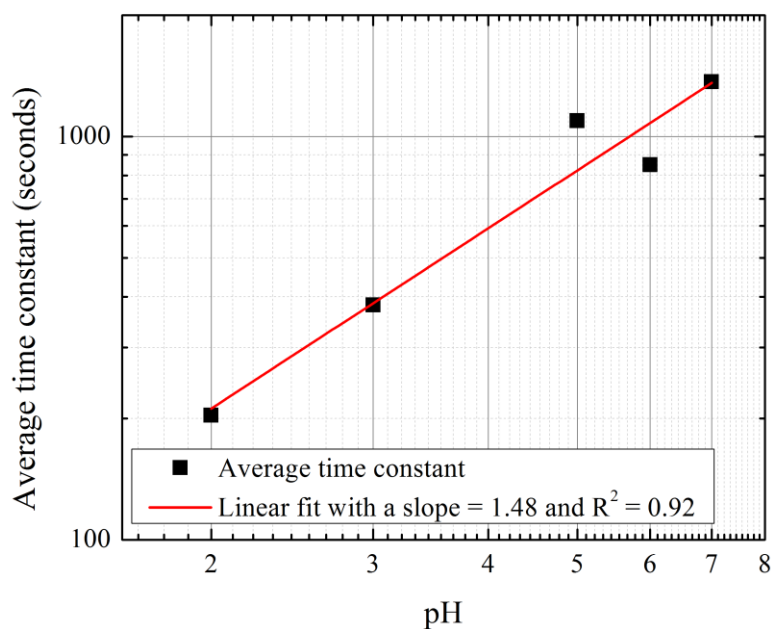


Figure 4-4: Time constant of the optrode versus pH of the test solutions with $100 \mu\text{mol L}^{-1}$ of H_2O_2 .

4.3.2. Sensing Behavior at PEM Fuel Cell's Operating pH

Sensing H_2O_2 and understanding the underlying conditions that promote its formation within a fuel cell are keys to understanding the mechanism of PEM fuel cell membrane degradation. Therefore, the sensing behavior of the optrode for detection and measurement of H_2O_2 has been studied at a pH typical of an operating PEM fuel cell (*i.e.* pH 2).

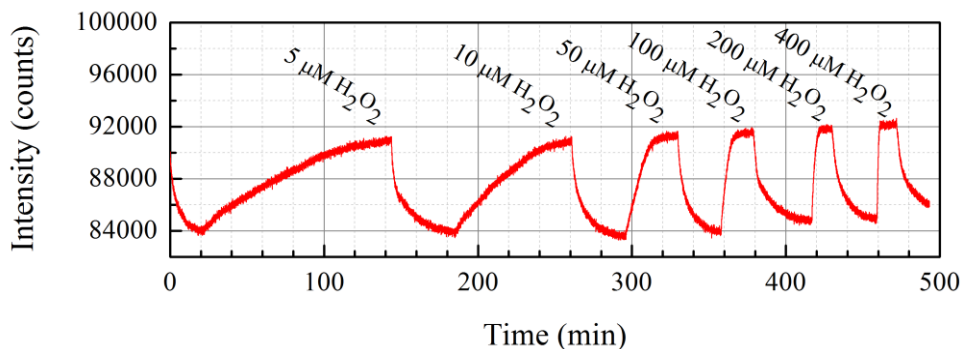


Figure 4-5: Intensity response of the optrode to immersion into solutions with different H_2O_2 concentrations at pH 2.

Fig. 4-5 shows the intensity response of the optrode to different H_2O_2 concentrations at pH 2. The intensity of the reflected light reaches approximately the same value after each immersion at different concentrations of H_2O_2 . Using the technique described in Section 3.1, the time constant, τ , is extracted from Fig. 4-5 and plotted versus H_2O_2 concentration in Fig. 4-6.

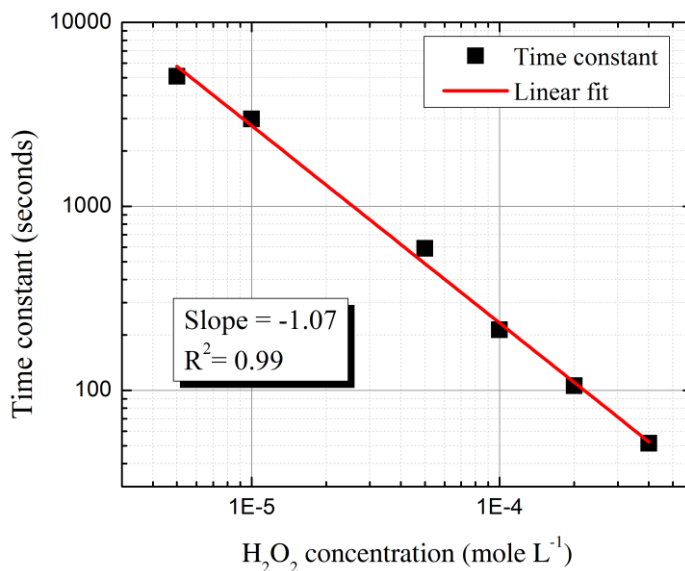


Figure 4-6: Time constant of the optrode versus H_2O_2 concentration at pH 2.

Fig. 4-6 shows that the time constant changes linearly (*i.e.* $R^2=0.99$) with H_2O_2 concentration, on a log-log scale. This linear behavior allows us to detect and quantify the concentration of H_2O_2 . Fig. 4-6 also shows that the time constant is smaller for the test

solutions with higher concentration of H_2O_2 . This behavior is governed by the increased diffusion rates associated with the higher concentration potentials.

4.3.2.1. Repeatability

To investigate the repeatability of the measurements, four experiments with 50, 100, 200, and 400 $\mu\text{mol L}^{-1}$ of H_2O_2 and with each one comprising three sensing tests are performed using the same optrode. Fig. 4-7 illustrates the intensity response of the optrode during these four experiments.

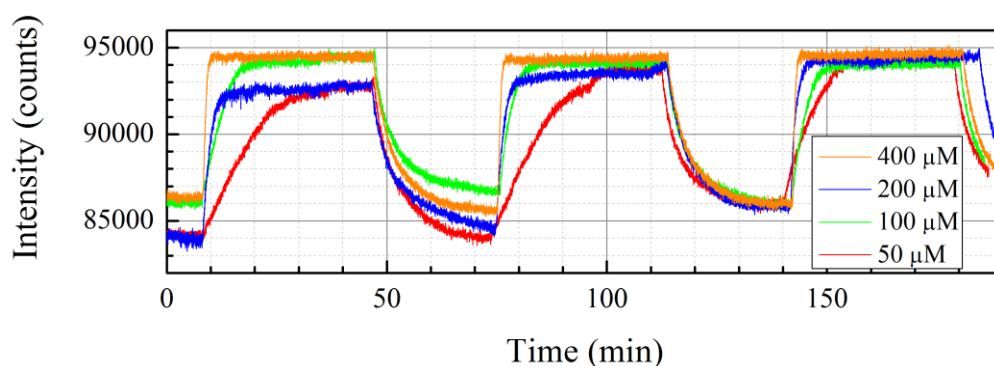


Figure 4-7: Successive intensity responses of the optrode to red) 50 $\mu\text{mol L}^{-1}$ of H_2O_2 , green) 100 $\mu\text{mol L}^{-1}$ of H_2O_2 , blue) 200 $\mu\text{mol L}^{-1}$ of H_2O_2 , and orange) 400 $\mu\text{mol L}^{-1}$ of H_2O_2 (For interpretation of the references to colour in this figure legend, the reader is referred to the web version of this article).

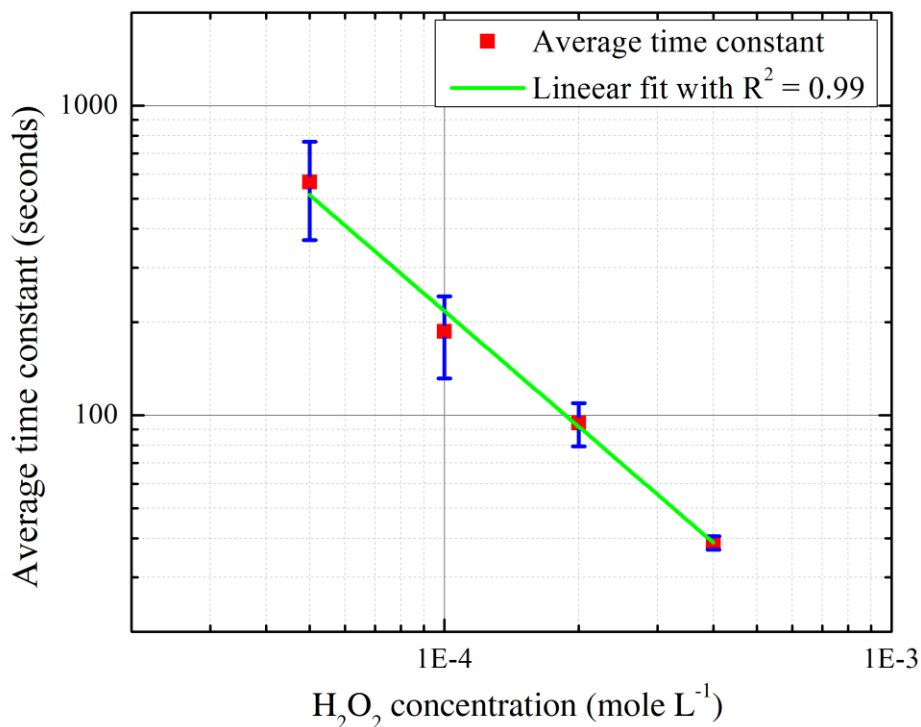
Fig. 4-7 shows that the intensity levels at minimum and maximum plateaued states are essentially the same and it is only the slope that increases following immersion into higher concentration H_2O_2 test solutions, leading to smaller time constants. The slope of intensity variation for each concentration of H_2O_2 is calculated during the first 60 seconds after the probe immersion into test solutions and presented in Table 4-1. The slopes for each concentration of H_2O_2 are close to each other, particularly at higher concentrations of H_2O_2 , which indicates the repeatability of the results. On the other hand, the slope of intensity variation during the probe immersion in ascorbic acid solutions is always the same with an average of negative 23 counts per seconds and standard deviation of 1.09 (*i.e.* slopes were calculated during the first 180 seconds after probe immersion in ascorbic acid). The same concentration of ascorbic acid was used in all tests, this behaviour further confirms the repeatability of the results with this optrode.

Table 4-1: Slopes of intensity variation at different concentrations of H₂O₂.

| H ₂ O ₂ concentration ($\mu\text{mol L}^{-1}$) | Slope of intensity variation (counts/seconds) | | | |
|---|---|-----------------|----------------|---------|
| | First response | Second response | Third response | Average |
| 50 | 16 | 12 | 22 | 16 |
| 100 | 23 | 38 | 38 | 33 |
| 200 | 63 | 65 | 81 | 70 |
| 400 | 118 | 129 | 125 | 124 |

Note: Slopes were calculated during the first 60 seconds after probe immersion into H₂O₂ test solution.

The time constant of the optrode versus H₂O₂ concentration is extracted from Fig. 4-7 and plotted in Fig. 4-8. The average time constant decreases linearly with increasing H₂O₂ concentration with an R^2 of 0.99. This is in a good agreement with the results presented in Fig. 4-6. The error, which is based on the Estimated Standard Deviation for each concentration, decreases as the H₂O₂ concentration increases (*i.e.* the optrode response is more reliable at higher concentrations of H₂O₂).

Figure 4-8: Time constant of the optrode versus H₂O₂ concentration.

4.3.2.2. Reproducibility

Two optrodes are prepared in the same manner at different times and multiple sensing experiments are performed with each. The time constants of both optrodes are plotted versus H_2O_2 concentration in Fig. 4-9. Both optrodes exhibit a linear behavior and a lower time constant with higher H_2O_2 concentration. The slopes for both optrodes are similar, -0.97 and -1.00 $\text{s mol}^{-1} \text{L}$. However, the extrapolation of the linear fits do not intercept the vertical axis at the same point. This suggests that each sensor will require an initial calibration with known concentrations of H_2O_2 . The different intercepts can be attributed to variations in sensing film thickness or microstructure which affect diffusive transport and lead to different diffusion times. However, the similarity of the slopes for the different optrodes suggests that this parameter depends mainly on the nature of the deposited PB/PW film under given experimental conditions (*i.e.* the temperature and pH of the sensing environment) and that is independent of the film thickness and structure.

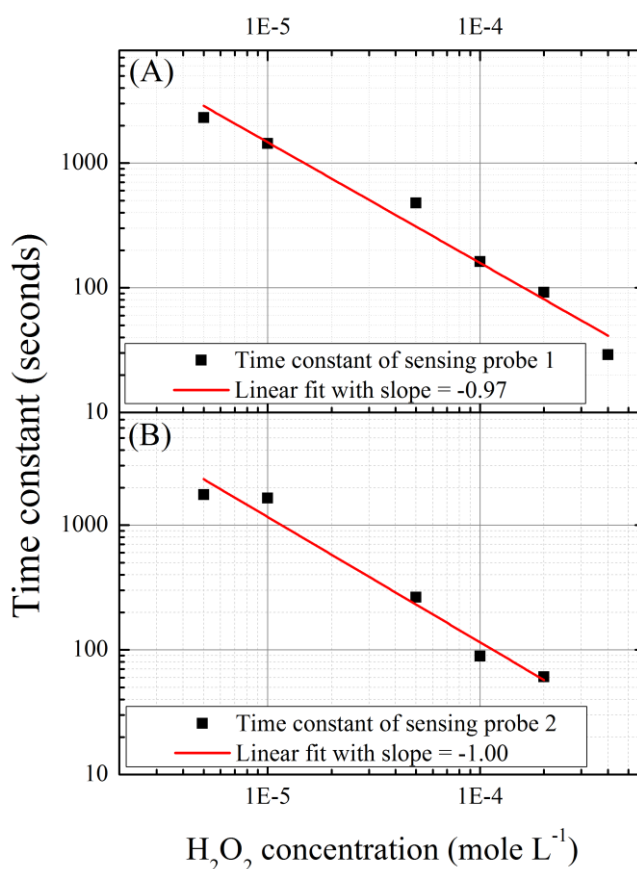


Figure 4-9: Time constant of two different optrodes versus H_2O_2 concentration at pH 2.

4.3.2.3. Durability

The durability of an optrode is evaluated by performing similar sensing experiments five, six, and nine months after fabrication. Fig. 4-10 presents the response of the optrode versus H_2O_2 concentration. The time constant of the optrode varies linearly with H_2O_2 concentration for all tests after five, six, and nine months, as shown in Fig. 4-10. The response and the slopes are similar with R^2 values of 0.97, 0.92, and 0.99 and slopes of -0.97, -1.04, and -1.07 for the best linear fits after five, six, and nine months, respectively. These features indicate acceptable durability of the optrode and a long-term stability of the PB film deposited on the tip of the optical fiber through the single-source precursor technique.

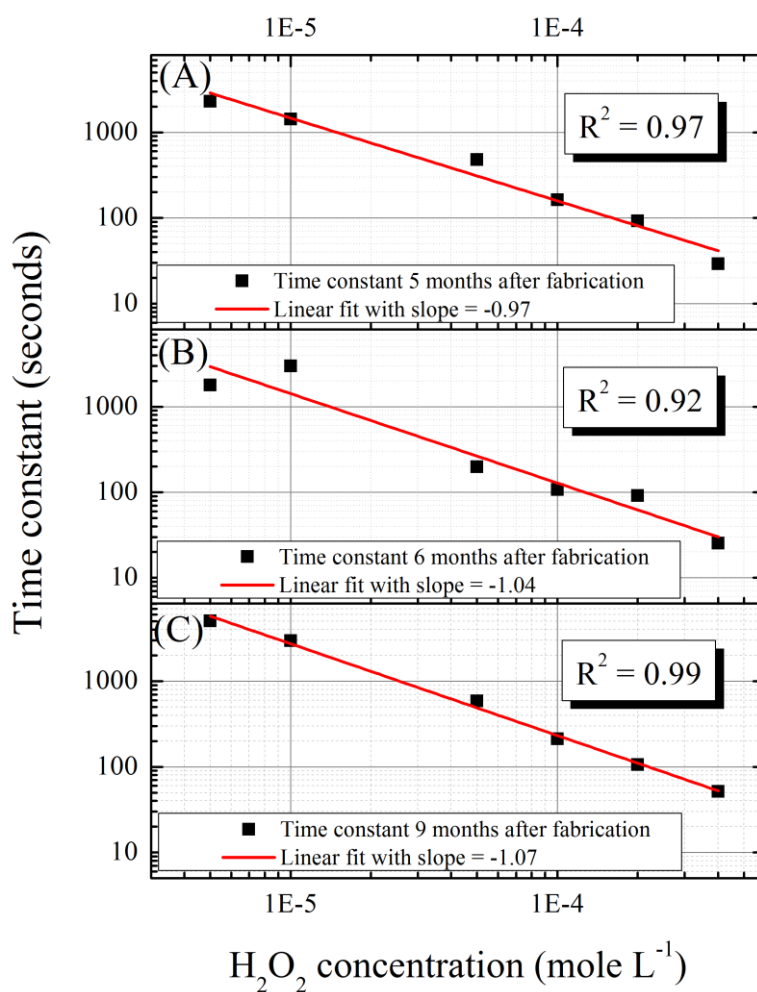


Figure 4-10: Time constant of an optrode versus H_2O_2 concentration (A) five, (B) six, and (C) nine months after its fabrication.

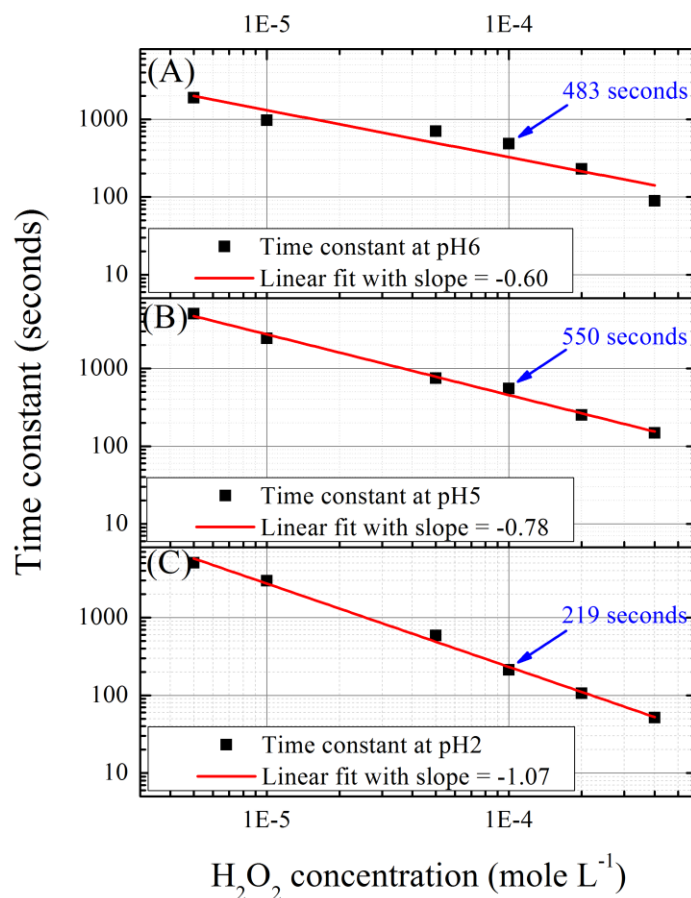


Figure 4-11: Time constant of an optrode versus H_2O_2 concentration in solutions with (A) pH 6, (B) pH 5, and (C) pH 2.

4.3.3. pH-dependent Sensitivity

The optrode time constant depends on the pH of the H_2O_2 test solutions, see Fig. 4-4. To further evaluate the dependency of the sensor response on the pH of the test solution, tests were performed at three different pH values (*i.e.* pH 2, 5, and 6) with different concentrations of H_2O_2 . Fig. 4-11A – 4-11C illustrate the response of an optrode versus H_2O_2 concentration at pH 6, 5, and 2, respectively. The sensor was found to be functional in all three pH values with a linear response to H_2O_2 concentration on a log-log scale. However, the slope of the best linear fit to the time constant of the sensor varies with pH value (*i.e.* -0.6, -0.78, and -1.07 at pH 6, 5, and 2 respectively). The sensor sensitivity ($\text{s mol}^{-1} \text{L}$) increases with decreasing pH of the H_2O_2 test solution. This suggests that the H_2O_2 reduction rate increases with increasing H_2O_2 concentration at lower pH values. We also note that the time constant of the sensor in $100 \mu\text{mol L}^{-1}$ of

H₂O₂ is lowest at pH 2 which confirms the results obtained in Fig. 4-4. The results also point to the need for independent pH monitoring in environments with unknown or fluctuating pH values.

4.4. Conclusions

The effect of pH on the sensing behavior of the PB-based H₂O₂ optrode was characterized and the optrode ability to detect H₂O₂ across a wide range of pH values (*i.e.* from pH 2 to pH 7) demonstrated. The pH dependency was quantified as the time constant of the optrode. Shorter time constants (*i.e.* faster response) were obtained at lower pH values. The linear response of the optrode to H₂O₂ concentration allows us to detect and quantify the concentration of H₂O₂ with good precision (*i.e.* R² of 0.99). The optrode shows repeatable response to H₂O₂ concentrations with improved reliability at higher concentrations. Sensing experiments with different optrodes exhibit the similar linear behavior with different time constants which indicates that each sensor requires individual calibration. The optrode also shows reliable responses five, six, and nine months after fabrications with the R² values of 0.97, 0.92, and 0.99, respectively, for the best linear fits on the time constant. This verifies the durability of the probe and long-term stability of the PB film deposited on the tip of the optical fiber through the single-source precursor technique. Sensing tests at three different pH values (*i.e.* pH 2, 5, and 6) with different concentrations of H₂O₂ reveal that the optrode remains functional at all pH values with a linear response to H₂O₂ concentration on a log-log scale. Moreover, the sensor sensitivity (s mol⁻¹ L) increases with decreasing test solution pH.

Although this work was primarily motivated by the need to develop *in situ* detection of H₂O₂ in an operating PEM fuel cell, where low pH values (~2) prevail, the optrode described in this paper can be used in a variety of industrial and environmental systems and could potentially be adapted to biological applications and physiological environments once appropriately calibrated.

Chapter 5

Effect of Deposition Conditions on Stability of PB Films at PEMFC's Operating Temperatures and pH

(Journal of The Electrochemical Society, volume **163** (6), 2016, B185–B187)

Reprinted with permission from *J. Electrochem. Soc.*, **163**, B185 (2016). Copyright 2016, The Electrochemical Society.

Preamble

Sensor development and detection of H₂O₂ concentrations at room temperature and different pH values including pH 2 (PEM fuel cell's operating pH) are shown in the previous chapters. Having established the functionality in an environment with pH value typical of an operating PEM fuel cell, it remains to establish the stability of the sensor at temperatures similar to an operating PEM fuel cell. For *in situ* detection of H₂O₂ in PEM fuel cells, the sensor must withstand the temperatures between 60 °C to °80 C. A set of experiments are performed and presented in this chapter, investigating the sensor stability at such temperatures. PB films are deposited under different conditions and the stability of the produced PB films is examined in solutions at elevated temperatures with pH 2. The deposition conditions under which the most stable PB film is obtained are identified and presented in this chapter.

The Body of this chapter was published in *Journal of The Electrochemical Society*.

Abstract

Optrodes based on Prussian blue (PB) are promising for hydrogen peroxide

detection within PEMFCs to study the Membrane-Electrode-Assembly degradation. The PB film is however required to sustain the harsh environment of PEMFCs. In this work, PB films were deposited through different conditions and soaked in Phosphate-Buffer-Solutions with pH 2 at elevated temperatures for a day. These PB films were characterized using FTIR to analyze their stability following PBS processing at operating temperature and pH corresponding to an operating PEMFC. The PB film prepared using the single-source precursor at the temperature of 60 °C is found to be the most stable.

5.1. Introduction

Hydrogen peroxide (H₂O₂) is one of the chemical species associated with degradation of the electrolyte membrane in PEMFCs [75, 4]. Understanding the underlying degradation mechanisms requires H₂O₂ sensors that function in the harsh environment of PEMFCs. Various approaches proposed to date for sensing H₂O₂ are reviewed in Botero et al, Sensors and Actuators 2013 [59]. Here we focus on sensing based on Prussian blue (PB), ferric ferrocyanide, which has been successfully demonstrated as an indicator of H₂O₂ [36]. However, PB film was found to leach into the sensing test solution at the temperatures and pH levels of an operating PEMFC, leading to an inconsistent sensing behavior [60]. This paper presents an experimental study of the stability of PB films deposited with alternative methods and at various temperatures.

The presence of H₂O₂ in PEMFCs has been detected by analysis of the effluent condensate from the anode and cathode [8, 76, 77]. Two pathways have been proposed for the formation of H₂O₂ in PEMFCs. First, oxygen reduction occurs at the cathode according to the reaction (5-1). The alternative view is based on the crossover of oxygen from the cathode to the anode side, which provides the oxygen needed to react with hydrogen, and produces H₂O₂ at the anode, reaction (5-2) and (5-3) [9].



Membrane degradation by H₂O₂ has been investigated by introducing Nafion

membranes to H₂O₂ solutions at 80 °C [4, 9]. After H₂O₂ processing of Nafion, fluoride and sulfate ions (F⁻ and SO₄²⁻) were detected in the solution which are derived from the C-F bonds and the sulfonic acid groups, respectively. Kinumoto et al. observed that the loss of sulfonic acid groups of Nafion reduces the proton conductivity, and the decomposition of the C-F bonds leads to membrane thinning and the formation of pinholes [4]. Qiao et al. showed that the proton conductivity, water uptake and the water self-diffusion coefficient gradually decrease with H₂O₂ processing [7]. Furthermore, Nafion is used in the catalyst layer to provide ionic conduction pathways. Therefore, decomposition of Nafion inside the catalyst layer also causes a reduction in the effective reaction area and increases the overpotential of the cell [4].

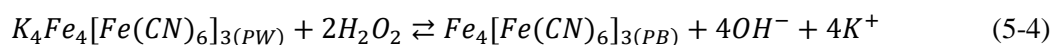
For *in situ* detection of H₂O₂ inside the fuel cell electrochemical and spectroscopic techniques are preferred among other conventional techniques such as titrimetric, colorimetric, and gasometric because of the challenges involved in *in situ* detection of H₂O₂. These challenges comprise the low concentration of H₂O₂, lack of space for insertion of a sensor into a cell, the corrosive environment, and the electrochemical noises inside a cell.

To date, the only report of *in situ* detection of H₂O₂ is based on an electrochemical method in which, Pt wires were used as electrodes to detect H₂O₂ in a PEMFC [7]. These sensors were able to detect H₂O₂ in the fuel cell but were not able to measure concentrations. The applicability of this or any other amperometric sensors in this application is limited by interference effects from the electrical fields created by fuel cell operation. The currents in fuel cells are a potential source of electromagnetic noise which can induce currents in the Pt wires, based on Faraday's law of induction, leading to inaccurate measurements.

Recently, optrodes have been demonstrated for *in situ* sensing of temperature and relative humidity in PEMFCs [21, 22]. Optrodes are well-suited to this application because their small size allows high spatial resolution and minimally disruptive access to the fuel cell. Furthermore, optical signals do not interfere with electrochemical processes in the fuel cell and are immune to electromagnetic interference. In addition, the fiber material (i.e. silica glass) is compatible with the electrochemically active environment

inside the fuel cell.

In a recent study, the authors developed an H₂O₂ optrode based on chemical deposition of PB onto the tip of an optical fiber [56]. The sensor detects H₂O₂ in a spectroscopic manner based on the oxidation of Prussian white (PW), PB reduced state, to PB in presence of H₂O₂, reaction (5-4), and evaluation of corresponding changes of the reflected light from the optrode. This sensor responds reliably to H₂O₂ concentrations in aqueous solutions at room temperature. However, the sensor responses are not consistent at higher temperatures which is likely attributed to leaching of the PB film into the sensing test solution.



In the present work, we want to address the stability of PB films at elevated temperatures. PB films were deposited on glass microscopy slides at different condition. The samples were immersed in Phosphate-Buffer-Solution (PBS) at elevated temperature and low pH to investigate the film stability in environment similar to that in an operating fuel cell. These PB films were characterized using Fourier transform infrared spectroscopy (FTIR) to assess their stability following PBS processing.

5.2. Experimental

5.2.1. Deposition of Prussian Blue Films

PB films were deposited on the substrates using three different processes. The first process comprises chemical deposition of PB through the sol-gel process and dip-coating technique. The sol-gel process was performed using a mixture of 25 mL of anhydrous ethanol, 25 ml of TEOS, 50 mL of an aqueous solution of 0.1 M hydrochloric acid, 50 mM potassium ferrocyanide, and 50 mM iron chloride (III). The prepared mixture was left at room temperature for 4 hours for gelation.

The second process comprises chemical deposition of PB films over a 5 hour period using a solution, containing both iron valences, of 5 mM potassium ferrocyanide and 5 mM iron chloride (III) in 50 mL of an aqueous solution of 0.1 M hydrochloric acid.

The third process involved deposition of PB films using potassium ferricyanide as a

single-source precursor (SSP). SSP is a synthesis approach in which all the elements that are required in the final product are incorporated into one compound. Following the procedure discussed in our previous work [56] to synthesize PB using potassium ferricyanide, photo-induced deposition of PB films was performed during 5 hours, in which 10 mM of potassium ferricyanide was added to 50 mL of an aqueous solution of 0.1 M hydrochloric acid [56]. All three processes were performed in solutions at 60 °C and the prepared samples were dried first at room temperature and then at 100 °C for 15 min. The sources of the chemicals are documented in table 5-1. Thermo Scientific glass microscopy slides were prepared and used as the substrate in all deposition processes. The chemical composition of the slide is: SiO₂ 72.20%, MgO 4.30%, Na₂O 14.30%, Al₂O₃ 1.20%, K₂O 1.20%, Fe₂O₃ 0.03%, CaO 6.40%, SO₃ 0.30%.

Table 5-1: Source of Chemicals.

| Chemicals | Product No. | Source |
|--|-------------|-------------------|
| Potassium ferrocyanide | 14459-95-1 | VWR International |
| Potassium ferricyanide | 13746-66-2 | Sigma-Aldrich |
| Iron chloride (III) hexahydrate | 7119.2 | Carl Roth |
| Tetraethyl orthosilicate (TEOS) | 86578 | Aldrich chemistry |
| Anhydrous ethanol | 64-17-5 | Fisher chemical |
| Di-sodium hydrogen phosphate dihydrate | 4984.1 | Carl Roth |
| Sodium dihydrogen phosphate dihydrate | 13472-35-0 | VWR International |

To increase the adhesion of PB films to the substrate, the OH groups on the surface of the substrate were activated by an acid treatment comprised of first washing with soap and distilled water and then treating with 68% HNO₃ for 5 minutes. The substrate was then rinsed with distilled water and cleaned with ethanol. Finally, the substrate was placed into the oven at 100 °C for 2 hours.

To study the effect of synthesis temperature on stability of PB films, additional samples were prepared through the SSP route at temperatures of 40 °C, 60 °C, and 80 °C. Deposition was also attempted at 20 °C, but the rate of deposition was found too slow.

Figure 5-1 shows the experimental procedure.

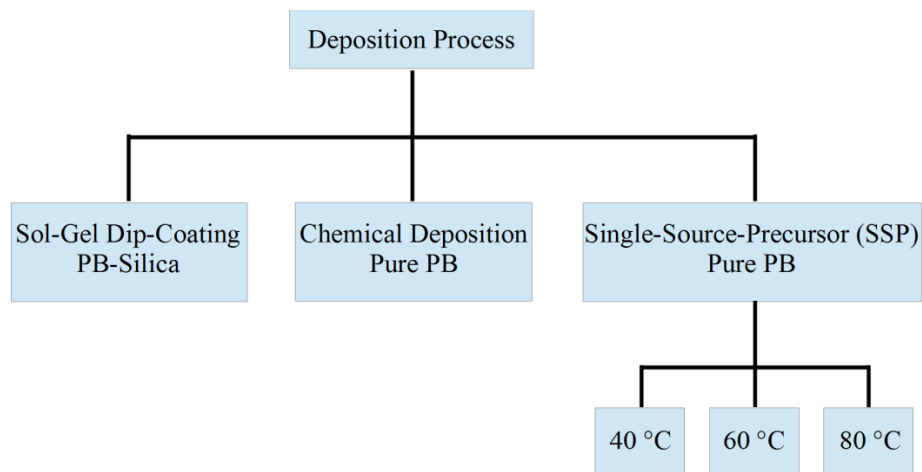


Figure 5-1: Experimental procedure

5.2.2. PBS Processing of Samples

PBS at pH 2 and buffer strength of 100 mM was prepared using di-sodium hydrogen phosphate dihydrate and sodium dihydrogen phosphate dihydrate. Two samples were prepared using each deposition processes, with one sample subjected to PBS processing, and each deposition process has been done twice to ensure the repeatability of the results. PBS processing was performed by immersing and leaving the samples in PBS at 80 °C for 21 hours and, thereafter, at 90 °C for 3 hours. Finally both samples prepared using each deposition processes were characterized using FTIR to study the effect of deposition process and synthesis temperature on stability of PB films.

5.3. Results and Discussion

5.3.1. Effect of Synthesis Process and Precursors

Figure 5-2 shows the FTIR spectra, in the range 2500 – 1500 cm^{-1} , of the samples synthesized through different processes before (solid lines) and after (dashed lines) PBS processing. The peak at 2083 cm^{-1} is the characteristic absorption peak of PB which is ascribed to the stretching vibration of $\text{C}\equiv\text{N}$ group in PB structure [78]. Considering the Beer-Lambert law, equation (5-5), the transmittance of light (T) through the material has an inverse relation with the amount concentration of material (c_i) within the pass length of the beam of light (l). Since just the characteristic absorption peak of PB is studied here

the molar attenuation coefficient (ε_i), which is an intrinsic property of a material, would be constant. Therefore, increasing the transmittance in FTIR spectra would be due to decreasing the amount of PB within the sample. This might happen in case of leaching PB film into the PBS.

$$T = 10^{-\sum_{i=1}^N \varepsilon_i \int_0^l c_i(z) dz} \quad (5-5)$$

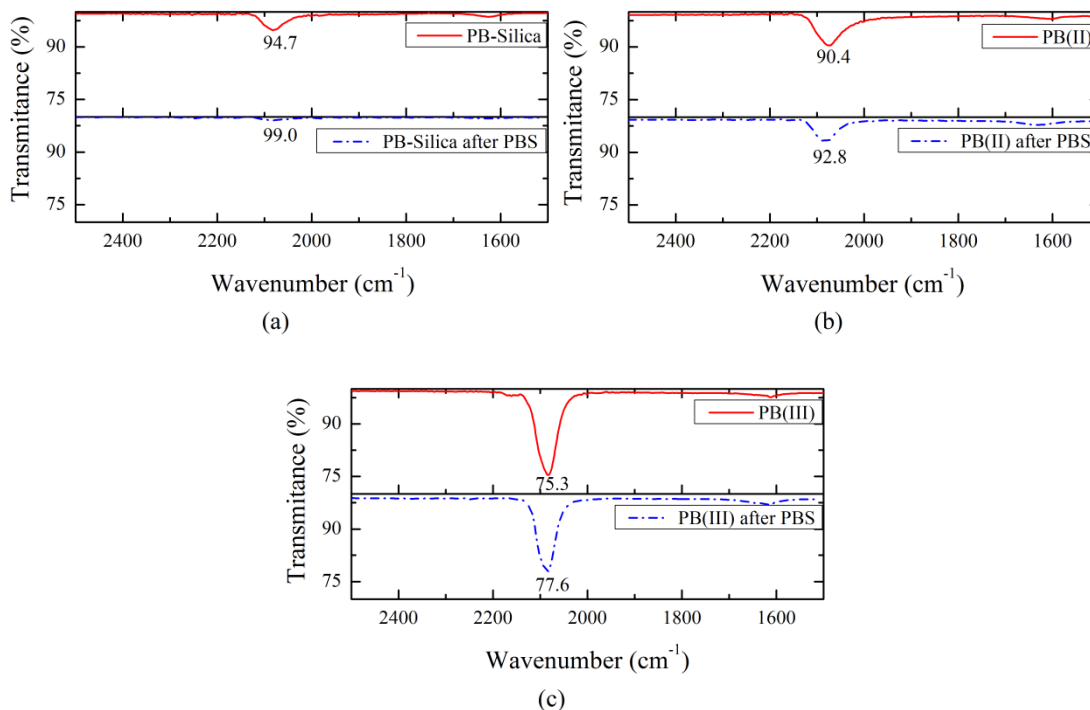


Figure 5-2: FTIR spectra of PB films synthesized through (a) sol-gel process, (b) chemical process using potassium ferrocyanide and iron (III) chloride, and (c) SSP process using potassium ferricyanide, before (solid line) and after (dashed line) PBS processing.

Among the three different deposition processes, the samples prepared through the sol-gel process, Figure 5-2 (a), exhibits the weakest peak at 2083 cm⁻¹ before PBS processing, and almost no characteristic peak after PBS processing. This indicates the PB film has completely leached into the PBS. Conversely, the sample prepared with the SSP process, Figure 5-2 (c), has the strongest peak at 2083 cm⁻¹ both before and after PBS processing, indicating this is the most stable PB film. The sample which was prepared with the chemical process using both iron valences, Figure 5-2 (b), does not suffer from complete leaching in PBS; however the characteristic peak of PB at 2083 cm⁻¹ is not as

strong as the peak for the samples prepared using SSP. We conclude that less PB is deposited onto the substrate through the second process compared to the SSP process.

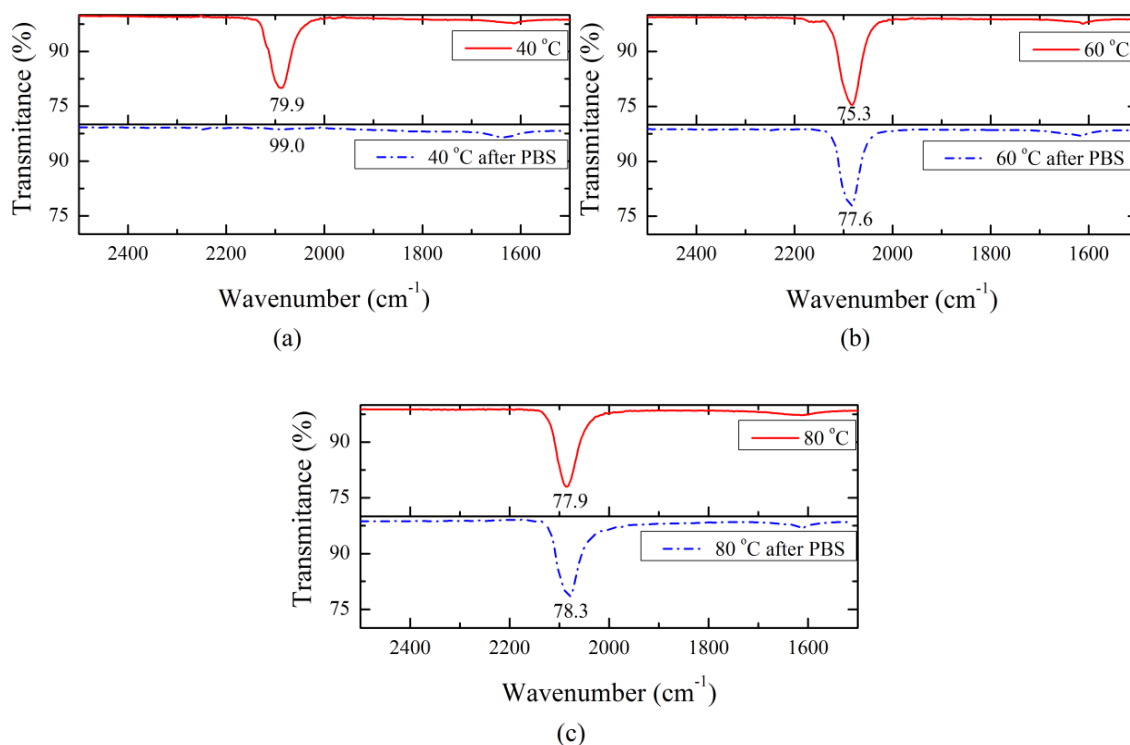


Figure 5-3: FTIR spectra of PB films synthesized at (a) 40 °C, (b) 60 °C, and (c) 80 °C, before (solid line) and after (dashed line) PBS processing.

5.3.2. Effect of Synthesis Temperature

The PB film prepared through the SSP process was the most stable both before and after PBS processing. Therefore, this process was chosen for further investigation with respect to the effect of synthesis temperature on the stability of PB films. Figure 5-3 depicts the FTIR spectra in the range of 2500 cm^{-1} to 1500 cm^{-1} for the samples synthesized at different temperatures ranging from 40 °C to 80 °C. The solid lines and dashed lines are the spectra of the samples before and after PBS processing, respectively. The sample which was prepared at 40 °C has no distinct peak at 2083 cm^{-1} after PBS processing which indicates the PB film has completely leached into the PBS, Figure 5-3 (a). On the other hand, the PB films prepared at 60 °C and 80 °C have a strong peak at 2083 cm^{-1} both before and after PBS processing (Figure 5-3 (b) and (c)) which confirms stability of PB films prepared at these temperatures. As there is no significant difference

between the PB films prepared at 60 °C and 80 °C, a temperature of 60 °C is selected as the synthesis temperature to achieve the most stable PB film through this technique.

5.4. Summary

PB films were synthesized using three different chemical processes. The stability of the films was assessed by PBS processing at temperature and pH corresponding to an operating PEMFC. The film prepared through SSP had the highest stability after PBS processing. The effect of synthesis temperature on stability of the PB films was also investigated by preparing films through SSP route at temperatures of 40 °C, 60 °C, and 80 °C, and by subsequently processing the samples in PBS solutions. This experiment revealed the film that was prepared at 40 °C was completely leached into the PBS, while the films that were prepared at 60 °C and 80 °C were sufficiently robust to sustain the PBS processing.

Preparing optrodes based on PB through SSP at temperature of 60 °C and performing sensing tests at temperature and pH corresponding to an operating PEMFC will be considered in future work.

Chapter 6

Conclusions and Future Work

This chapter links the contributions of this dissertation and summarizes the findings from the three studies presented in Chapters 3 to 5. Possible avenues for future work are also discussed in this chapter.

6.1. Conclusions and Contributions

This dissertation presents the development of a novel optrode, and demonstrates the sensing behavior of the proposed sensor toward detection and measurement of H_2O_2 under a range of conditions. The motivation for carrying out this research was to develop a sensor that can be used for detection and measurement of H_2O_2 concentrations in an environment similar to that in an operating PEM fuel cell. However, the development of such a sensor is challenging because the sensor is required to have specific characteristics to be able to work and sustain the harsh environment inside an operating PEM fuel cell. The first stage in this research focused on a review of previous work and state of the art to select a suitable sensing technique. Based on a preliminary assessment and the fact that there are active electrical and electromagnetic fields inside an operating PEM fuel cell, a spectroscopic technique was deemed preferable to other techniques (e.g. electrochemical or amperometric techniques). Several challenges, mainly related to the stability of the sensor at PEM fuel cells operating conditions, needed to be addressed to allow successful implementation of the technique. These challenges were addressed in three studies presented as contributions in Chapters 3 to 5.

6.1.1. Spectroscopic Detection of Hydrogen Peroxide with an Optical Fiber Probe using Chemically Deposited Prussian Blue

In the first study (Chapter 3), an H_2O_2 optrode was developed by chemical deposition of PB onto the tip of an optical fiber. The main objective of this study was to prepare a sensor with repeatable sensing response to H_2O_2 concentrations.

Multiple optrodes were prepared using the same procedure and sensing tests protocols. The sensing behavior of the optrodes to H_2O_2 concentrations was found to be inconsistent between different optrodes. Examination and analysis of the results prompted a change of this study from assessing the sensing behavior of the optrode to investigating the chemical deposition of PB films.

PB films prepared through the same chemical technique with different deposition parameters were characterized using Raman spectroscopy. This revealed that fluorescent lamp light (Philips Alto, F28T5 25W) exposure affects the purity of the prepared films. The light exposure leads to the formation of pure PB film, whereas deposition in darkness leads to co-precipitation of PB and BG.

After resolving the above problem several new optrodes were prepared under controlled light exposure during deposition of PB films. The new set of optrodes were found to behave consistently, and additional sensing tests were performed to assess the repeatability and reproducibility of sensor response. The durability of the optrode was also established by subjecting an optrode to multiple experiments during seven months and comparing the sensor responses to H_2O_2 concentrations four and seven months after the optrode preparation.

This study resulted in a novel H_2O_2 optrode in which the PB film is deposited onto the tip of an optical fiber through the photoinduced SSP technique. Using this sensor, H_2O_2 can be detected and measured in buffered solutions at room temperature with pH 4. The sensor characteristics (i.e. repeatability, reproducibility, and durability) were examined and the sensor response found to be reliable under this condition.

6.1.2. pH-dependent Response of a Hydrogen Peroxide Sensing Probe

The performance of the PB-based H₂O₂ optrode prepared through other methods (e.g. LbL technique) is limited in environments with different pH values. Therefore, in the second study (Chapter 4), the sensor's capability for detection and measurement of H₂O₂ under a range of pH values was investigated, including pH value corresponding to a PEM fuel cell environment.

The sensor response was initially assessed in solutions with a constant concentration of H₂O₂ at different pH (i.e. 2 to 7) to demonstrate the sensor capability to detect H₂O₂ at different pH values. However, the sensor response was found to be affected by the pH, with faster response times obtained at lower pH values.

Further sensing tests were carried out at pH 2 with multiple optrodes prepared at different times through the same process. These optrodes are capable of detecting and measuring different concentrations of H₂O₂ at pH 2 and show repeatable response to H₂O₂ concentrations with the more reliable response at higher concentrations. The results also indicate acceptable durability of the probe and long-term stability of the PB film.

Investigation of the effect of pH on sensitivity of the optrode confirmed the sensor capability to detect and measure different concentrations of H₂O₂ at different pH values, and showed the sensitivity of the sensor is also affected by the pH, whereby optrode has higher sensitivity to H₂O₂ concentrations at lower pH values.

In summary, the optrode was found to be functional at the pH corresponding to an operating PEM fuel cell. This paves the way for developing a sensor for *in situ* detection of H₂O₂ inside PEM fuel cells. Moreover, the sensor works in a wide range of pH values (i.e. from pH 2 to pH 7) that suggests this sensor as a suitable candidate for applications in environments with the pH values in the range of 2 to 7. Investigating the effect of pH on sensing behavior of the optrode shows the sensor has faster response times and higher sensitivities at lower pH values.

6.1.3. Effect of Deposition Conditions on Stability of PB Films at PEMFC's Operating Temperatures and pH

Although the sensor is functional at PEM fuel cell's operating pH, the stability of the sensor at PEM fuel cell's operating temperature needed to be established. In the third study (Chapter 5), PB films were prepared under different conditions and the stability of the films in solutions with pH 2 and at elevated temperatures were assessed by FTIR analysis.

PB films were deposited by sol-gel dip coating, direct chemical process, and SSP techniques. Experiment and FTIR analysis revealed that the film prepared through SSP technique has the highest stability after PBS processing.

The effect of synthesis temperature on stability of PB films was also investigated. The FTIR analysis of these samples shows the film prepared at 40 °C is completely leached into PBS, while the films prepared at 60 °C and 80 °C are sufficiently robust to sustain the PBS processing.

A key conclusion is that optrodes prepared using the SSP technique at 40 °C might not be stable for *in situ* sensing in PEM fuel cells. Instead, the optrode should be prepared using the same technique but at a synthesis temperature of 60 °C to sustain the high temperatures inside PEM fuel cells.

6.1.4. Conclusions

This work presents a novel optrode for detection and measurement of H₂O₂ concentrations at temperatures and pH corresponding to an operating PEM fuel cell. The proposed optrodes capitalize on some of the unique advantages of the fiber-optic devices such as small size, flexibility, and immunity to electromagnetic interference. The effect of synthesis conditions on properties of PB films was systematically studied, revealing the effect of light exposure during deposition of PB films on purity of the films and the effect of deposition technique and temperature on stability of PB films at elevated temperatures. The proposed optrodes pave the way for developing high performance H₂O₂ sensor applicable for *in situ* PEM fuel cell measurements, as well as portable H₂O₂ sensors for a range of applications with environments with a pH range of 2 to 7 and temperatures of

less than 90 °C.

6.2. Future work

Although the initial motivation for this research was to develop a sensor that can be used for detecting H₂O₂ concentrations inside PEM fuel cells, the functionality of the developed sensor is only demonstrated *ex situ* in solutions with pH 2 (PEM fuel cell's operating pH).

Extension of this research should next focus on the development of optrodes based on PB films through SSP technique at temperature of 60 °C, and deployment of the sensors for *in situ* PEM fuel cell tests. The *in situ* sensing tests might be done by embedding multiple sensors into the flow channels to increase the chance of H₂O₂ detection, and running the fuel cell under stress conditions conducive to H₂O₂ formation. One major challenge in this work might be related to placement of the sensors into the fuel cell in such a way as to allow the recovery of the sensor in ascorbic acid after exposure to H₂O₂. In his doctoral dissertation, Botero-Cadavid suggests a method for integration of this kind of sensors in PEM fuel cells [79].

Further work will also be required to develop *in situ* calibration procedures to allow sensing in an operating PEM fuel cell. For this, an H₂O₂ vapor generator is necessary. In an H₂O₂ vapor generator, a hot air stream with a temperature around 100 °C is introduced to a container of liquid mixture of H₂O₂/H₂O. The resultant flow exiting from the container of H₂O₂/H₂O mixture is at sufficiently high temperature for all components (i.e. air, H₂O₂, and H₂O) to be in the gaseous phase. This stream can be introduced to a fuel cell through the flow field. On the other hand, a coolant flow through bipolar plates is necessary to keep the flow fields at the desired (lower) temperatures and decrease the temperature of the air/H₂O₂/H₂O stream. This causes some portion of H₂O₂/H₂O mixture condenses into liquid.

Bibliography

- [1] Matthew M. Mench. *Fuel cell engines*. John Wiley & Sons, Inc., 2008.
- [2] N Djilali and PC Sui. Transport phenomena in fuel cells: from microscale to macroscale. *International Journal of Computational Fluid Dynamics*, 22(1-2):115–133, 2008.
- [3] Jing Zhao, Yalin Yan, Li Zhu, Xiaoxi Li, and Genxi Li. An amperometric biosensor for the detection of hydrogen peroxide released from human breast cancer cells. *Biosensors and Bioelectronics*, 41:815–819, 2013.
- [4] Taro Kinumoto, Minoru Inaba, Yoko Nakayama, Kazuhito Ogata, Ryota Umebayashi, Akimasa Tasaka, Yasutoshi Iriyama, Takeshi Abe, and Zempachi Ogumi. Durability of perfluorinated ionomer membrane against hydrogen peroxide. *Journal of power sources*, 158(2):1222–1228, 2006.
- [5] A Pozio, RF Silva, M De Francesco, and L Giorgi. Nafion degradation in pefcs from end plate iron contamination. *Electrochimica acta*, 48(11):1543–1549, 2003.
- [6] Haolin Tang, Shen Peikang, San Ping Jiang, Fang Wang, and Mu Pan. A degradation study of nafion proton exchange membrane of pem fuel cells. *Journal of Power Sources*, 170(1):85–92, 2007.
- [7] Wen Liu and David Zuckerbrod. In situ detection of hydrogen peroxide in pem fuel cells. *Journal of The Electrochemical Society*, 152(6):A1165–A1170, 2005.
- [8] Vishal O Mittal, H Russell Kunz, and James M Fenton. Is h₂o₂ involved in the membrane degradation mechanism in pemfc? *Electrochemical and Solid-State Letters*, 9(6):A299–A302, 2006.
- [9] Jinli Qiao, Morihiro Saito, Kikuko Hayamizu, and Tatsuhiko Okada. Degradation of perfluorinated ionomer membranes for pem fuel cells during processing with h₂o₂. *Journal of The Electrochemical Society*, 153(6):A967–A974, 2006.
- [10] Vijay A Sethuraman, John W Weidner, Andrew T Haug, Sathya Motupally, and Lesia V Protsailo. Hydrogen peroxide formation rates in a pemfc anode and cathode effect of humidity and temperature. *Journal of The Electrochemical Society*, 155(1):B50–B57, 2008.
- [11] Biyan Zhou, Jihua Wang, Zhenfei Guo, Huoquan Tan, and Xiaochuan Zhu. A simple colorimetric method for determination of hydrogen peroxide in plant tissues. *Plant Growth Regulation*, 49(2-3):113–118, 2006.
- [12] George Eisenberg. Colorimetric determination of hydrogen peroxide. *Industrial & Engineering Chemistry Analytical Edition*, 15(5):327–328, 1943.
- [13] William M Dehn. A gasometric method for the determination of hydrogen peroxide. *Journal of the American Chemical Society*, 29(9):1315–1319, 1907.

- [14] Jian Yao Zheng, Yongli Yan, Xiaopeng Wang, Wen Shi, Huimin Ma, Yong Sheng Zhao, and Jiannian Yao. Hydrogen peroxide vapor sensing with organic core/sheath nanowire optical waveguides. *Advanced Materials*, 24(35):OP194–OP199, 2012.
- [15] Robert Koncki, Tomasz Lenarczuk, Anna Radomska, and Stanislaw Glab. Optical biosensors based on prussian blue films. *Analyst*, 126:1080–1085, 2001.
- [16] Ignacio DelVillar, Ignacio R. Matías, Francisco J. Arregui, and Richard O. Claus. Esa-based in-fiber nanocavity for hydrogen–peroxide detection. *IEEE TRANSACTIONS ON NANOTECHNOLOGY*, 4(2):187–193, March 2005.
- [17] Ignacio DelVillar, Ignacio R. Matias, Francisco J. Arregui, Jes´us Echeverr´a, and Richard O. Claus. Strategies for fabrication of hydrogen peroxide sensors based on electrostatic self-assembly (esa) method. *Sensors and Actuators B*, 108:751–757, 2005.
- [18] Li Wang, Haozhi Zhu, Yonghai Song, Li Liu, Zhifang He, Lingli Wan, Shouhui Chen, Ying Xiang, Shusheng Chen, and Jie Chen. Architecture of poly (o-phenylenediamine)–ag nanoparticle composites for a hydrogen peroxide sensor. *Electrochimica Acta*, 60:314–320, 2012.
- [19] Qiang Yan, Zhiliang Wang, Jian Zhang, Hui Peng, Xuejiao Chen, Huina Hou, and Chunran Liu. Nickel hydroxide modified silicon nanowires electrode for hydrogen peroxide sensor applications. *Electrochimica Acta*, 61:148–153, 2012.
- [20] Xuemi Hu and Shiquan Tao. An optical fiber h₂o₂-sensing probe using a titanium(iv) oxyacetylacetonate immobilized nafion coating on a bent optical fiber probe. *IEEE Sensors Journal*, 11:2032–2036, 2011.
- [21] Nigel A David, Peter M Wild, Jingwei Hu, and Nedjib Djilali. In-fibre bragg grating sensors for distributed temperature measurement in a polymer electrolyte membrane fuel cell. *Journal of Power Sources*, 192(2):376–380, 2009.
- [22] NA David, PM Wild, J Jensen, T Navessin, and N Djilali. Simultaneous in situ measurement of temperature and relative humidity in a pemfc using optical fiber sensors. *Journal of The Electrochemical Society*, 157(8):B1173–B1179, 2010.
- [23] Xnemei Hu Shiquan Tao, Joseph C. Fanguy. Fiber optic sensors for in situ real-time monitoring pem fuel cell operation. In *Proceedings of FUELCELL2005 Third International Conference on Fuel Ceil Science, Engineering and Technology*, 2005.
- [24] Ignacio DelVillar, Ignacio R. Matías, Francisco J. Arregui, and Richard O. Claus. Fiber-optic hydrogen peroxide nanosensor. *IEEE SENSORS JOURNAL*, 5(3):365–371, June 2005.
- [25] Chandrakant Tagad, Sreekantha Dugasani, Rohini Aiyer, Sungha Park, Atul Kulkarni, and Sushma Sabharwal. Green synthesis of silver nanoparticles and their application for the development of optical fiber based hydrogen peroxide sensor. *Sensors and Actuators B: Chemical*, 183:144– 149, 2013.

- [26] Edgar Pick and Yona Keisari. A simple colorimetric method for the measurement of hydrogen peroxide produced by cells in culture. *Journal of immunological methods*, 38(1):161–170, 1980.
- [27] Makoto Mizoguchi, Munetaka Ishiyama, and Masanobu Shiga. Water-soluble chromogenic reagent for colorimetric detection of hydrogen peroxide—an alternative to 4-aminoantipyrine working at a long wavelength. *Anal. Commun.*, 35(2):71–74, 1998.
- [28] Craig Gay and Janusz M Gebicki. A critical evaluation of the effect of sorbitol on the ferric–xylenol orange hydroperoxide assay. *Analytical biochemistry*, 284(2):217–220, 2000.
- [29] Aleksandra Lobnik and Merima Cajlakovic. Sol–gel based optical sensor for continuous determination of dissolved hydrogen peroxide. *Sensors and Actuators B: Chemical*, 74(1):194–199, 2001.
- [30] Evan W Miller, Orapim Tulyathan, Ehud Y Isacoff, and Christopher J Chang. Molecular imaging of hydrogen peroxide produced for cell signaling. *Nature chemical biology*, 3(5):263–267, 2007.
- [31] Evan W Miller, Aaron E Albers, Arnd Pralle, Ehud Y Isacoff, and Christopher J Chang. Boronate-based fluorescent probes for imaging cellular hydrogen peroxide. *Journal of the American Chemical Society*, 127(47):16652–16659, 2005.
- [32] Thompson M Freeman and W Rudolf Seitz. Chemiluminescence fiber optic probe for hydrogen peroxide based on the luminol reaction. *Analytical Chemistry*, 50(9):1242–1246, 1978.
- [33] Azra Tahirovic, Amira Copra, Enisa Omanovic-Miklicanin, and Kurt Kalcher. A chemiluminescence sensor for the determination of hydrogen peroxide. *Talanta*, 72(4):1378–1385, 2007.
- [34] TS Francis, Shizhuo Yin, and Paul B Ruffin. *Fiber optic sensors*. CRC press, 2010.
- [35] Erick L Bastos, Paulete Romoff, Camila R Eckert, and Wilhelm J Baader. Evaluation of antiradical capacity by h₂o₂-hemin-induced luminol chemiluminescence. *Journal of agricultural and food chemistry*, 51(25):7481–7488, 2003.
- [36] Robert Koncki, Tomasz Lenarczuk, and Stanisaw Gab. Optical sensing schemes for prussian blue/prussian white film system. *Analytica chimica acta*, 424(1):27–35, 2000.
- [37] Meng Lin, Jiao Yang, Misuk Cho, and Youngkwan Lee. Hydrogen peroxide detection using a polypyrrole/prussian blue nanowire modified electrode. *Macromolecular Research*, 19(7):673–678, 2011.
- [38] Robert Koncki. Chemical sensors and biosensors based on prussian blues. *Critical Reviews in Analytical Chemistry*, 32(1):79–96, 2002.

- [39] Kingo Itaya, Tatsuaki Ataka, and Shinobu Toshima. Spectroelectrochemistry and electrochemical preparation method of prussian blue modified electrodes. *Journal of the American Chemical Society*, 104(18):4767–4772, 1982.
- [40] Vernon D Neff. Electrochemical oxidation and reduction of thin films of prussian blue. *Journal of the Electrochemical Society*, 125(6):886–887, 1978.
- [41] Dan Du, Minghui Wang, Yuehua Qin, and Yuehe Lin. One-step electrochemical deposition of prussian blue–multiwalled carbon nanotube nanocomposite thin-film: preparation, characterization and evaluation for h₂o₂ sensing. *Journal of Materials Chemistry*, 20:1532–1537, 2010.
- [42] Ru Yang, Zaibo Qian, and Jiaqi Deng. Electrochemical deposition of prussian blue from a single ferricyanide solution. *Journal of the Electrochemical Society*, 145(7):2231–2236, 1998.
- [43] SA Agnihotry, Punita Singh, Amish G Joshi, DP Singh, KN Sood, and SM Shivaprasad. Electrodeposited prussian blue films: Annealing effect. *Electrochimica acta*, 51(20):4291–4301, 2006.
- [44] Ming Hu, Shuhei Furukawa, Ryo Ohtani, Hiroaki Sukegawa, Yoshihiro Nemoto, Julien Reboul, Susumu Kitagawa, and Yusuke Yamauchi. Synthesis of prussian blue nanoparticles with a hollow interior by controlled chemical etching. *Angewandte Chemie*, 124(4):1008–1012, 2012.
- [45] Sani Demiri, Metodija Najdoski, and Julijana Velevska. A simple chemical method for deposition of electrochromic prussian blue thin films. *Materials Research Bulletin*, 46:2484–2488, 2011.
- [46] Xinglong Wu, Minhua Cao, Changwen Hu, and Xiaoyan He. Sonochemical synthesis of prussian blue nanocubes from a single-source precursor. *Crystal Growth & Design*, 6(1):26–28, 2006.
- [47] Junfeng Zhai, Yueming Zhai, Liang Wang, and Shaojun Dong. Rapid synthesis of polyethylenimine-protected prussian blue nanocubes through a thermal process. *Inorganic chemistry*, 47(16):7071–7073, 2008.
- [48] Ignacio Del Villar, Ignacio R Matás, FJ Arregui, and RO Claus. Esa based fiber-optic sensor for continuous detection of hydrogen peroxide concentration. In *Sensors, 2003. Proceedings of IEEE*, volume 1, pages 393–396. IEEE, 2003.
- [49] Xiaomiao Feng, Zhengzong Sun, Wenhua Hou, and Jun-Jie Zhu. Synthesis of functional polypyrrole/prussian blue and polypyrrole/ag composite microtubes by using a reactive template. *NANOTECHNOLOGY*, 18:195603 (7pp), 2007.
- [50] Subramanian Bharathi and Ovadia Lev. Sol-gel-derived prussian blue-silicate amperometric glucose biosensor. *Applied biochemistry and biotechnology*, 89(2-3):209–216, 2000.

- [51] Silvia Zamponi, Anna M Kijak, Andre J Sommer, Roberto Marassi, Pawel J Kulesza, and James A Cox. Electrochemistry of prussian blue in silica sol-gel electrolytes doped with polyamidoamine dendrimers. *Journal of Solid State Electrochemistry*, 6(8):528–533, 2002.
- [52] Yu-Lin Hu, Jin-Hua Yuan, Wei Chen, Kang Wang, and Xing-Hua Xia. Photochemical synthesis of prussian blue film from an acidic ferricyanide solution and application. *Electrochemistry communications*, 7(12):1252–1256, 2005.
- [53] Akihito Gotoh, Hiroaki Uchida, Manabu Ishizaki, Tetsutaro Satoh, Shinichi Kaga, Shusuke Okamoto, Masaki Ohta, Masatomi Sakamoto, Tohru Kawamoto, Hisashi Tanaka, et al. Simple synthesis of three primary colour nanoparticle inks of prussian blue and its analogues. *Nanotechnology*, 18(34):345609, 2007.
- [54] D Ellis, M Eckhoff, and VD Neff. Electrochromism in the mixed-valence hexacyanides. 1. voltammetric and spectral studies of the oxidation and reduction of thin films of prussian blue. *The Journal of Physical Chemistry*, 85(9):1225–1231, 1981.
- [55] Robert Koncki and Otto S. Wolfbeis. Composite films of prussian blue and n-substituted polypyrroles: Fabrication and application to optical determination of ph. *Analytical Chemistry*, 70(13):2544–2550, July 1 1998.
- [56] Hamed Akbari Khorami, Juan F Botero-Cadavid, Peter Wild, and Ned Djilali. Spectroscopic detection of hydrogen peroxide with an optical fiber probe using chemically deposited prussian blue. *Electrochimica Acta*, 115:416–424, 2014.
- [57] Hamed Akbari Khorami, Peter Wild, Alexandre G Brolo, and Ned Djilali. ph-dependent response of a hydrogen peroxide sensing probe. *Sensors and Actuators B: Chemical*, 237:113–119, 2016.
- [58] Hamed Akbari Khorami, Nadine Jacobs, Peter Wagner, Alexander Dyck, Peter Wild, Alexandre G Brolo, and Ned Djilali. Effect of deposition conditions on stability of pb films at pemfc's operating temperatures and ph. *Journal of The Electrochemical Society*, 163(6):B185–B187, 2016.
- [59] Juan F Botero-Cadavid, Alexandre G Brolo, Peter Wild, and Ned Djilali. Detection of hydrogen peroxide using an optical fiber-based sensing probe. *Sensors and Actuators B: Chemical*, 185:166–173, 2013. In Press.
- [60] Juan F Botero-Cadavid, Peter Wild, and Ned Djilali. Temperature response and durability characterization of an optical fiber sensor for the detection of hydrogen peroxide. *Electrochimica Acta*, 129:416–424, 2014.
- [61] Paulette BL Chang and Thomas M Young. Kinetics of methyl< i> tert</i>-butyl ether degradation and by-product formation during uv/hydrogen peroxide water treatment. *Water research*, 34(8):2233–2240, 2000.

- [62] T Pottage, C Richardson, S Parks, JT Walker, and AM Bennett. Evaluation of hydrogen peroxide gaseous disinfection systems to decontaminate viruses. *Journal of Hospital Infection*, 74(1):55–61, 2010.
- [63] RK Root, J Metcalf, N Oshino, and B Chance. H₂O₂ release from human granulocytes during phagocytosis. i. documentation, quantitation, and some regulating factors. *Journal of Clinical Investigation*, 55(5):945, 1975.
- [64] Yu Jeong Byun, Seong Keun Kim, Young Mi Kim, Gue Tae Chae, Seong-Whan Jeong, and Seong-Beom Lee. Hydrogen peroxide induces autophagic cell death in c6 glioma cells via bnip3-mediated suppression of the mtor pathway. *Neuroscience letters*, 461(2):131–135, 2009.
- [65] Subhashinee SK Wijeratne, Susan L Cuppett, and Vicky Schlegel. Hydrogen peroxide induced oxidative stress damage and antioxidant enzyme response in caco-2 human colon cells. *Journal of agricultural and food chemistry*, 53(22):8768–8774, 2005.
- [66] Dam TV Anh, W Olthuis, and P Bergveld. A hydrogen peroxide sensor for exhaled breath measurement. *Sensors and Actuators B: Chemical*, 111–112:494–499, 2005.
- [67] Louise Samain, Bernard Gilbert, Fernande Grandjean, Gary J Long, and David Strivay. Redox reactions in prussian blue containing paint layers as a result of light exposure. *J. Anal. At. Spectrom.*, 28(4):524–535, 2013.
- [68] Ivanildo Luiz de Mattos, Lo Gorton, and Tautgirdas Ruzgas. Sensor and biosensor based on prussian blue modified gold and platinum screen printed electrodes. *Biosensors and Bioelectronics*, 18(2):193–200, 2003.
- [69] Bernhard AH Von Bockelmann and Irene LI Von Bockelmann. Aseptic packaging of liquid food products: a literature review. *Journal of agricultural and food chemistry*, 34(3):384–392, 1986.
- [70] Malcolm S Purdey, Jeremy G Thompson, Tanya M Monro, Andrew D Abell, and Erik P Schartner. A dual sensor for ph and hydrogen peroxide using polymer-coated optical fibre tips. *Sensors*, 15(12):31904–31913, 2015.
- [71] F Ricci and G Palleschi. Sensor and biosensor preparation, optimisation and applications of prussian blue modified electrodes. *Biosensors and Bioelectronics*, 21(3):389–407, 2005.
- [72] Minmin Liu, Ru Liu, and Wei Chen. Graphene wrapped cu₂o nanocubes: non-enzymatic electrochemical sensors for the detection of glucose and hydrogen peroxide with enhanced stability. *Biosensors and Bioelectronics*, 45:206–212, 2013.
- [73] Robert Koncki and Otto S Wolfbeis. Optical chemical sensing based on thin films of prussian blue. *Sensors and Actuators B: Chemical*, 51(1):355–358, 1998.
- [74] Behrooz Zargar and Amir Hatamie. Prussian blue nanoparticles: a simple and fast optical sensor for colorimetric detection of hydralazine in pharmaceutical samples. *Analytical Methods*, 6:5951–5956, 2014.

- [75] Shinji Kato, Yuya Masahira, Kazuhiko Noda, and Hatiro Imai. Degradation of solid polymer membrane in pefc by hydrogen peroxide. *ECS Transactions*, 16(48):1–5, 2009.
- [76] Minoru Inaba, Taro Kinumoto, Masayuki Kiriake, Ryota Umebayashi, Akimasa Tasaka, and Zempachi Ogumi. Gas crossover and membrane degradation in polymer electrolyte fuel cells. *Electrochimica Acta*, 51(26):5746–5753, 2006.
- [77] Kazuhiro Teranishi, Kentaro Kawata, Shohji Tsushima, and Shuichiro Hirai. Degradation mechanism of pemfc under open circuit operation. *Electrochemical and Solid-State Letters*, 9(10):A475–A477, 2006.
- [78] AM Farah, C Billing, CW Dikio, AN Dibofori-Orji, OO Oyedeji, D Wankasi, FM Mtunzi, and ED Dikio. Synthesis of prussian blue and its electrochemical detection of hydrogen peroxide based on cetyltrimethylammonium bromide (ctab) modified glassy carbon electrode. *Int. J. Electrochem. Sci*, 8:12132–12146, 2013.
- [79] Juan F Botero-Cadavid. *Fiber-optic sensor for detection of hydrogen peroxide in PEM fuel cells*. PhD thesis, University of Victoria, 2014.

Appendix A: Polymer Electrolyte Membrane Fuel Cell

PEM fuel cells have the potential to be used in portable (0-100W), stationary (0-25kW), and transportation (~ 80kW) applications. Among those, using PEM fuel cells in transportation systems is attracted more attention because of its low operating temperature (from room temperature to ~ 80°C) and high relative performance. Current and voltage of PEM fuel cells are required to be adjusted in order to generate the required power. Fuel cell current is adjustable simply by changing the size of the active electrode area. The higher active electrode area leads to higher current in a single fuel cell. On the other hand, the output voltage of a single fuel cell is always less than 1 V. This is because of the limitation that is caused by the fundamental of electrochemical potential of reactant and product species. Therefore, the voltage of a fuel cell stack is tunable by connecting several individual fuel cells in series to achieve compact design, and higher voltage and power. To have a better understanding about the fundamental of fuel cells operation, the mechanism of energy conversion within PEM fuel cells, key components of PEM fuel cells and the materials that are used in PEM fuel cells are explained below.

The basis of electricity generation in the fuel cell is electrochemical reactions that take place inside it. In general, the energy difference between products and reactants states in an exothermic electrochemical reaction minus various losses of the fuel cell system gives the operating voltage of the fuel cell. The operating voltage of the fuel cell is a driving force for electrons to flow through the external circuit and drive the load. For an electrochemical reaction to happen, there are several necessary components [1]:

1. *Anode and cathode electrodes*: electrochemical reactions happen on electrodes. Oxidation occurs at anode side and electrons are produced. Reduction occurs at cathode side and electrons are consumed. A pair of oxidation and reduction reactions is called a redox reaction and explains the overall reaction of a system.
2. *Electrolyte*: an electrolyte can be a liquid or a solid that physically separates electrodes, or in other words, fuel and oxidizer. It is ion conductive and electron insulator that prevents electron short-circuiting between electrodes. The produced ions in a half redox reaction are conducted to the other electrode through the electrolyte and the other half redox reaction happens there.

3. *External connection between electrodes for current flow:* the external circuit connects electrodes to each other. The produced electrons at anode side flow through an external circuit, drive the load, and reach to the cathode side to complete the circuit.

A PEM fuel cell also consists of an anode electrode, a cathode electrode, and a proton exchange membrane (PEM) that all together called as Membrane Electrode Assembly (MEA). Anode and cathode electrodes are connected together with an external circuit. At the anode electrode, hydrogen fuel is oxidized to hydrogen cations and produces electrons. Hydrogen cations migrate to cathode side through the electrolyte membrane. Conversely, electrons are blocked by electrolyte membrane, and flow through the external circuit, drive the load, and return to the cathode side. On the other hand, at the cathode electrode, oxygen reacts with hydrogen cations and consumes electrons. As long as anode and cathode are fed with hydrogen and oxygen, the electrons flow through the external circuit [1, 2]. Figure A-1 is a schematic of fuel cell's components and shows the general reactions happen in the fuel cell.

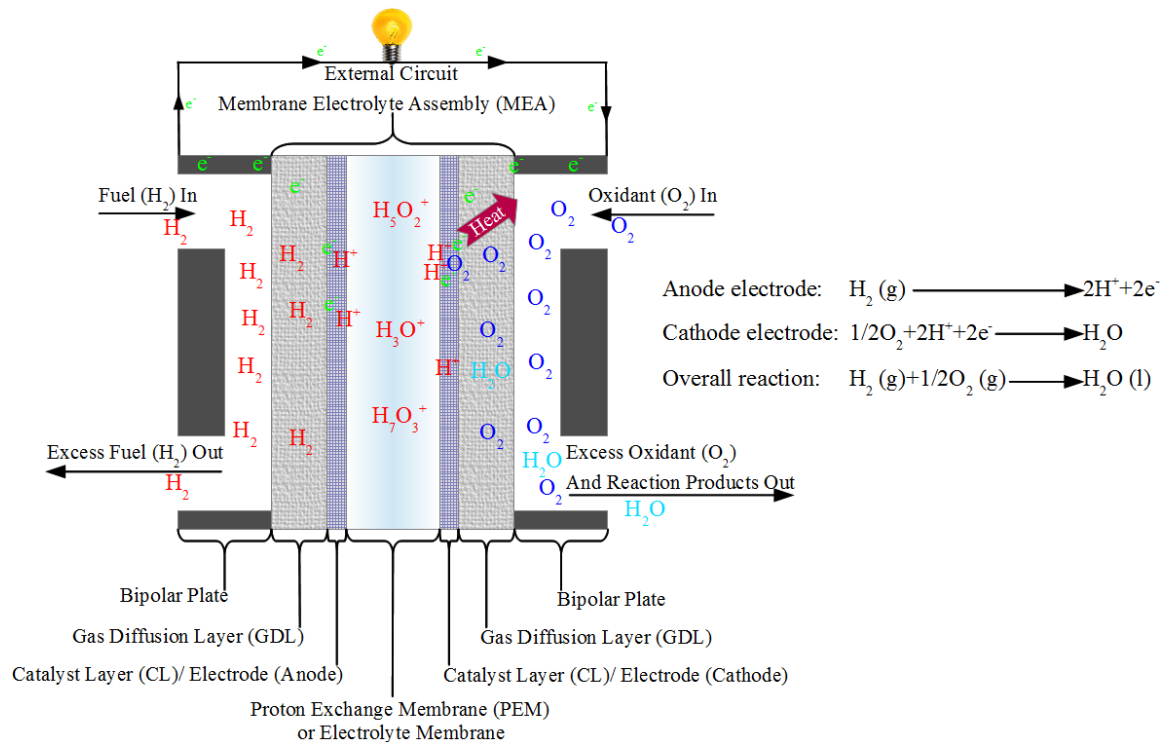


Figure A-1: Schematic of fuel cell's components and reactions.

PEM fuel cells include the following key components: polymer electrolyte membrane, catalyst layers (CL), gas diffusion layers (GDL), and bipolar plates with flow channels for reactants, products, and coolant in larger stacks [1].

The solid electrolyte membrane in the PEM fuel cell is formed from a hydrophobic and inert polymer backbone which sulfonated with hydrophilic and ionically conductive acid clusters. Nafion is the most well-studied polymer electrolyte for fuel cells which is created by sulphonation (SO_3^-) of the basic polytetrafluoroethylene (PTFE) structure, as shown in Figure A-2. Although the PTFE is not ionically conductive but provides chemical stability and durability of membrane. Clustering of the sulfonic acid side groups and hydration level are determining factors on the ionic conductivity of the electrolyte.

A catalyst layer (CL) in a PEM fuel cell is a three-dimensional porous structure consists of carbon-supported catalyst and ionomer. Electrochemical reactions at anode and cathode happen in catalyst layers. For example a reduction reaction occurs in cathode when oxygen, hydrogen ions, and electrons meet in presence of catalyst particles. For the reactions to happen ions, electrons, reactants, and products are required to be easily transported in CL. The CL must also have a high electrochemically active surface area. Ionomer and high conductive carbon particles function as an ion conductor and electron conductor, respectively. Catalyst particles decrease the required activation energy of the electrochemical reaction and promote the electrochemical reaction. Highly porous structure of the CL facilitates transport of reactants and products. Figure A-3 shows the CL at cathode electrode.

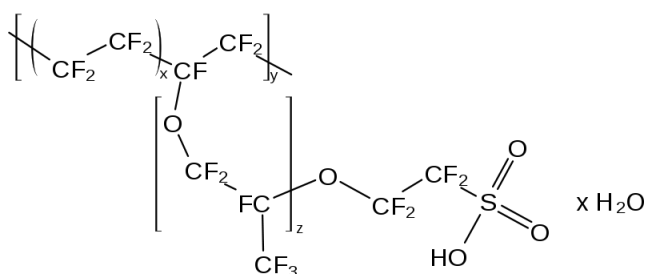


Figure A-2: Nafion structure
(<http://en.wikipedia.org/wiki/File:Nafion2.svg>).

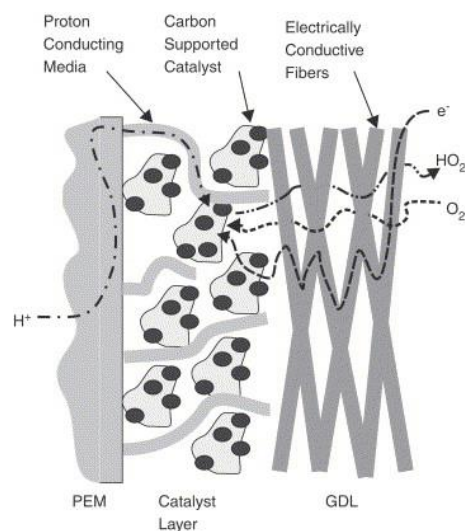


Figure A-3: CL at cathode electrode
(taken from [2], Reproduced with permission from Elsevier).

A gas diffusion layer (GDL) consists of a carbon fiber or woven cloth microporous layer. The GDL functions as an electron conductor to/from the CL and reactant transport to or product removal from the CL. It also provides heat transport from the CL to the bipolar plate and is a mechanical support for the CL.

A bipolar plate or flow field utilizes polymer-sealed high-conductivity graphite material. Bipolar plates conduct electrons from the anode to the external circuit and from the external circuit to the cathode. It delivers fuel flow through flow channels and provides structural integrity of the stack. A bipolar plate also dissipates waste heat generated by inefficiencies of the reaction, often with a coolant flow through itself. A polymer sealing is used in bipolar plates to ensure the normally porous graphite is impermeable to water.

Appendix B: Prussian Blue

PB is a ferric ferrocyanide with the basic face-centered-cubic crystalline structure consisting of iron ions linked by the cyanide groups with two chemical forms $\text{Fe}_4^{\text{III}}[\text{Fe}^{\text{II}}(\text{CN})_6]_3$ and $\text{KFe}^{\text{III}}\text{Fe}^{\text{II}}(\text{CN})_6$, Figure B-1 [39, 40]. These two chemical forms are commonly known as “insoluble” and “soluble”, respectively [40]. Both insoluble and soluble forms of PB are highly insoluble ($K_{\text{sp}} = 10^{-40}$), the difference refers to the simplicity of potassium peptization [54]. Large metal cations and water molecules, as well as other small molecules like H_2O_2 , can be accommodated in the open structure of PB [54]. Chemical reduction and oxidation of PB leads to Prussian White (PW) (potassium ferrous ferrocyanide) and Berlin green (BG) (ferric ferricyanide), with chemical formula $\text{K}_2\text{Fe}^{\text{II}}\text{Fe}^{\text{II}}(\text{CN})_6$, and $\text{Fe}^{\text{III}}\text{Fe}^{\text{III}}(\text{CN})_6$, respectively [39, 54]. Reactions (B-1) to (B-4) show the reduction and oxidation for soluble and insoluble forms of PB, respectively.

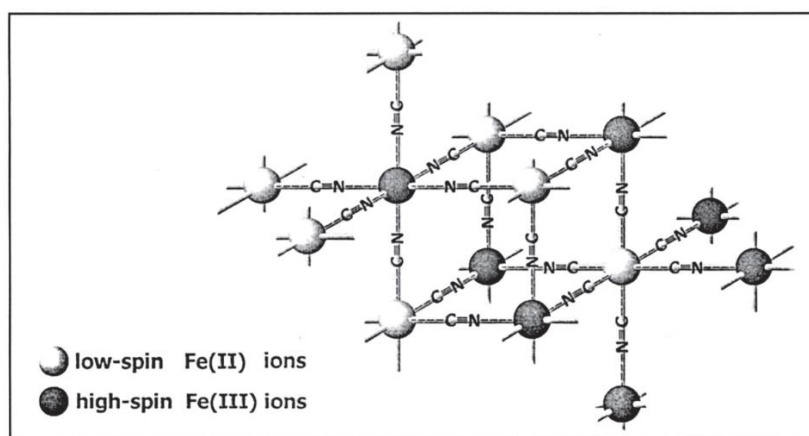


Figure B-1: Face-centered-cubic crystal structure of PB (taken from [38], Reproduced with permission from Taylor & Francis).

